STRUCTURE AND METAMORPHISM OF THE HAAST SCHIST AND TORLESSE ZONES BETWEEN THE ALPINE FAULT AND THE D'URVILLE VALLEY, SOUTH NELSON.

A Thesis
submitted in partial fulfilment of
the requirements for the Degree
of
Master of Science in Geology
in the
University of Canterbury
by

R.V.Rose

University of Canterbury
1986

Frontispiece

Mt Una and the Spenser Mountains

from Burn Creek Bivy

"Quality is better seen up at

the timberline than here obscurred

by smokey windows and oceans of

words"

Robert M. Pirsig

(Zen and the Art of Motorcycle maintenance)

CONTENTS

LIST OF TABLES AND FIGURES

Tables

Figures

ABSTRACT

Within the bends region of the Alpine Fault two structural trends have been identified. These are a D_1-D_2 "Rangitata" trend and a D_3 "Kaikoura" trend. The D_1-D_2 trend maintains a northeasterly strike of both bedding and S_2 schistosity which is independent of the Alpine Fault, intersecting in such a way as to verge into the Fault from the south at an acute angle. Within the Glenroy section, the relative angle changes such that this trend approaches obliquely from the north. The D_3 trend overprints D_2 close to the Alpine Fault and is subparallel to the fault.

Two metamorphisms (M_2 and M_3) are identified, M_2 being associated with D_2 and M_3 with D_3. S_3 schistosity, L_3 lineations and F_3 folds are associated with strain in, and adjacent to the Alpine Fault Zone.

There is no direct evidence that the Haast Schists slip around and past a fixed bend in the Alpine Fault Zone. The double bend of the Alpine Fault is thus fixed with respect to the "Wairau Block" (that area between the Alpine/Wairau and Awatere Faults), and forms the leading edge of a wedge shaped body of Haast Schist and Torlesse Zone metasediments.

L_3 lineations including quartz rodding, trend and plunge at approximately 060/50° northeast, and are assumed to reflect the transport direction in non-coaxial plane strain within the Alpine Fault Zone. The Haast Schists are being thrust over the Western Province with the vector direction and rate of movement of the rock mass remaining relatively constant at all points around the curve of the Alpine Fault.

Likely orientations of the XY plane of strain in the Alpine Fault Zone are discussed. It is concluded that a distinctly separate schistosity will not form unless

pre-existing metamorphic layering is suitably oriented with respect to the shear zone. Consequently, transition from M_2 (Rangitata Phase) schists to M_3 (Alpine Fault generated) schists may be subtle and difficult to determine either in the field or in thin section.

Rotation of the D_2 structural trend by ductile drag on a macroscopic scale within the Alpine Fault Zone appears to be counterclockwise. This is to be expected if (as is the case in the bends region) the early anisotropy has a more northerly strike than the convergence vector.

Equal area projection plots of post-metamorphic brittle shear surfaces cluster strongly, defining dominant shear sets oriented west-northwest to northwest and east-northeast respectively. Those shears which strike northwest exhibit minor movement of sinistral sense, whereas those striking northeast show a dextral movement. No large brittle offsets have been demonstrated, and cumulative offset on these shear systems has not altered the gross structural trends.

CHAPTER ONE

THE ALPINE FAULT PROBLEM

1.1 THE ALPINE FAULT

1.1.1 Introduction

Although some matters concerning the Alpine Fault are still quite contentious, a certain degree of consensus has been reached as to the nature and history of this major tectonic feature. Unfortunately there have been no recent review papers. However, Cutten (1976) and Suggate (1963) provide access to most of the early literature. Naturally research on various aspects of the Indo-Pacific plate boundary has continued since 1976. The following is a list of the main problematical themes:

(1) The history of lateral offset by the Alpine Fault and "splay" faults.

(2) The importance of the Alpine Fault in the uplift history of the Haast Schists and Southern Alps.

(3) The nature of the Fault Zone, it's width, attitude, movement mechanisms, and the orientation of the slip vector.

(4) The contribution of the Alpine Fault to the Indo-Pacific plate boundary.

Cutten (1976) defined five lines of enquiry into the movement history of the fault. These as well as several additional categories are outline here:

(a) Extrapolation into the past, of modern rates of movement on the Alpine Fault.

(b) Displacement by the Fault system of older features such as lamprophyre dykes, and mylonites.

(c) The ages of deformation structures associated with the Alpine Fault.

(d) Potassium-Argon dating of the uplifted schists.

(e) (i) The thermal regime of the Southern Alps.
(ii) General theoretical work on shear heating.

(f) Plate tectonics
(i) Seafloor spreading and magnetic anomalies.
(ii) General crustal stress and strain.

(g) Geophysical profiling.

(h) Contemporaneous sedimentation patterns.

A selective history of the literature on the Alpine Fault is included prior to outlining several of the above categories. Potassium-Argon dating of the schists and shear heating are discussed in Section 4.6.2. Stress patterns and their significance are discussed briefly in Section 5.2.

1.1.2 Early Recognition and the Question of the Attitude of the Alpine Fault

Although credit for naming the Alpine Fault may go to Henderson (1937), it's earliest recognition as a major feature must date back at least to Morgan (1908) in the Mikonui subdivision. He termed it a "Great Fault", the geomorphic expression of which is termed the Gregory Valley. As to the nature of the Fault, Morgan wrote ..."It may be

concluded that the uplift of the Southern Alps was largely a product of bodily forward movement of the folds up the incline plains of an overthrust fault." His cross section clearly shows this fault as a wide zone of intense shear.

A structural break between the Arahura Series (Haast Schists) and the granites to the west was also suggested by Bell and Fraser (1906). This was recorded as a "Sinuous boundary line" ... "constituting one of the most striking physical features of the region."

Cox (1883) and McKay (1895) both noted that schists overlie marbles and slates in the Alfred River area, although no fault was recognised.

It is rather curious that although the early workers recognised that schists lay above the rocks of the Western Foreland, this seems to have been either ignored or discredited by the next generation. One notable exception was J.T. Kingma (1959, 1974).

It was not until 1942 that Wellman and Willet recognised the Alpine Fault as a continuous feature from Milford Sound as far north as Lake Rotoroa, and 1949 when Wellman, in an address to the Pacific Science Congress, postulated 480 kilometres of dextral strike slip movement along the fault.

Over the ensuing years the Alpine Fault and related topics have been the source of considerable debate. The literature to 1963 is reviewed by Suggate (1963). This summary produced no consensus and debate continued to rage.

Kupfer (1964) re-emphasized Morgan's view that the fault was a wide and complex zone of deformation, and also noted that very little information detailing this zone had so far been forthcoming.

The first recognition of the Alpine Fault as a plate boundary is usually attributed to Le Pichon (1968).

However, this could also be awarded to Wilson (1963) who produced plate tectonics, all but in name, and mentioned the Alpine Fault-Macquarie Ridge system in this context.

In 1953 Wellman catalogued all available data on fault attitudes and recent offsets for the South Island. At this time it was still thought that the Alpine Fault was a structure which dipped at a moderate angle to the southeast. However, by 1955 Wellman had altered his views and published a cross section showing the Alpine Fault to be vertical, a view which remained entrenched in the literature for many years. Sibson et al (1979) discuss the attitude of the fault and modify Wellman's cross section, significantly, returning to the view of a dipping fault of earlier years.

1.1.3 The Age of the Alpine Fault

(a) Introduction

In an historical context, the most vigorously contested aspect of the Alpine Fault is it's age. Debate has quietened somewhat of recent times as it is now generally accepted that the entire dextral strike slip displacement can be accommodated by Cenozoic tectonics. Most workers now assign the maximum age at late Oligocene to early Miocene, although the process of initiation of the plate boundary through New Zealand may date back slightly further.

The age of the Alpine Fault is crucial to any tectonic model of the bends area, therefore it is useful to here outline some of the arguments present in the literature on the Fault.

(b) Displacement by the Alpine Fault of Older Features

On the basis of a 180-210 km separation of Mid-Cretaceous lamprophyre dyke swarms across the Alpine Fault in Westland, Wellman (1956), Grindley (1963) and

Wellman and Cooper (1971) suggested this recorded the maximum possible post Cretaceous dextral offset on the Alpine Fault (a hypothesis which Wellman had rejected by 1964).

After examining the distribution of lamprophyre dykes in the South Island, Hunt and Nathan (1976) concluded "... Rather than a single belt of lamprophyre dykes, there appears to be a number of geographically distinct dyke swarms around source bodies inferred from magnetic evidence". Hunt and Nathan suggested "... roughly synchronous emplacement of lamprophyre magma at widely separated localities" and saw no reason to conclude that the dykes can be used as structural markers for recording Alpine Fault movement.

(c) Deformation Structures Associated with the Alpine Fault

Grindley (1963) suggested that mylonites offset by the Alpine Fault in Westland could be used as structural markers similar to the lamprophyre dykes. As the mylonites were thought to be Cretaceous is age, a maximum of 161 km of post Cretaceous offset was implied.

Young (1968) considered the Fraser Formation of central Westland to be part of the Alpine Fault Zone. Mid Cretaceous lamprophyre dykes which were seen to cut the Fraser Formation gave a minimum age of mylonitization.

The significance of the Fraser Formation is still a matter of some contention. It has been shown by Rattenbury (1985) that Cretaceous dykes in the Fraser Formation cut gneisses rather than mylonites, and are themselves mylonitized, thus providing a maximum age of mylonitization. K-Ar dating indicates these mylonites are post Mid-Eocene in age. Mylonites of the Fraser Formation could be either unrelated to the Alpine Fault, or represent a proto-Alpine Fault. There is no proof at this stage that mylonites of the Fraser Formation are part of the Alpine Fault Zone.

Kupfer (1964) and Sibson et al. (1979, 1981) show that the Alpine Fault is a narrow but complicated zone 1-1.5 km wide. Reed (1964) identified three types of fault rock: (a) incoherent fault pug, fault breccia and shattered rocks; (b) coherent cataclasite, mortared and brecciated rocks; and (c) mylonite, augen mylonite, ultramylonite and blastomylonite. He associated groups (a) and (b) with Quaternary and late Tertiary movement phases, and group (c) with Jurassic to early Cretaceous movement. However Sibson et al. (1979) have shown that all three rock types have been generated since the beginning of the Kaikoura Orogeny, with mylonitic lineations subparallel to the present day Indo-Pacific plate boundary.

1.1.4 Total Offset and Movement Rates on the Alpine Fault

Movement rates including both horizontal and vertical components, are relevant to models of the tectonics of the bends region. The Alpine Fault is recognised as an integral part of the Indo-Pacific plate boundary zone (Walcott, 1979) with crustal strain widespread and not confined to a single lineament. The Marlborough Faults are also an integral part of this zone although the age and early movement histories of these faults is not well understood.

The most striking feature associated with the Alpine Fault is the 480 km strike separation of the Dun Mountain Ophiolite and the Maitai Group. It should not be assumed that all rocks adjacent to the Alpine Fault have suffered this same displacement.

Movement rates on the Fault must decrease northward from the Taramakau River if current models of the plate boundary are credible. Alternatively the Alpine Fault must systematically absorb a large proportion of the strain recorded across the Marlborough Fault system. Therefore it follows that rates of movement on the north-south "Glenroy" or "Bends" section of the Alpine Fault are roughly

equivalent to that on the Wairau Valley extension further northeast. If this is so then an interesting question arises: Have the Haast Schists of southeast Nelson suffered as large a displacement as the Dun Mountain Ophiolite and the Maitai Group. The answer must be, not necessarily. (see fig. 1.1).

A number or factors are involved in the slowing of movement on the northern section of the Alpine Fault. These include:

(1) Absorption of strain by the Marlborough Fault System (although how far back in time this can be projected is unknown).

(2) Southward displacement of the Marlborough Fault system with respect to the Western Foreland.

(3) Initiation of new Marlborough type faults under Canterbury as the Hikurangi Subduction Complex migrates southward.

(4) General slowing of transcurrent movement by an increase in compression and reverse movement across the Alpine-Marlborough Fault System.

It is not justifiable to assume that the Western Foreland can be regarded as a rigid block uninvolved in the plate boundary zone, however convenient it may be to do so. There is ample evidence of significant tectonic movements west of the Alpine Fault during the Kaikoura Orogeny (see Rattenbury, 1985; Campbell and Cutten, 1985; Berryman, 1980, as examples).

Estimates of the actual movement rates at various localities on the Alpine-Marlborough Fault System have shown a variable but generally increasing trend since the Alpine Fault was "discovered" in 1942. An exhaustive review of the conflicting estimates is beyond the scope of this discussion. Walcott (1978) and Bibby (1976) estimated strain

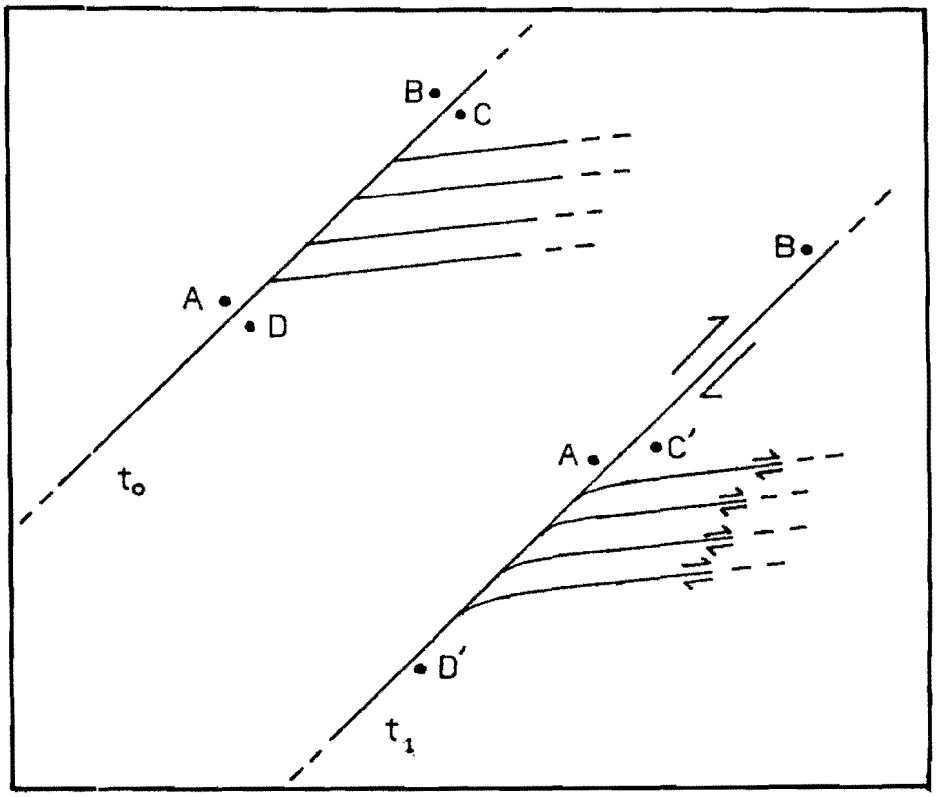

FIG 1.1 Relative displacement across a master fault and associated splay faults.

$\overline{AB} = \overline{CD} \neq \overline{C'D'}$, $\overline{AD'} \neq \overline{BC'}$

rates across the "axial tectonic belt" (Walcott) at 4.5 x 10^{-7}/yr and 5±1 x 10^{-7}/yr respectively, up to 75% of which was located at the major faults (Walcott).

Estimated cumulative horizontal displacement rates across the axial tectonic belt vary from 10±5 mm/yr to 35 mm/yr (Wellman, 1985). Berryman (1979) favoured a cumulative rate of 25 mm/yr across the Marlborough Faults, 3.8 mm/yr on the Wairau Fault, and between 6.75 and 25 mm/yr for the central overthrust section of the Alpine Fault.

1.1.5 Geophysical Exploration of the Alpine Fault

There have been a number of geophysical studies aimed at outlining the crustal structure of the South Island, and in particular the Indo-Pacific plate boundary. These include the interpretation of Bouguer anomalies from regional gravitational surveys, detailed investigation of gravity profiles at selected localities, and the interpretation of compilations of earthquake epicentre data.

The seismic record is significant with respect to the Alpine Fault as there is a relative paucity of discrete slip events which are demonstrably associated with the Alpine Fault. This situation could either represent cyclical seismic activity at the Alpine Fault (and perhaps associated with a buildup in elastic strain) or it could reflect asiesmic strain in the Alpine Fault Zone and the Southern Alps. There is abundant evidence indicating that seismic slip postdating the last glacial period has caused the offset of glacial and post glacial geomorphic features.

Seismicity in the South Island is described by Smith (1971), Evison (1971), Scholz et al. (1973), Davey and Broadbent (1980), Arabasz and Robinson (1976), Haines et al. (1979) and Hatherton (1980).

Gravity investigations include those of Malahoff (1965), Hatherton and Hunt (1968), Woodward (1972, 1979) and Allis (1981). Hatherton and Hunt (1968) found that due to a

lack of density contrast across the Alpine Fault Zone it was not possible to determine the attitude of the fault zone at depth. Malahoff (1965) found that where the Dun Mountain Ophiolite terminates against the Alpine Fault (near Tophouse) there was sufficient density contrast to allow estimation of the attitude of the fault plane. The figure obtained was 67° southeast. Both Woodward (1979) and Allis (1981) illustrated the Alpine Fault plane with dips of around 60° and 30° respectively. These two models were based on the regional Bouguer anomalies. Allis (1981) suggests substantial crustal underthrusting of the Indian Plate under the Pacific Plate along the Alpine Fault, particularly south of Mt Cook.

In the southeast Nelson area topography exerts a marked influence on the strike of the Alpine Fault which "V's" from ridge to valley indicating an easterly to southeasterly dip.

1.2 OBJECTIVES OF THIS STUDY

One of the most striking features on any topographic or geologic map of the South Island is the Alpine Fault. This lineament extends on land from Milford Sound in the south to Blenheim in the north and is essentially straight for most of it's length. However, in the present study area the strike swings through an angle of approximately 50° in a marked double bend.

To the west of the bends the geology is now well known. East of the fault however there has been little detailed mapping. Several authors have attempted to explain why there should be a bend in the Alpine Fault. None have been entirely convincing, partly due to a lack of in depth knowledge of the structure east of the fault.

The aim of this thesis is to examine, in some detail, the structure of the basement rocks within that area immediately east of the "Alpine Fault bends". From this

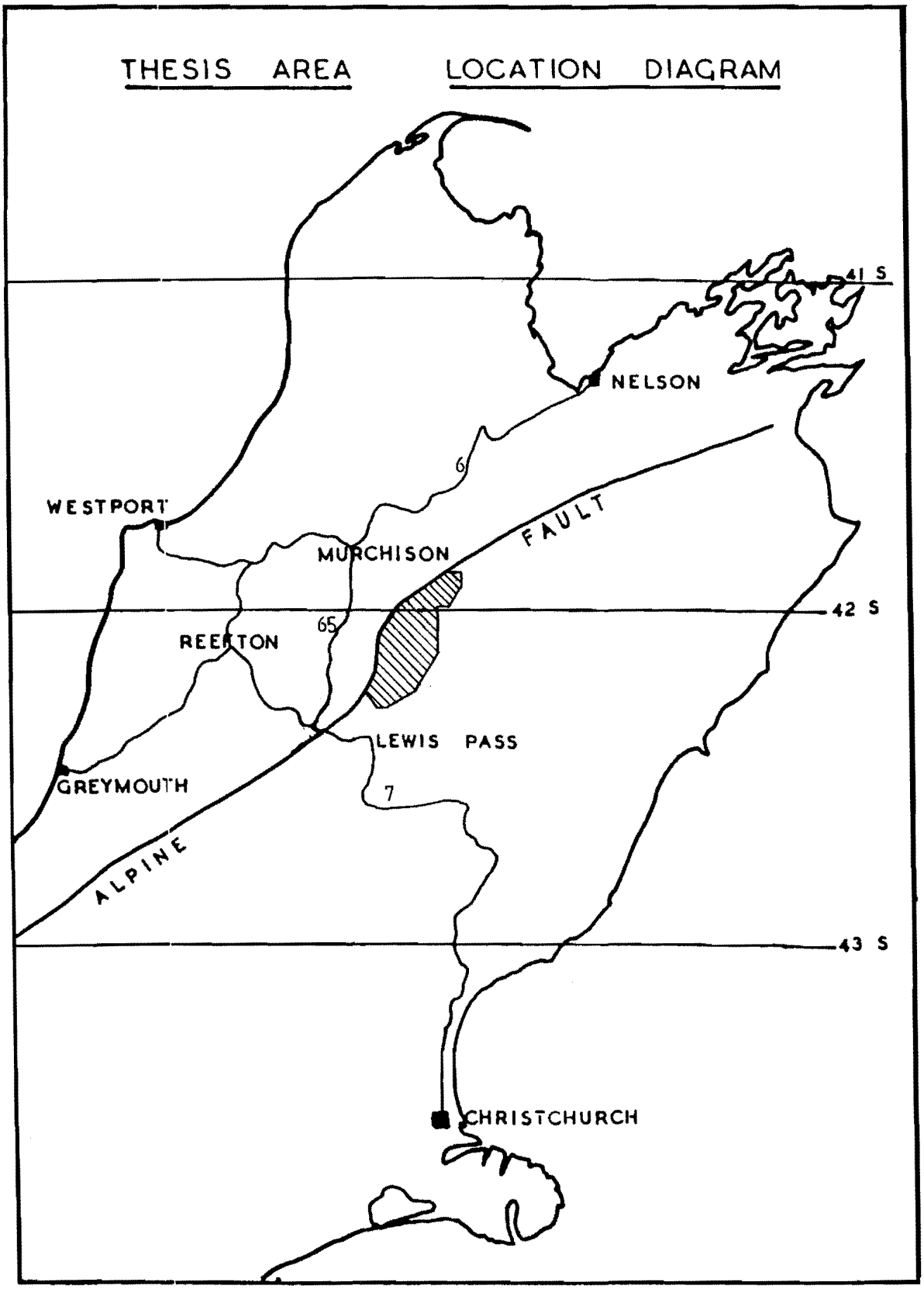
THESIS AREA LOCATION DIAGRAM
41 S
NELSON
6
WESTPORT
FAULT
MURCHISON
42 S
65
REEFTON
LEWIS PASS
GREYMOUTH
7
ALPINE
43 S
CHRISTCHURCH

FIG 1.2

basic data an attempt is made to describe the way in which these bends have affected the structure of the surrounding rocks, to model likely movement mechanisms on the fault itself, and to further discuss possible causes of the formation of the bends.

1.3 LOCATION

The area mapped in this study lies some 25 kilometres southeast of Murchison, 15 kilometres northeast of Springs Junction, and 140 kilometres north of Christchurch. Boundaries of the area coincide with the Alpine Fault in the west and north, the Spencer Mountains in the south and southeast, the Mahaunga range in the east, and the Sabine River in the northeast. This constitutes roughly the southwestern half of Nelson Lakes National Park. The approximate extent of the area is outlined on the location map (fig. 1.2).

1.4 PHYSIOGRAPHY AND VEGETATION

Topographic relief in the area is considerable. From a minimum valley elevation of 1400 ft above sea level, the mountains rise to a maximum of 7400 ft (Mt Ella). The region contains portions of the catchments of a number of rivers including: the Glenroy, Matakitaki, D'Urville and Sabine Rivers draining to the north; the Alfred and Maruia Rivers draining southwest; and Sheriff River, which drains towards the west. The landscape is quite clearly glacially moulded. On shaded slopes of the higher peaks snow may still lie all the year round.

Vegetation cover is of three main types. In low lying valleys, open grasslands are utilised by local farmers. Mountain Beech forest covers the remaining valley bottom areas and the valley sides up to the bush line. Above the bushline, tussock grassland, unvegetated scree and bare outcrop dominates.

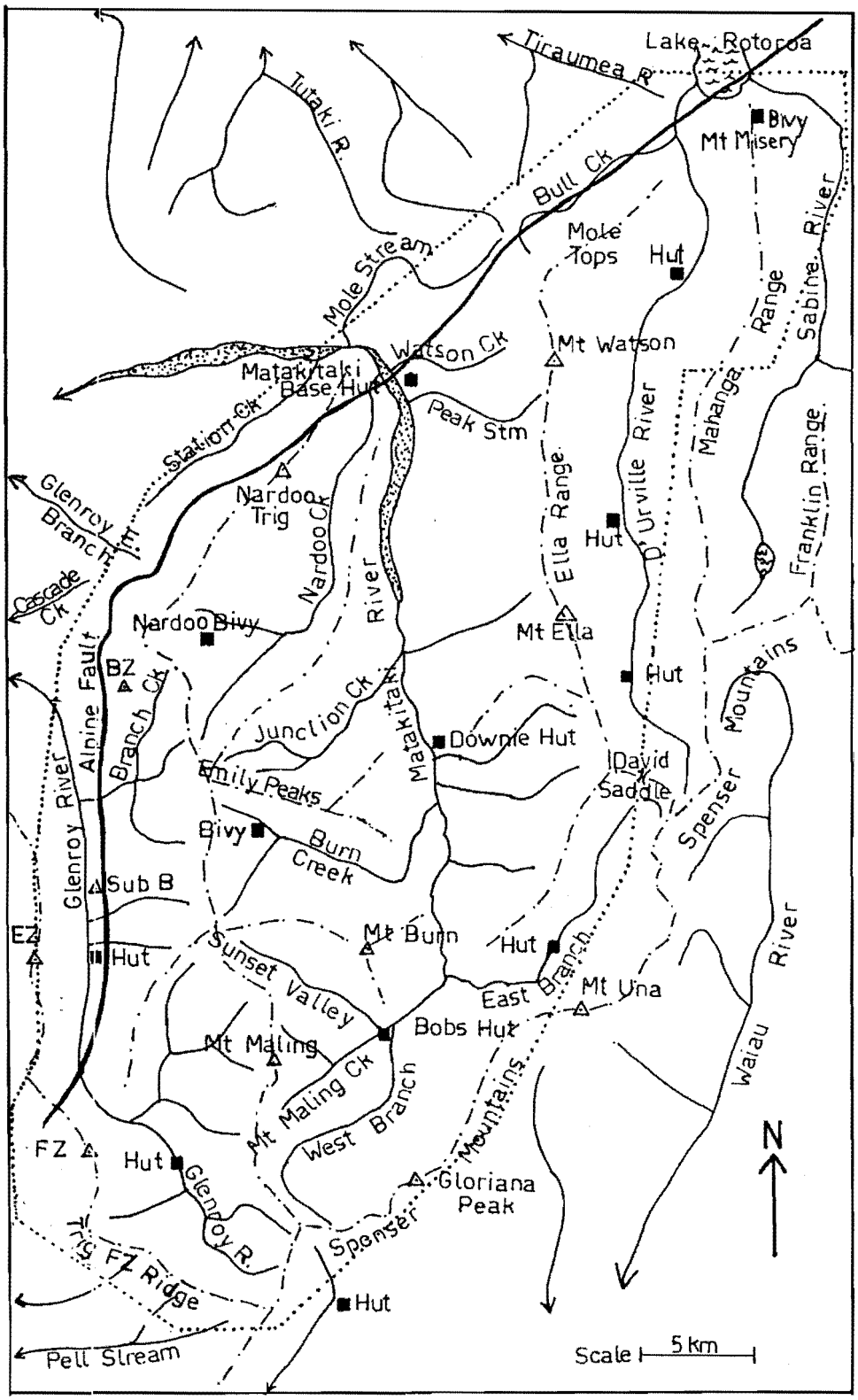

FIG 1.3 Locations within the study area

1.5 PREVIOUS WORK

The first geological investigation of this part of the Nelson province was carried out by Julius von Haast in 1861. With respect to the present study area Haast noted that the Spenser Mountains were composed of sedimentary strata which became more crystalline towards the core of the range. It should be noted that this survey was carried out under extreme physical hardship. No maps were previously available, these being drawn as the trip progressed, from high vantage points, by Haast and his assistant Charles Burnett.

The next explorations of note were carried out by Herbert S. Cox in 1883. Rocks encountered in the present area include "foliated quartz schists resembling those of Otago". These were seen to extend little further north than the Matakitaki river. Cox noted that the metamorphic schists overlie fossiliferous strata (Sheriff and Alfred Rivers), and that greywackes at the head of the Tiraumea River overlie metamorphic crystalline rocks (Rotoroa Igneous Complex of Fyfe). He did not recognise the Alpine Fault, but did note a zone of soft mica and chlorite schists in the Alfred and Sheriff Rivers. These relationships are clear in two cross sections through this region.

In 1895 Alexander McKay followed Cox in assuming the Paleozoic rocks of Springs Junction formed a continuous sequence with the mica schists east of the Alpine Fault. Although the fault is not recognised, it's trend can be recognised on McKay's map.

Fyfe (1929, 1930, 1968) described the geology of the Murchison Subdivision. The Wairau Fault is extended as far south as the Matakitaki river. Rocks equivalent to the Haast Schist and Torlesse Zones (of the Alpine Assemblage, Carter et al 1974) are assigned the local names Glenroy and Mt Robert Series respectively. Following Cox (1883), the Mt

Robert Series is seen as unconformable upon the Glenroy Series. That section of Fyfe (1968) dealing with the petrology of the Mt Robert Series and Glenroy Series, was written by J. J. Reed, who equated these rocks with the Alpine Feldspathic Association of Wellman (1952). The mapping for Fyfe (1968) was completed by 1936. Reed (1958) recognised no unconformity between Mt Robert and Glenroy Series rocks. He identified a "thick succession of alternating greywackes, argillites, and rare conglomerates extending from Lewis Pass to Lake Rotoiti" which "grade westward with increasing metamorphism into fully reconstituted quartzofeldspathic schists, chlorite schists, and actinolite schists". Within the schists he mapped chlorite, biotite, and garnet zones (garnets were also noted by Cox 1883), the chlorite zone being subdivided into Ch11, Ch12, and Ch13 subzones of Hutton and Turner (1936).

Bowen (1964) compiled the New Zealand Geological Survey map at 1:250,000 Sheet 15, Buller from previously published and unpublished surveys. Additional surveys were also carried out. He incorporated structural data not seen in either Fyfe (1968) or Reed (1958), and also modified the position of Reed's isograds.

Adamson (1966) mapped the area roughly bounded by the Alpine Fault, and the Glenroy and Matakitaki Rivers. Some structural data from the schists were recorded for the area about the junction of Nardoo Creek and the Matakitaki River.

Sheppard, Adams, and Bird (1975) dated schists from the Upper Glenroy Valley and Branch Creek, Matakitaki River at the Alpine Fault, and the D'Urville River. From the distribution of K-Ar ages obtained, Sheppard et al. concluded that an uplift phase commenced 4 ± 2 m.y. ago, with argon outgassing at this time, possibly due to shear heating on the Alpine Fault.

Turnbull and Forsyth (in press) mapped the area between the Alpine Fault, the Maruia River, and the Traverse Range during the 1982/83 field season. This work was aimed

towards elucidation of the structure of the region. One of the main findings was the identification of two metamorphic events, one of which they relate to movement on the Alpine Fault. Various aspects of the work of Turnbull and Forsyth are discussed in the main text of this thesis.

CHAPTER TWO

LITHOLOGY

2.1 MAP UNITS BASED ON THE DEVELOPMENT OF METAMORPHIC FABRIC

2.1.1 Introduction

There is still some dispute as to the nomenclature which should be used in high level classification of the main units of the "New Zealand Geosyncline". For the purposes of this thesis the terminology of Carter et al. (1974) has been adopted. The Torlesse (greywacke) Zone and Haast Schist Zone of the Alpine Assemblage are here separated by the Textural Zone I/IIA isotect. Division along this line is purely arbitrary, many sedimentary structures still being visible inside the Haast Schist Zone.

In the field the rocks were described in terms of their metamorphic textural development, the attitude of one or more schistosity planes, the presence or absence of key metamorphic minerals, their primary lithological character, and where possible, the facing direction and attitude of bedding.

2.1.2 Textural Zonation Scheme (after Bishop 1972)

This scheme was adopted as the means by which general development of metamorphic foliation was identified. It is based on the degree to which medium grained sandstone has developed a metamorphic fabric.

Textural Zone I - Indurated sandstone with no metamorphic fabric. Hand specimens show no tendency to split in any preferred direction.

Textural Zone IIA - Metasandstones bear a spaced or weak moderately developed slaty cleavage and have a tendency to split parallel to it. Original grain boundaries are indistinct.

Textural Zone IIB - Slaty cleavage is penetrative and the rocks usually split parallel to it. Segregation laminae are not developed.

Textural Zone IIIA - Metasandstone is strongly schistose and fine grained with incipient leucocratic segregation laminae 1 to 10 mm long.

Textural Zone IIIB - Strongly schistose rocks with thin segregation laminae less than 2 mm thick and 10 mm or more in length.

2.2 PRIMARY LITHOLOGIC CHARACTER OF THE HAAST SCHIST AND TORLESSE ZONES

The immediate appearance of the rocks of this area is that of fairly typical metasediments of the Haast Schist and Torlesse Zones. In the southwest portion of Nelson Lakes National Park, there is an unusually large proportion of pelitic rocks. Overall, the ratio of pelitic to psammitic rocks is around 1:3 but, in the west particularly (Textural Zones IIB to IIIA), the ratio is somewhat higher.

In general, strata strike consistently northwest and dip either steeply southeast or northwest. Those packages which are rich in metapelite tend to exhibit a more subdued topographic expression than those rich in metapsammite, the latter being more resistant to weathering and erosion.

Compositionally these rocks are similar to those of the Alpine Assemblage elsewhere in the Southern Alps. Reed (1958) analysed weight percentages of the various oxides in nine quartzofeldspathic samples from southeast Nelson. These

were shown to be very similar to samples previously analysed from other parts of the Alpine Assemblage

Even in the lower textural grades crystallisation, recrystallisation, and deformation of the matrix, of monocrystalline feldspar grains, and the feldspathic component of the lithic grains, make original grain boundaries difficult to distinguish. Distortion of the quartzose component by recrystallisation and pressure solution also presents problems. Therefore it was deemed unrealistic to attempt precise arenite classification.

During mapping a loose subdivision of these metasediments into sedimentary associations was useful. The associations are: (1) massive/very thick bedded sandstone; (2) Thin bedded association; (3) mudstone - siltstone association; (4) conglomerates.

A second subdivision was made on the basis of overall composition into: (1) Grey quartzofeldspathic metasediments and (2) Grey-green to green clastic metasediments. This subdivision will be discussed under metamorphism.

In the higher textural grades pelite and psammite are distinguished by difference in grain size (although the original grainsize can only be estimated) and by colour contrast due to the presence or absence of relict carbonaceous material.

2.3. SEDIMENTARY ASSOCIATIONS

2.3.1 Massive and Very Thick Bedded Sandstone Association

Included within the massive sandstone association are those strata in which pelite is either absent, or forms only a minor proportion of the total thickness. With few exceptions, bedding planes are not visible unless pelitic horizons are present. In rocks of low textural grade, the

massive sandstone association is dominated by medium to coarse grained sandstones. As a mapping unit at 1:25,000, areas shown as massive sandstone may include horizons composed of mudstone-siltstone association, and of thin bedded association.

By comparison with other regions, it is inferred that this association was deposited by mass flow mechanisms under the influence of gravity, and represents deposits proximal to the mass flow source.

2.3.2 Thin Bedded Association

The thin bedded association (see fig. 2.2) is characterised by interbedded sandstones, siltstones, and mudstone. In general, the psammite to pelite ratio is between 3:1 and 1:3. The attitude of bedding can be reliably measured at most localities outside the TZ-IIIA isotect. Bed thickness is variable from around 2-3 cm to 1 m. The most common grainsize for sandstone is fine, coarse sands being rare in this association. Fining and coarsening sequences are common, as this association is often transitional into either the mudstone-siltstone association, or the massive sandstone association. Thin bedded association can also grade laterally into either mudstone-siltstone, or massive sandstone association. Flysch like sequences are not uncommon, and at some localities Bouma B to E sequences are still preserved. The mapped association contains occasional thicker sandstones and mudstones, which owing to scale, cannot be separated out. Depositional mechanisms are assumed to be similar to those of the massive sandstone association, only more distal, and with significant fine-grained background sedimentation.

2.3.3 Mudstone/Siltstone Association

This association is characterised by massive and thin bedded mudstone and siltstone with layer spacing from less than 1 mm to 5 cm. Interspersed within this association there may occur occasional packages of the massive

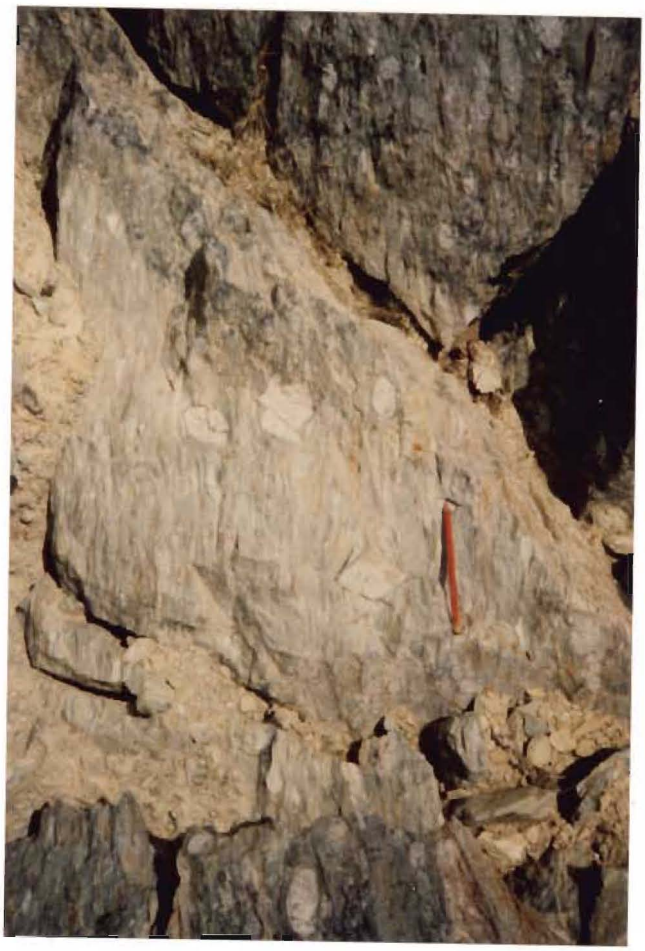

FIG. 2.1
Deformed clast-supported conglomerate from the Ella Range 2 km north of Mt Watson (M30 4750 9120). Flattening is grainsize sensitive Coarse grained plutonic cobbles are the least deformed and are often offset by brittle shear planes which do not extend through the surrounding pebbles.

FIG. 2.2 Typical thin bedded association of TZ IIB in the Upper Glenroy Valley. Metric grid reference M31 4595 8820. Note the small sinistral fault with an offset of approximately 20 cm.

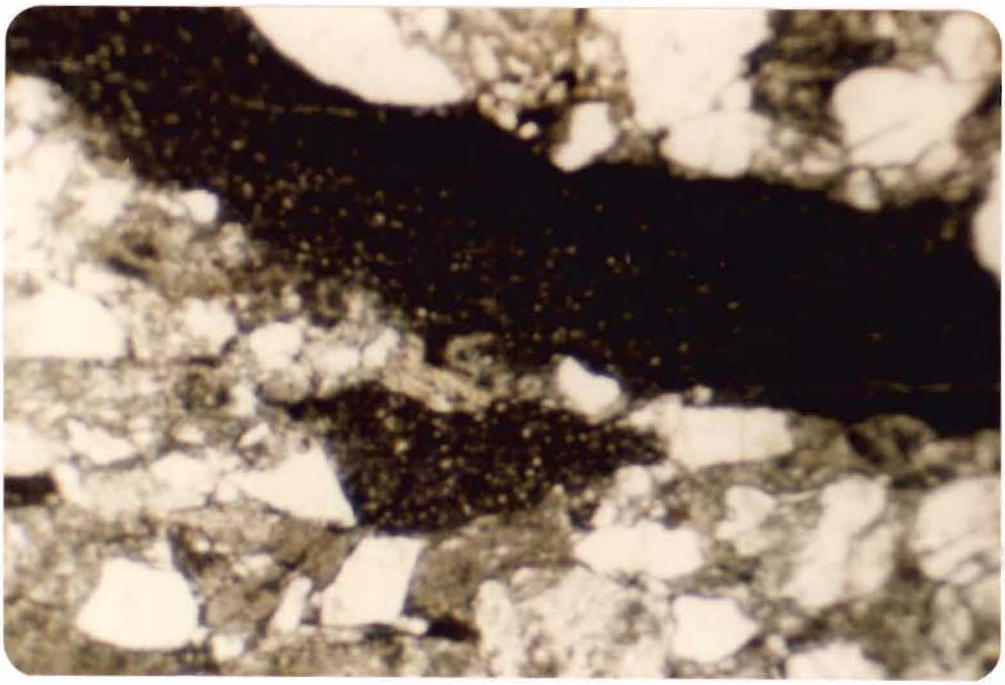

FIG. 2.3 Thin section (UC10657), TZ IIA chipwacke. Components include mudstone, siltstone and very fine sandstone fragments, chert, strained and unstrained quartz, polycrystalline quartz and feldspar grains. Metric grid reference M30 4732 9001.

FIG. 2.4 Mudstone rip-up breccia, TZ IIA semischist. Mudstone clasts are aligned with their long and intermediate axes within the plane of bedding (and schistosity). The clasts are embedded in a matrix of coarse to granular sandstone. Metric grid reference M30 4735 9001.

sandstone, or thin bedded associations. Mudstone-sandstone associations can pass gradationally into the thin bedded association both laterally, and stratigraphically up or down sequence.

This association exhibits a rather dark grey to black colour due to the large component of unabsorbed carbonaceous material, and fine iron rich opaques. Some outcrops have a reddish colouration due to the oxidation of iron rich minerals.

To the west of David Saddle, and through David Saddle (Turnbull and Forsyth, in press), Torlesse metasediments and mudstone-siltstone association in particular, often have a rather green colouration. A significant change in the type of sediment supplied for an unknown length of time, may be the cause. The mineralogy of these green rocks suggests a contrast in chemical composition between these green phyllites and the more widespread grey metasediments.

Individual examples of the mudstone-siltstone association are up to 700 m in thickness, as seen in the upper reaches of Burn and Junction Creeks. Several examples are laterally continuous over distances as large as ten kilometres. This association covers no less than one fifth of the total area mapped.

Depositional mechanisms are not known, but may include sedimentary gravity mass flow, working by traction currents, and background pelagic sedimentation.

2.3.4 Conglomerate

The most distinctive marker horizons of this region are those in which conglomerate is a significant component. Conglomerate only occurs in sequences rich in coarse granular sandstone, although mudstone can be a subsidiary component.

No premetamorphic internal structure has been recognised within conglomerate horizons. Cobbles and pebbles are invariably flattened and elongated in the plane of schistosity.

Several varieties of conglomerate are recognised within the field area. These are: (a) chipwacke and mudstone ripup breccia; (b) pebbly sandstone and matrix supported conglomerate; (c) clast supported conglomerate; and (d) pebbly mudstone.

(a) Chipwacke (fig. 2.3) and ripup breccia (fig. 2.4). - The matrix is always medium to coarse sand enclosing large penecontemporaneous mudstone clasts. The coarse sand fraction is well rounded where it can be seen in rocks of low textural grade. Mudstone clasts are invariably angular, and generally matrix supported. They are elongate parallel to bedding with internal layering parallel to external bedding and the long axes of the clasts. Occasional folds within individual clasts have been observed. The matrix itself appears to be transitional into pebbly sandstone in some instances. These features indicate high energy processes were involved in the origin of the mudstone clasts, probably including scouring during mass flow of coarse sandy material.

(b) and (c) Pebbly sandstones, matrix supported conglomerate, and clast supported conglomerate. - These lithologies occur in association and appear to be transitional, each into the others, and into coarse to granular sandstone. Cobbles and pebbles in conglomerate of this type are always well, to very well rounded. Pebble lithologies include both acid and basic plutonics, probable basic volcanics altered to greenschists, vein quartz, as well as the more numerous grey sandstone, siltstone, and mudstone

lithologies. Clast supported conglomerate is illustrated in figs. 2.1, 3.6 and 3.7.

(d) Pebbly mudstones - This lithology consists of dark masssive mudstone with scattered flattened pebbles, and was noted at one locality only. Here it was associated with clast supported conglomerates (fig. 3.7).

The dominant conglomerate lithology encountered was the clast supported variety. Proportions of each type are difficult to estimate as conglomerates were found in situ only at a small number of localities. Average diameters of cobbles in the clast supported conglomerates are 3-5 cm. The largest individual clast observed was approximately 20 x 15 cm in the plane of observation.

In all cases the conglomerates appear to have been deposited by mass flow mechanisms. No channel scours have been observed. A conglomerate bearing unit is continuous along strike for at least five kilometres on the range separating Burn and Branch Creeks. This conglomerate almost certainly extends into Junction Creek as float was noted in the lower reaches. Lateral persistance on this scale may indicate sheet flow conditions.

Conglomerate appears to grade laterally into massive medium and coarse sandstone between Mt Watson and the Mole Tops.

2.4 AGE AND DEPOSITIONAL ENVIRONMENT

Processes associated with metamorphism have obscured much of the small scale sedimentary structure, therefore environmental interpretation is necessarily limited. However, some inferences can be made.

The nature of the sedimentary associations, the intimate relationships between individual packages of each,

and the probable dominance of sedimentary mass flow mechanisms under the influence of gravity indicate a subaqueous environment of deposition. Such features as already outlined are all common to a deep sea fan setting similar to that outlined by Walker (1979). Several workers concerned with the origin of the Torlesse have suggested a similar setting. These include MacKinnon (1980, 1983), Carter et al. (1978), Howell (1981), Webby (1959) and Hicks (1981). Others have shown that not all of the Torlesse sediments were deposited in deep water, including Andrews (1974), Andrews et al. (1976), Beggs (1980), Bradshaw (1972), and Brodie (1953). The problems of provenance and environment of deposition of the Torlesse are outside the scope of this project. However composition of conglomerates does indicate that a significant component of the sediments was of sialic continental derivation.

No fossils have been identified within this study area, nor any evidence of bioturbation. Torlessia has been identified from immediately south and east by G. McLean (pers. comm.) and to the northeast by J.K. Campbell (pers. comm.). This suggests an Upper Triassic age for these rocks.

2.5 THE HAAST SCHIST ZONE

By definition the Haast Schist - Torlesse zonal boundary is the TZ-I/IIA isotect. This position is arbitrary as there is neither a structural break, nor a fundamental change in rock composition, nor geological history across the boundary. An east to west traverse of the Torlesse and Haast Schist Zones is a prograde section through metasediment and rare metabasites of pumpellyite-actinolite, greenschist and amphibolite facies.

The main changes associated with increasing textural grade are the attenuation and progressive transposition of bedding into schistosity, the loss of delicate sedimentary structures, and thus of younging, progressive increase in

the development of mineralogic segregation and increasingly common mesoscopic folding. Also loosely associated with increasing textural grade are changes in the dominant mineral assemblages (Section 3.1.2). As metamorphic grade increases new minerals crystallize, including actinolite, biotite, garnet, hornblende and oligoclase. Crystallization of new phases is accompanied by the replacement of others eg. pumpellyite, actinolite, stilpnomelane and detrital plagioclase.

2.5.1 Lithologies

During fieldwork the Haast Schists were subdivided informally, into greyschist and greenschist. Unlike the division between the Haast Schist and Torlesse Zones, this classification is based on fundamental compositional differences. Classification into greyschist and greenschist also transcends the sedimentary associations, as no difference in either mechanisms or environment of deposition is implied.

(a) Greyschist

By volume greyschist constitutes the bulk of the Haast Schist Zone in this region. Greyschist includes rocks of all four sedimentary associations previously described. In this region, lateral stratigraphic continuity is most clearly demonstrated in greyschist of TZ-IIB between Mt Maling and Junction Creek. Here exposure is good due to high elevation, steep relief and a relatively small proportion of bush cover.

Compositionally the greyschists are broadly quartzo-feldspathic. Analyses of the weight percentage of the various oxides by Reed (1958) shows SiO_2 in the range 64-78 %, Al_2O_3 11.4-18.03 %, FeO 2.34-5.04 %, Na_2O 1.10-5.7 %, K_2O 0.3-4.93% and variable proportions of the other main oxides, although never greater than 4 %. Molecular norms are in the range qtz 24.3-36.0 %, or 1.5-31.0 %, ab 10.5-40.5 %, an 2.5-10.0 %, c (corundum) 1.0-10.9 %, en 4.0-6.4 %, fs

1.4-6.2 %, with variable proportions of the remaining normative minerals, but all less than 2 %.

(b) Greenschist

Greenschist is limited in distribution and forms a much smaller proportion of the total rock volume than does greyschist. As with the greyschists attenuated bedding can be seen, indicating a sedimentary origin. Overall composition suggests these metasediments are of andesitic volcanoclastic derivation. Contacts between greyschist and greenschist are not obviously tectonic. In several instances segregation laminae and schistosity were observed to run parallel to the contact for distances of several metres (the limit of exposure). Here any tectonic juxtaposition must be pre-metamorphic. In that area between Mt Dorothy, Downie Creek, and David Saddle, green quartz-poor metasediments are in conformable sedimentary contact with grey quartz-rich metasediments.

Generally the greenschists are characterised by much lower quartz content and higher albite, epidote and chlorite contents when contrasted with the greyschists. Reed (1958) performed analyses of the major oxides and normative analysis on three "chlorite" schists from the Haast Schists of southeast Nelson. Weight percentages of the major oxides are: SiO_2 52.5-58.4 %, Al_2O_3 12.1-18.5 %, Fe_2O_3 2.94-8.7 %, FeO 4.48-8.80 %, MgO 1.69-7.0 %, CaO 2.5-6.26 %, with variable proportions of the other oxides, all less than 5 %. Molecular norms are in the range qtz 12.9-20.6 %, or 2.0-12.0 %, ab 19. -39.5 %, an 12.5-29.5 %, fs 2.0-8.2 %, mt 3.3-9.8 %.

CHAPTER THREE

D_1 AND D_2 DEFORMATION

3.1 METAMORPHISM

3.1.1 Introduction

Two metamorphic events have contributed to the formation of pumpellyite-actinolite and greenschist facies schist of the Haast Schists in this region. Turnbull and Forsyth (in press) were first to recognise the existence of two schistosities, and related the second of these to the Alpine Fault metamorphism. Sheppard et al. (1975) suggested that shear heating on the Alpine Fault was responsible for outgassing of radiogenic argon and the observed K/Ar age pattern. There is a general pattern of increasing age with distance from the Alpine Fault.

Originally Reed (1958) recognised only one phase of metamorphism (Triassic-Jurassic). However, Reed's work was petrographic rather than structural and his sample density in the Glenroy Valley, where the obliquely intersecting surfaces are most obvious, was sparse.

The early (M_2) event was a regional metamorphism associated with compressive tectonics probably during latest Triassic and early Jurassic times. M_3 was dynamothermal in nature, and was associated with deformation in the Alpine Fault Zone. Two isograds (biotite and garnet) and three isotects (TZ-I/IIA, IIA/IIB, and IIB/IIA) were mapped. These surfaces represent a combination of the influence of both metamorphisms. The isograds are significantly modified with respect to those of Reed (1958), Bowen (1964) and Turnbull and Forsyth (in press).

It should be noted that the chlorite zone includes rocks of both pumpellyite-actinolite and greenschist facies. The Facies boundary is not defined in terms of mineral isograds or isotects used in this study.

3.1.2 Petrography

The results of petrographic work undertaken in this study are in broad agreement with those of Reed (1958). In the field, the metasediments of this region were subdivided into quartz rich greyschist and quartz poor greenschist. On the basis of thin section petrography the dominant mineral assemblages within the chlorite, biotite and garnet sones were identified. In the chlorite zone the dominant assemblage is quartz-albite-sericite-and the epidote family. Minor minerals include chlorite, pumpellyite (Reed, 1958), allanite, piemontite, sphene, zircon, tourmaline, actinolite, haematite, apatite, magnetite, illmenite, stilpnomelane, calcite and carbonaceous material.

In the biotite zone the dominant assemblage is quartz-albite-muscovite-chlorite or the epidote family, $\pm$ biotite. Minor minerals include all those of the chlorite zone except pumpellyite, as well as occasional apatite.

In the garnet zone the dominant assemblage is epidote- albite-quartz-chlorite or biotite, $\pm$ garnet and/or hornblende. Minor minerals include oligoclase, sphene, zircon, tourmaline, calcite, apatite, magnetite, illmenite, haematite, and carbonaceous material. Most of the greenschists sampled also lie within the garnet zone. The dominant assemblage in the greenschists is epidote-chlorite-albite-quartz-muscovite, $\pm$ hornblende and/or garnet. Minor minerals include calcite, magnetite, illmenite, haematite, sphene and biotite.

3.2 NOMENCLATURE OF DEFORMATION

The Haast Schists of southeast Nelson have been subjected to a multiphase deformational history. Correlation of the timing of structural events with the schists of Marlborough and Otago and the Southern Alps is not attempted. However, the terminology adopted for this study is similar to that used by McLean (1986) for the adjacent Lewis Pass area.

TERMINOLOGY

Deformational Period	Metamorphism	Schistosity	Folds
D_1	-	-	F_1
D_2	M_2	S_2	F_2
D_3	M_3	S_3, brittle shear fabric	F_3, F_4

In this scheme there is no M_1 event, M_2 being the first recognised metamorphism. Therefore there is no S_1 schistosity, S_2 being the first recognised. For the purposes of discussion in this thesis the D_4 deformation of McLean (1986) is included in D_3. Therefore D_3 here includes F_3, F_4, S_3 and S_4 of McLean. S_4 is equivalent to the late brittle shear fabric described in this study. These four features appear to be forming synchronously but at different structural levels within the Alpine Fault Zone, therefore F_4 and the brittle shear fabric overprint F_3 and S_3 (as uplift and unroofing cause the downward migration of the brittle field through the rock mass).

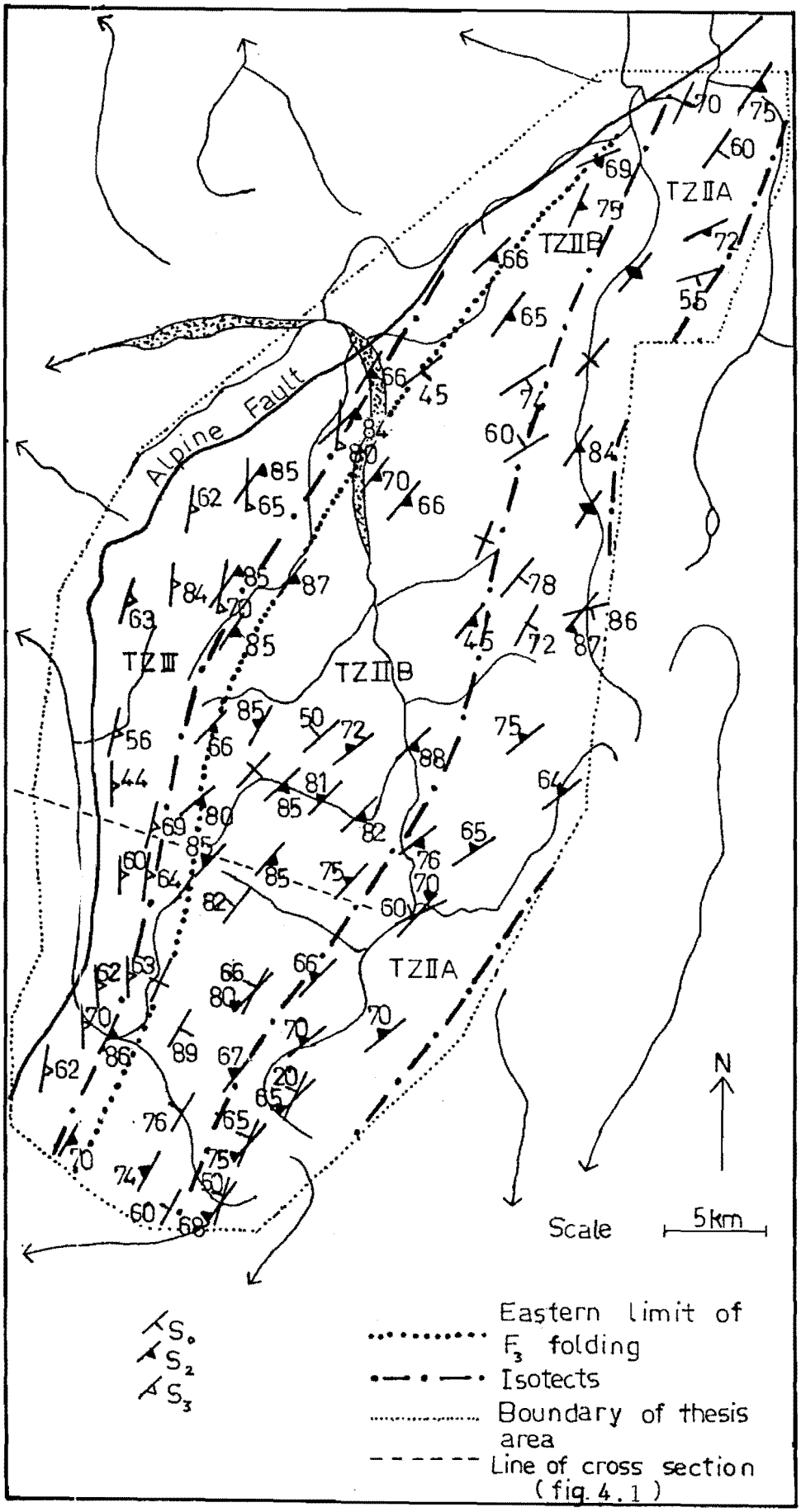

FIG 3.1 Simplified sketch map showing the general stucture within the study area

3.3 DEFORMATION ASSOCIATED WITH THE D_1 AND D_2 EVENTS

3.3.1 The D_{1-2} Structural Grain

The D_2 structural grain (see fig. 3.2) runs northeast-southwest and is largely unaffected by the Alpine Fault on a regional scale. In the south across Trig FZ Ridge D_2 structures parallel the Alpine Fault, trending at approximately 030°. Northward across the upper Glenroy River D_2 structures swing clockwise through an angle of 10-15° to a northeasterly trend which is maintained throughout the remainder of the region outside of the Alpine Fault Zone. Thus the D_2 trend approaches the north-south Glenroy section of the Alpine Fault obliquely from the northeast. D_2 structures include S_2 schistosity, the attitude of bedding, F_2 folds in bedding, and the TZ-I/IIA and TZ-IIA/IIB isotects.

The attitude of S_2 is only casually related to the trend of M_2 isotects. Where the isotects swing from northeast to east-northeast in S_2 schistosity does not, crossing these at an acute angle. Strain in metamorphism has not produced large rotation of the stratigraphy in the horizontal profile. Stratigraphy runs uninterrupted along strike through the TZ-IIA and TZ-IIB isotects. It appears likely that bedding had suffered sufficient rotation prior to metamorphism such that it lay dominantly within the extensional field of M_2 strain. Bedding is oriented subparallel to schistosity generally, therefore its early rotation occurred about an axis which lies within the S_2 plane. Macroscopic reversals of younging are present. The possibility of macroscopic F_2 folding and/or pre F_2 folding is discussed in Sections 3.5.1 and 3.5.4. Structural stacking by tectonic sliding may have been important in deformation prior to metamorphism, although no slides have been identified in this study. Turnbull and Forsyth (in press) describe a tectonic slide in the Spenser Mountains, just outside this study area.

FIG. 3.2 Panorama illustrating the structural trend (D_2) in the upper reaches of Burn Creek. The view is from Emily Peaks, looking southwest towards the Matakitaki-Glenroy Divide. Strike ridges which reflect a combination of S_2 schistosity, sedimentary stratigraphy and late brittle shear surfaces are prominent in this and other parts of the study area. Ridges and depressions are cored by metapsammite and metapelite respectively.

In adjacent areas macroscopic tight to isoclinal folding and early faulting/tectonic sliding have been identified (see Johnston, in press; Turnbull and Forsyth, in press; Campbell and McLean, 1985). Axial planes of these folds and axial planar cleavage are roughly on strike with the S_2 surface in this study area.

Some water polished stream exposures in Sunset Valley and Burn Creek exhibit structures which appear to predate S_2 schistosity particularly in the mudstone-siltstone association. Small rootless mesoscopic folds, brittle and brittle-ductile shears appear to be related to syn-sedimentary deformation and are included within D_1.

3.4 M_2 METAMORPHISM

3.4.1 Introduction

M_2 metamorphism is responsible for development of the bulk of the pumpellyite-actinolite and greenschist facies Haast Schist of this region. Those rocks deformed in M_3 metamorphism were crystalline M_2 schists of TZ-IIB and higher prior to M_3.

Structural relationships suggest that M_2 is related to deformation during the Rangitata I Orogeny (of Bradshaw et al., 1980). This is supported by K/Ar dating by Sheppard et al. (1975) in this region. Ages range from 6 to 143 m.y., and increase with distance away from the Alpine Fault and the zone of M_3 metamorphism.

S_2 schistosity is the dominant surface east of a line defining the eastern limit of F_3 folding (fig. 3.1) first described by Turnbull and Forsyth (in press). Schists in which S_2 is the only penetrative schistosity reach biotite grade in mineralogy. In a few samples biotite is being replaced by chlorite, although only in a small percentage of grains. Retrograde metamorphism in M_2 schists is rare and may relate to M_3 overprint.

3.4.2 Development of S_2 Schistosity

One of the major effects of M_2 metamorphism was the formation of S_2 schistosity. Development of this penetrative surface is closely associated with finite strain in M_2. The textural zonation scheme is a system whereby schists may be subdivided into mappable units, and is based on the progressive development of schistosity. Thus increasing textural grade reflects increasing finite strain (see Section 3.5), cf. Norris and Bishop (1985).

Processes involved in the development of S_2 schistosity include crystallization, recrystallization, pressure solution and possibly grain boundary sliding. S_2 is first seen in mudstones of Textural Zone I, as a weak slaty cleavage. Sandstones may display a weak fracture cleavage. Across the TZ-I/IIA isotect S_2 becomes a more or less penetrative slaty cleavage. In TZ-IIA individual sand grains have suffered little strain or pressure solution. Unstable grains such as plagioclase are often replaced by sericite, chlorite and epidote. Similarly the fine grained matrix in sandstone is totally reconstituted into sericite, chlorite and epidote in TZ-IIA. Schistosity is defined by pressure solution lamellae, and preferred orientation of sericite. Pressure solution lamellae are surfaces of concentration of residual carbonaceous material and other opaques such as haematite, magnetite and illmenite. Quartz grains are not generally recrystallized (other than that inherited from metamorphic rock fragments). Pressure solution along S_2 cleavage planes and the development of pressure shadows tends to give quartz grains a slightly elongate shape parallel to S_2. Schistosity planes wrap around and anastomose between sand grains, as does the preferred orientation of sericite grains. Sericite in pressure shadows and replacing unstable grains tends to show little dimensional preferred orientation.

Although development of S_2 is more rapid in mudstone than sandstone, the same processes operate. Finer grainsize

and more carbonaceous-micaceous composition make the above processes more effective in mudstone.

Deformation is more intense with increasing textural grade. In TZ-IIB individual sand grains are less distinct. The S_2 surface is still best defined as slaty cleavage. Pressure solution of quartz grains is more advanced and pressure shadows more pronounced, often linking sand grains. Quartz veins are strongly deformed (see Section 3.5.2). Small folds of bedding are tight to isoclinal with attenuated limbs (e.g. UC10647, UC10653, UC10665). Rotation of quartz veins, deformation of conglomerate cobbles, and microfabric, together indicate that S_2 schistosity formed parallel to the XY plane of finite strain during coaxial deformation.

Processes in TZ-IIA and IIB are dominated by grainsize reduction, grains being restricted to the dimensions of spacing of S_2 schistosity planes. In TZ-IIIA compositional layering has developed, usually as attenuated and boudinaged quartz veining, or as grain aggregates linked by pressure shadows. Metapsammite and metapelite are difficult to distinguish, although the higher carbonaceous content of metapelite tends to give it a darker colour.

There is evidence of strongly non-coaxial deformation in the M_2 microfabric. In particular quartz aggregates show little tendency to develop any marked degree of crystallographic preferred orientation.

The progressive development of S_2 schistosity in this study area is similar to that reported from the Martinsburg formation in Eastern Pennsylvania by Woodland (1982).

3.4.3 Biotite "Cross Mica" Fabric

The biotite isograd is located approximately in the centre of Textural Zone IIB. In the area between the biotite isograd and the eastern limit of F_3 folding, biotite crystals in metapsammite show a remarkable lack of

dimensional preferred orientation. This "cross mica" fabric is the result of a single period of nucleation and growth, and is defined by long axes and basal planes of biotite oblique to S_1 schistosity. Features which recur in all samples exhibiting this fabric include:

(a) Well developed dimensional and crystallographic preferred orientation (parallel schistosity) where S_2 is closely spaced, especially in fine grained samples.

(b) Poor dimensional and crystallographic preferred orientation in coarse grained samples, and in particular within quartzose domains between schistosity planes. Basal sections of biotite, giving good optic axis figures, are common in thin sections perpendicular to schistosity.

(c) There is no preferred sense of vergence between basal planes of biotite and S_1 schistosity.

(d) There is evidence of basal slip in some biotite crystals with basal planes oblique to S_2.

(e) Biotite is most common close to the edges of quartzose domains, and close to well developed schistosity planes which anastomose about the quartzose domains (fig. 3.3).

(f) Where the basal planes of biotite are oblique to schistosity these terminate against schistosity without crossing it. This is part of the evidence for pressure solution on schistosity planes.

The S_2 surface was active during nucleation and growth of biotite in these schists. There is no clear evidence of simple shear parallel to S_2 schistosity. Crystallographic orientations displayed by biotite could indicate slightly mimetic growth during a low strain thermal

FIG. 3.3 Thin section (UC 10664). Biotite "cross mica" fabric in metapsammite of TZ IIB. UC10664 was collected from the ridge separating the catchments of Burn Creek and the Glenroy River (metric grid reference M30 4621 8943). Plane polarized light. Field of view 2.5 x 1.7mm.

FIG. 3.4
F_2 folds in TZ IIA mudstone-siltstone association between the Matakitaki River and its stern branch. The pencil is aligned vertically parallel to the F_2 axial plane and approximately normal to the fold axis.

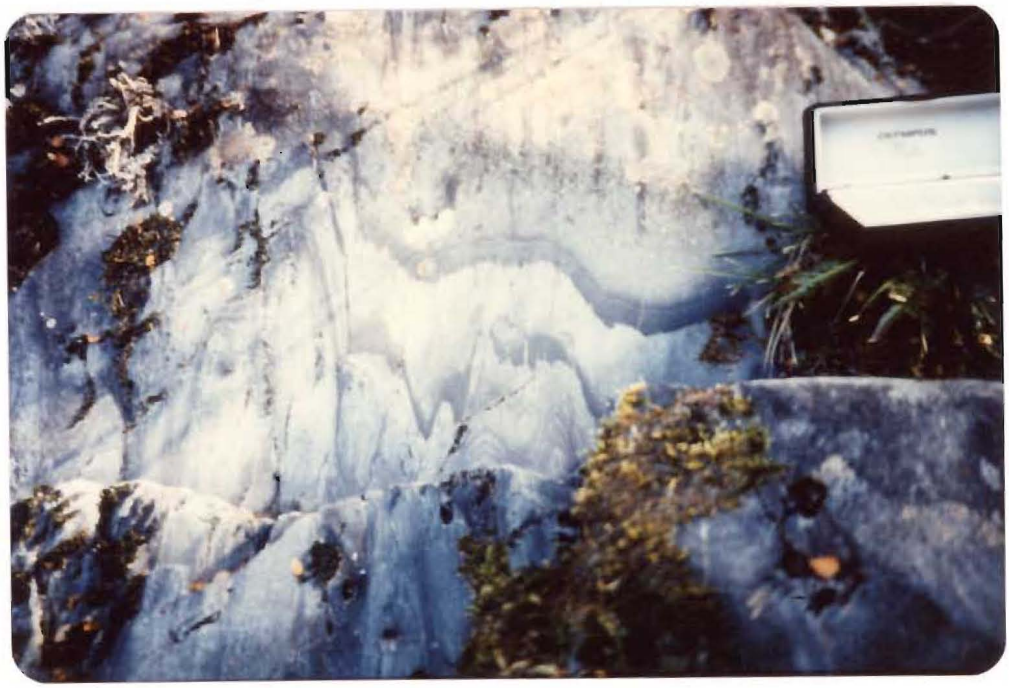

FIG. 3.5 F_2 folds in Burn Creek. Vertical S_3 schistosity is axial planar to the folds with fold axes sub-horizontal and parallel to the direction of view. Note that graded bedding is still preserved in these TZ IIB semischists.

M_3 overprint. Associated reactivation of the S_2 surface (see Section 4.4.3) would inhibit the extension of basal planes across S_2 schistosity. It should be noted that biotite is not common in TZ-IIB schists of other regions [exception - Murray Hawkes, 1980] underlain by Haast Schist.

A list of samples which display typical "cross mica" fabric is included on Table 1. Cross micas can be seen in figs. 3.3 (UC10664).

3.5 STRAIN IN D_2

3.5.1 F_2 Folding In Bedding

Strain in D_2 is recorded primarily by S_2 schistosity. The S_2 surface is axial planar to F_2 folds (see figs. 3.4 and 3.5), although it is not restricted to those localities with mesoscopic folding. Folding is poorly developed for the most part, although F_2 folds occur throughout the study area. F_2 folds are most common in the west where the textural grade of the schists is higher, and particularly common in the mudstone-siltstone, and thin bedded associations.

Mesoscopic F_2 folds in TZ-IIA have rounded profiles and closure is tight to isoclinal. Flexure slip appears to have been the dominant mechanism here. In TZ-IIB and IIIA fold hinges are more angular, and show the effects of flow by cleavage slip. In most cases these folds probably developed initially by flexure slip.

Mesoscopic F_2 folds exhibit reversal of S_o-S_2 vergence across the hinge. The folds are asymmetric with fold vergence reflecting the macroscopic vergence of S_2 and S_o in any particular area. In this context it is notable that bedding rarely shows a greater dip than schistosity. At the macroscopic scale any reversal in dip direction of bedding is also accompanied by a reversal in dip direction of S_2, a reversal of S_0-S_2 vergence, of mesoscopic F_2 fold

vergence and a reversal a younging direction in several instances (unequivocal indications of younging direction are not common). The bedding-schistosity intersection lineation (LS_1/S_o) generally plunges at a shallow angle to the southwest. Bedding- schistosity vergence reversals usually result in schistosity-lineation vergence reversals (as seen in the horizontal profile). Reversals of younging and the various vergence relationships indicate the likely presence of macroscopic folds, either F_2, or from an earlier phase now obscured by M_2 metamorphism. If macroscopic folds are present then the lack of turn arounds (in hinge zones) of stratigraphy indicates these folds have axes with shallow plunges.

Stereographic projection of schistosity, bedding and their intersection lineation (figs. 3.8, 3.9, 3.10, 3.11) demonstrates that the lineation clusters about the F_2 fold axis. Axes of mesoscopic F_2 folds have a low plunge towards the southwest in general, the only notable exception being that area about Burn Creek Bivy, where the axes plunge gently towards the northeast (fig. 3.8(b)). Lineations cluster less strongly in Textural Zone IIA than in Textural Zones IIB and IIIA. In TZ-IIA rocks have suffered less finite strain. The angle between bedding and schistosity is wider on average in TZ-IIA as a result.

Stretching lineations defined by deformed conglomerate pebbles are coincident with the F_2 fold axis and the bedding-schistosity lineation. It is assumed that the X axis of the strain ellipsoid of D_2 deformation is parallel to the F_2 fold axis throughout the region.

3.5.2 Deformed Quartz Veins

Metamorphism of greenschist and pumpellyite-actinolite facies occurs under a temperture and pressure range sufficient to allow ductile deformation in rocks of quartzo-feldspathic composition. Although mesoscopic folding of bedding is curiously poorly developed, folds as strain indicators are common. Quartz veins are particularly common

in the greyschists, either randomly oriented, and/or as spaced (often conjugate) sets. No regionally consistent dominant sets have been recognised. The initial orientation of veins is usually oblique to schistosity, which is invariably axial planar to F_2 folds of veins. Axes of these folds have no preferred rake angle on the S_2 surface. Folding is a response to compression perpendicular to S_2. The operative mechanisms are folding by cleavage slip, pressure solution on cleavage planes and single layer buckling of veins where there is a viscosity contrast between veins and the bulk rock.

Folding is best developed in veins at high angles to S_2. These buckles are assumed to be geniune folds. The degree of flattening observed in folded veins is consistent with that of deformed conglomerates in nearby localities. Quartz veins are not perfectly planar when they are introduced. Many irregularities amplify during progressive deformation to become folds, or become indistinguishable from folds (cf. Shelley, 1968).

Those veins which have a low initial angle of incidence on S_2 generally do not develop folds, but often exhibit attenuation and boudinage.

Quartz veins appear to be of variable age, as there is considerable variance in the degree to which veins of the same orientation are deformed at any one locality. Thus F_2 folds must also be of variable age. Vein introduction was probably by hydraulic fracture, and fracture infilling, a process which may have been active throughout M_2 metamorphism.

On passing from psammite to pelite single quartz veins often show abrupt changes in attitude and thickness. The veins are rotated towards bedding in the pelite and are reduced in thickness, reflecting a greater degree of flattening in the pelite. Rapid rotation of veins in pelite gives these rocks a better segregated appearance particularly in TZ-IIIA.

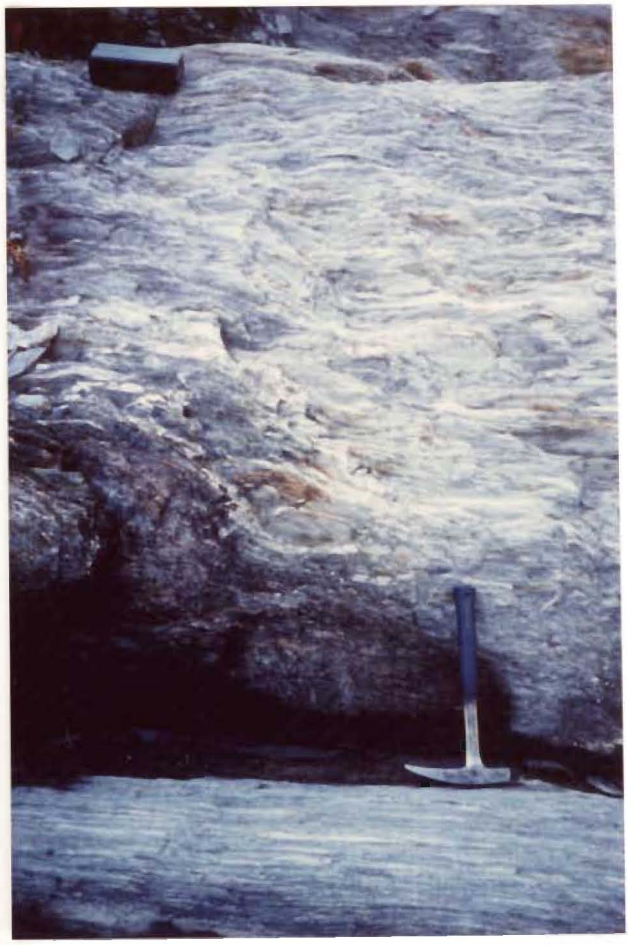

FIG. 3.6
Deformed, clast-supported conglomerate of TZ IIB, 1 km northwest of Burn Creek Bivy. Cobbles and pebbles are flattened in the plane of S_2 schistosity. Note the stretching lineation which plunges gently northeast(left). Figs and 3.7 show a sharp contrast in the degree to which cobbles are flattened over the zone between the handle and head of the hammer. Metric grid reference, M30 4623 8936

FIG. 3.7 Deformed, clast-supported conglomerate (top) and pebbly mudstone (bottom) of TZ IIB. Length to width ratios of cobbles (centre) are as high as 20:1. Pebbles within the mudstone are less deformed than those in the adjacent clast-supported conglomerate. Same locality as above.

3.5.3 Deformed Conglomerates

Deformed conglomerates (see figs. 2.1, 3.6, 3.7), which are present at a number of localities in the study area, provide a reasonable estimate of strain during D_2. Conglomerates are progressively flattened and stretched with increasing textural grade. The textural grade in all lithologies is closely related to the imposed finite strain. Flattening is invariably within the plane of S_2 schistosity, and the stretching lineation is parallel both F_2 bedding fold axes and the S_2-S_o intersection lineation.

In TZ-IIA a,b,c ratios of deformed cobbles are low. On the Mahanga Range, Mt Ella and at the head of the Matakitaki River East Branch, ratios are approximately 4:3:2 or lower. In TZ-IIB ratios are somewhat higher. At Mt Watson average ratios vary from 3:2:1 to 8:3:1 between different outcrops. Conglomerate float in Peak Stream exhibit ratios which are again variable and reach 8:3:1. At the three wire walkway across the Matakitaki River near its junction with Burn Creek ratios are as high as 10:5:1. West of Burn Creek Bivy (close to the TZ-IIB/IIIA isotect) average ratios range from approximately 12:5:1 to 20:10:1. In TZ-IIB deformation in D_2 has produced ellipsoidal pebbles by general strain which was probably coaxial in nature.

3.5.4 D_2 Strain - An Overview

The deformation which produced S_2 schistosity, F_2 folding of veining and bedding and strained conglomerates was penetrative, but also inhomogeneous. Deformation was coaxial with S_2 schistosity parallel to the XY plane of the finite strain ellipsoid.

Textural grade is closely related to the average finite strain of any area in question. The regular pattern of isotects indicates increasing finite strain towards the west, and has been produced, at least in part, by differential uplift, probably in at least two phases.

Schistosity is not parallel the isotects in plan view, nor is there any reason to assume parallelism in cross section. Isograds and isotects probably dip at moderate angles towards the east and southeast, although control in mapping is not sufficient for precise determination.

The schistose sequence of southeast Nelson is 20 km in a maximum width across strike. This is probably indicative of the true thickness of schists, however it is unlikely that the true stratigraphic thickness is this large. Processes such as isoclinal folding and tectonic sliding were almost certainly important in assembling the thick pile of sediments, which must have totalled more than 20 km before ductile strain in M_2. Bedding had been rotated prior to M_2 metamorphism such that it generally lay within the extensional field of the M_2 strain ellipsoid. Whether this rotation occurred in D_2 or an earlier D_1 deformation is difficult to determine from the evidence within this study area. Mapping to the northeast (see Campbell and McLean, 1985) suggests steeply plunging isoclinal folds were generated during the early stages of D_2 deformation.

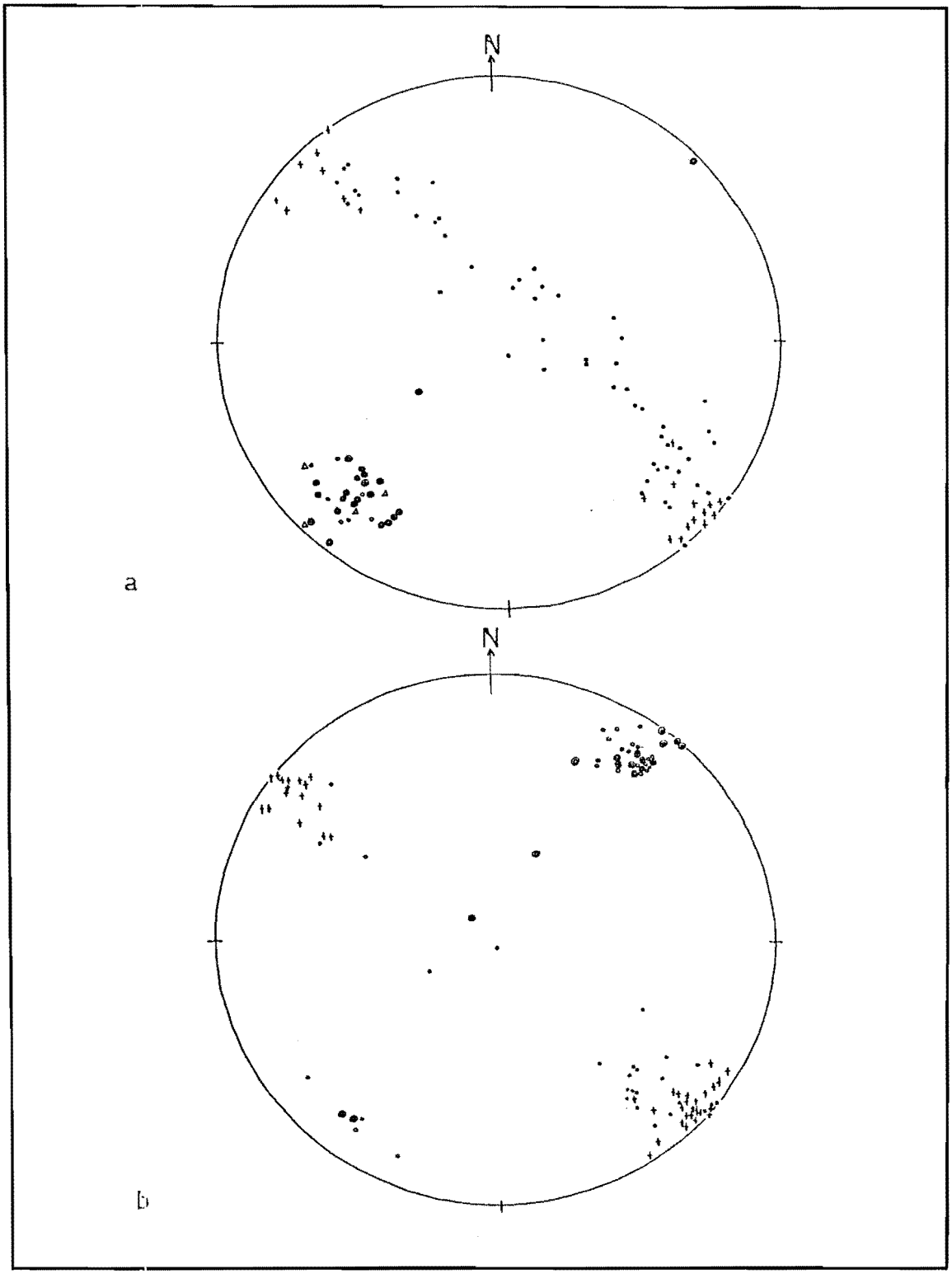

FIG 3.8 Structural Data Legend-see pg

a. Mt Burn and Lower Burn Creek

b. Burn Creek Bivy

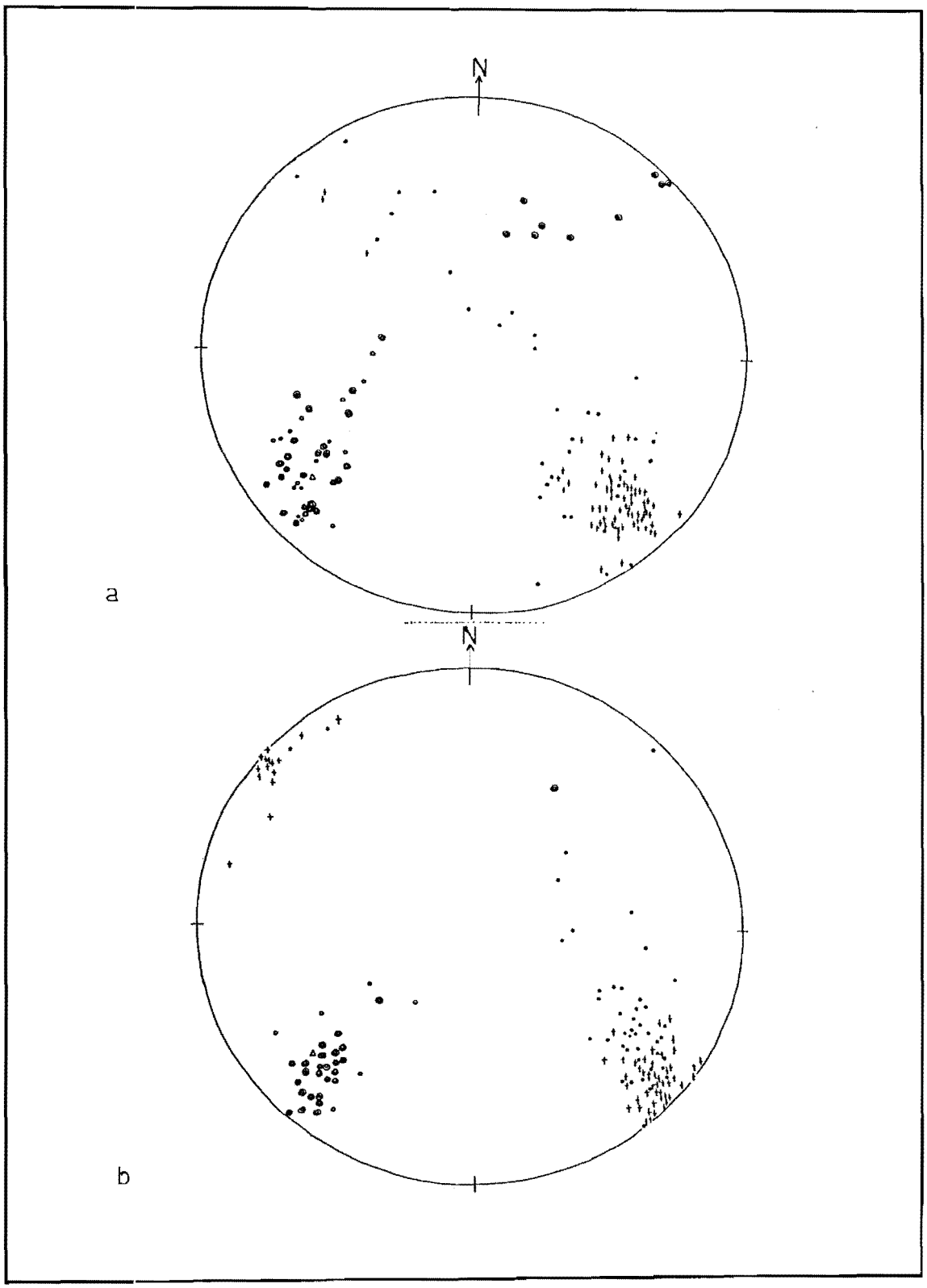

FIG 3.9 Structural Data Legend-see pg

a. Upper Glenroy Valley, Trig FZ Ridge, and Spenser Mts west of Gloriana Peak.

b. Bobs Hut (Upper Matakitaki Valley)

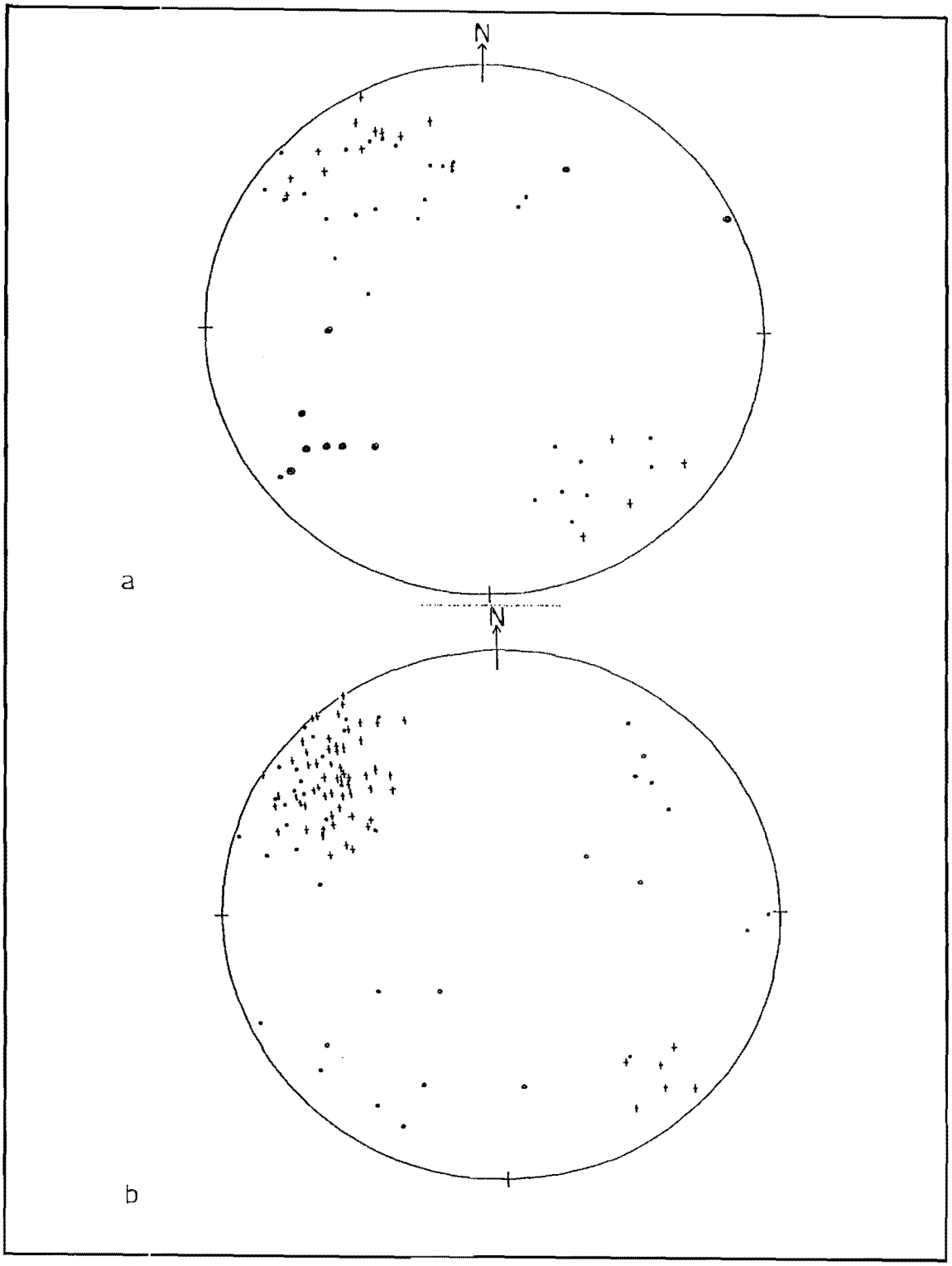

FIG 3.10 Structural Data Legend–see pg

a. Ella Range between Mt Ella and the Mole Tops

b. Mahanga Range north of Mt Windward

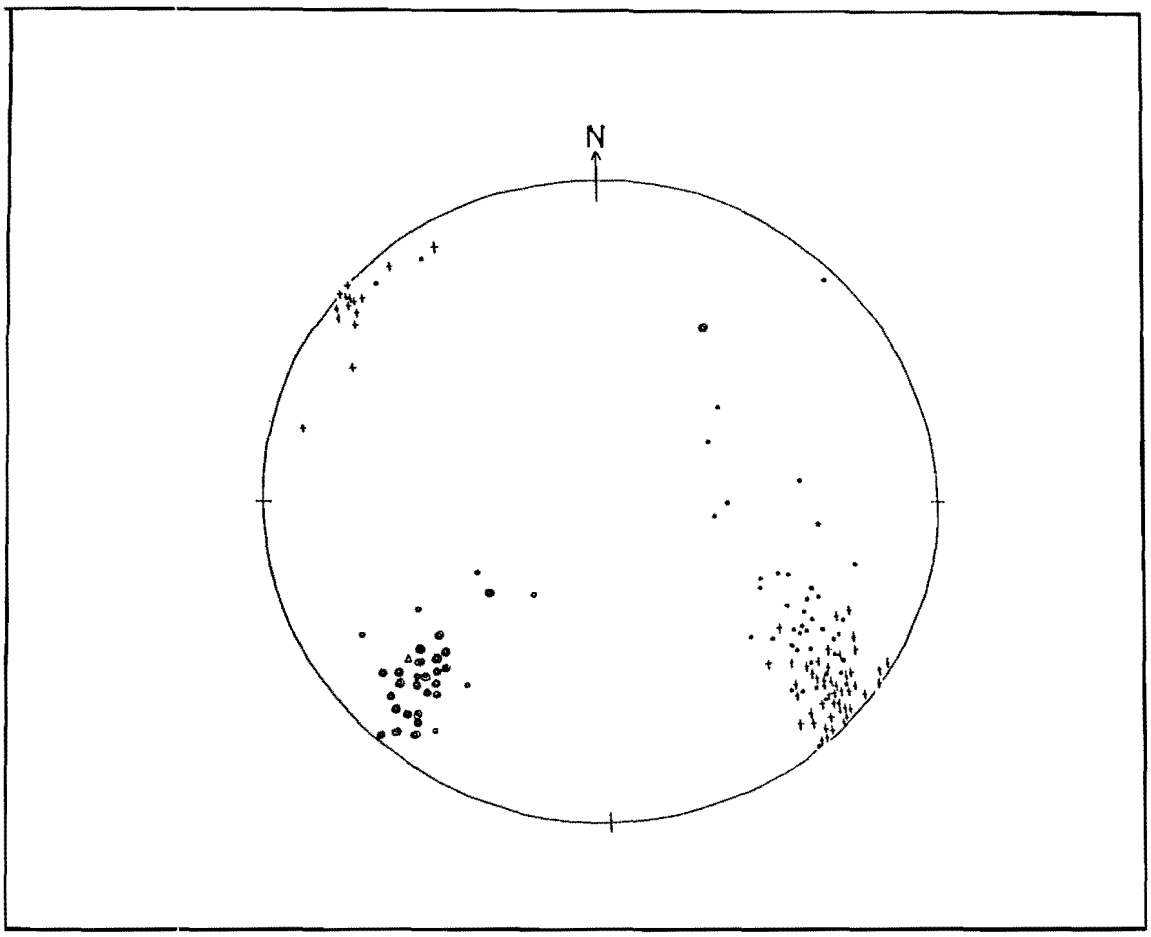

FIG 3.11 Structural Data Sunset Valley

Legend

- poles to bedding
- poles to S_2 schistosity
- $L^{S_2}_{S_0}$ calculated
- $L^{S_2}_{S_0}$ measured
- stretching lineation
- F_2 fold axes (mesoscopic)

CHAPTER FOUR

D_3 DEFORMATION

4.1 M_3 METAMORPHISM

Textural evidence of M_3 metamorphism in thin section is restricted to an elongate zone adjacent, and subparallel to the Alpine Fault. This zone extends from Trig FZ Ridge at the southern extent of mapping, to the Mole Tops in the north, and is coincident with the zone of F_3 folding.

The mineral assemblage at the eastern limit of S_3 cleavage is dominated by those phases crystallized during M_2. Biotite in these rocks may be of M_3 origin (see Sections 3.4.3, 4.4.3). There is little evidence of low grade M_3 retrogression in M_2 schists outside that zone where S_3 cleavage/schistosity is present. Retrogression in M_3 appears to be late stage, and restricted to the zone in which S_3 is present. Several samples show retrogressive chlorite replacing biotite.

Metamorphism in M_3 reached garnet grade greenschist facies and possibly amphibolite facies, as sample UC10689 contains oligoclase feldspar (N.B. Reed, 1958 considered albite within the garnet zone of south Nelson to be retrogressive from oligoclase). Those samples containing garnet in thin section are listed in Table 1. Chemical analyses of garnets from quartzo-feldspathic schists of Trig FZ Ridge by Reed (1958) indicates these are almandine. Samples containing hornblende-actinolite are also listed in Table 1.

M_3 metamorphism and F_3 folding are associated with elevated temperature and enhanced ductility produced in strain/shear heating in the Alpine Fault Zone (Section

4.6.2) Potassium-Argon dating by Sheppard et al. (1975) suggests these schists were at the Argon retention limit some 6 mys ago. Unroofing of M_3 schists has occurred as a result of uplift on the Alpine Fault.

Although the ages of schists in southeast Nelson reach a minimum of 6 mys this does not imply that metamorphism at depth has necessarily halted, or even reached its climax. The Alpine Fault is still active and metamorphism is an ongoing event associated with the Alpine Fault.

4.2 DEFORMATION ASSOCIATED WITH THE M_3/F_3 EVENT (D_3)

4.2.1 Introduction

D_3 deformation is intimately associated with the Alpine Fault and thus the Indo-Pacific plate boundary. This involves metamorphism, ductile deformation including folding, and brittle shear. There is ample evidence suggesting strong vertical tectonics during the ongoing Kaikoura Orogeny especially over the last 6 mys (Sections 4.6.1, 4.7.3(b)). The Alpine Fault is the most significant single feature within the plate boundary zone. A large proportion of deformation within this zone occurs at the Alpine Fault. The following Sections are a discussion of D_3 deformation, deformational mechanisms, and structural trends which are related to processes within the Alpine Fault Zone.

4.2.2 General D_3 Structural Trends

As structures formed in D_2 are regionally consistent in trend, D_3 can be appraised in terms of its impact upon D_2 structures.

South of the study area the Alpine Fault strikes at 050-055°. Just north of Lake Daniels the strike swings towards the north, finally running north-south in the Glenroy Valley. At Branch Creek the strike begins to swing

FIG 4.1 THE ALPINE FAULT : ESE - WNW CROSS SECTION IN THE UPPER GLENROY

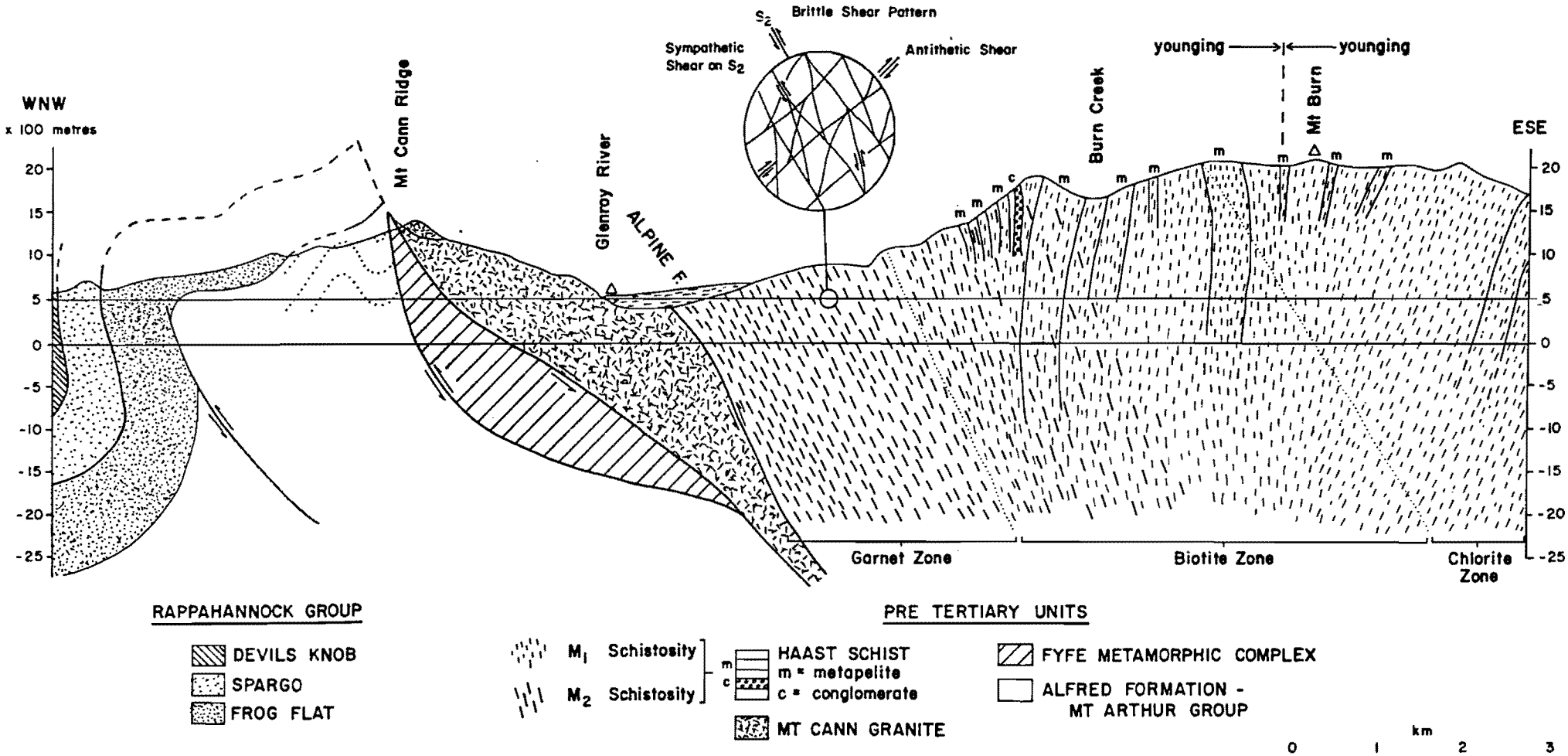

by Campbell, Cutten and Rose

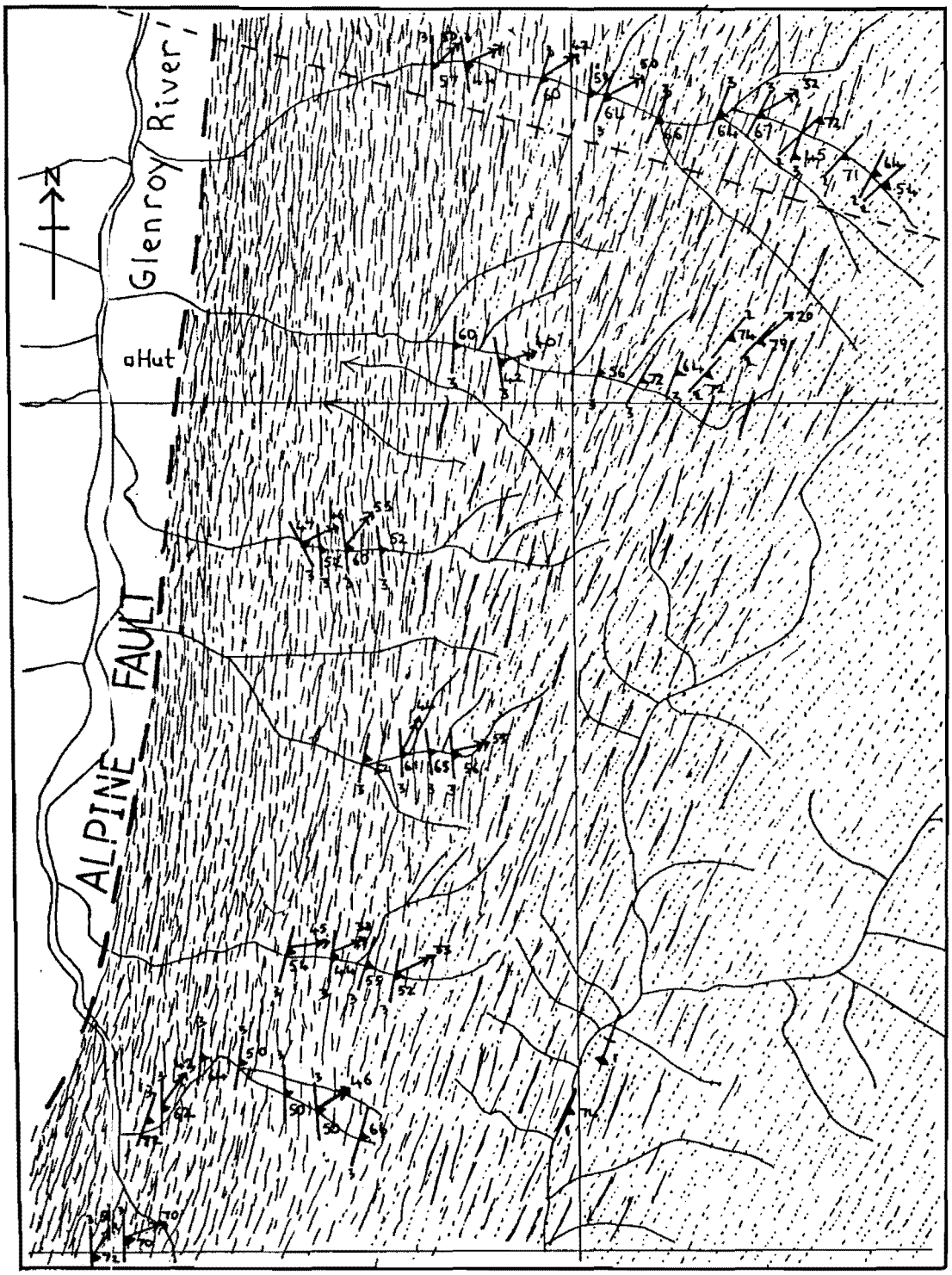

FIG 4.2 Scale 1 km

Sketch map of D_2 and D_3 strutural trends within the zone of M_3 metamorphism

D_2 trend

D_3 trend

------ Line of crosseclion (fig 4.1)

back towards the dominant northeast direction, this being completed at the head of the Glenroy River's East Branch. The trends of the garnet isograd, the TZ-IIB/IIIA isotect and the eastern margin of the F_3 fold belt are subparallel to the Alpine Fault, the fold belt attaining its maximum width at the head of Nardoo Creek. F_3 axial planes and S_3 schistosity diverge from the Alpine Fault, but in the opposite sense to that expected for a dextral shear zone. This divergence is discussed in Section 4.4. S_3 schistosity deviates from the strike of the Alpine Fault by as much as 25° (north- northeast). The dip of S_3 close to the Alpine Fault is assumed to reflect the attitude of the fault itself. The relation of S_3 to the finite strain ellipsoid is discussed in Sections 4.3.1, 4.3, 4.4.

Brittle shear in D_3 is widespread and regionally penetrative on the macroscopic scale. Brittle shear can be subdivided into shear within the Alpine Fault Zone (Section 4.7.3), and shear to the west of the Alpine Fault Zone (Section 4.7.4).

The combined effects of brittle and ductile strain across the Alpine Fault Zone are thought to cause drag of the D_2 structural trend. The drag pattern is outlined in Section 4.6.3.

4.2.3 Development of S_3 Schistosity

The S_3 schistosity is intimately associated with deformation in, and adjacent to the Alpine Fault Zone. Bedding and S_2 schistosity are essentially parallel, and are rotated on the limbs of F_3 folds. These folds have axial planes which strike between 350° and 025°. Fold vergence is almost invariably dextral. S_3 schistosity is axial planar to F_3 folds. Hinge zones rapidly develop crenulation cleavage westward towards the Alpine Fault. With rotation of the limbs and reconstitution in hinge zones of F_3 folds attenuated bedding and S_2 schistosity become difficult to distinguish from S_3. Primary sedimentary layering is still recognised at some localities within 1 km of the Alpine

Fault in the Glenroy Valley as extremely attenuated layers defined by relict carbonaceous material. Figs. 4.5, 4.9, 4.13 show F_3 folds with S_3 axial planar cleavage and a form surface defined by S_1, S_o and veins.

Development of S_3 crenulation cleavage follows a pattern similar to that described by Cosgrove (1976). In the Glenroy Valley the early S_2-S_o anisotropy is obliquely inclined to the direction of maximum compression (cf. a mirror image of figs 14 and 17, Cobbold et al., 1971; Plate 2 a,b,c, Cosgrove, 1976; fig. 11, Patterson and Weiss, 1966) in the horizontal profile (see also Section 4.4). The S_2-S_o anisotropy is also oblique to the likely vector of convergence across the Alpine Fault Zone (the horizontal projection of the transport direction). Where S_2 has been rotated quickly in folding, crenulation is less well developed, with S_2 now in the extensional field (on limbs of F_3 folds).

In the south of the study area along Trig FZ Ridge F_3 folds are rare and S_3 crenulation cleavage is less well developed than further north in the Glenroy Valley. Here S_2 is apparently rotated towards S_3 without suffering intense F_3 folding and crenulation. Variations in the style of D_3 deformation are discussed in Section 4.4.

4.2.4 M_3 Microfabric and Microstructure

Close to the Alpine Fault in the Glenroy Valley the Haast Schists display a selection of features commonly associated with high finite strain. These include:

(a) asymmetric pressure shadows (of Simpson and Schmid, 1983) about resistant grains.

(b) deformed and recrystallized quartz aggregates with moderate to strong crystallographic preferred orientation.

(c) quartz rodding and other mineral lineations.

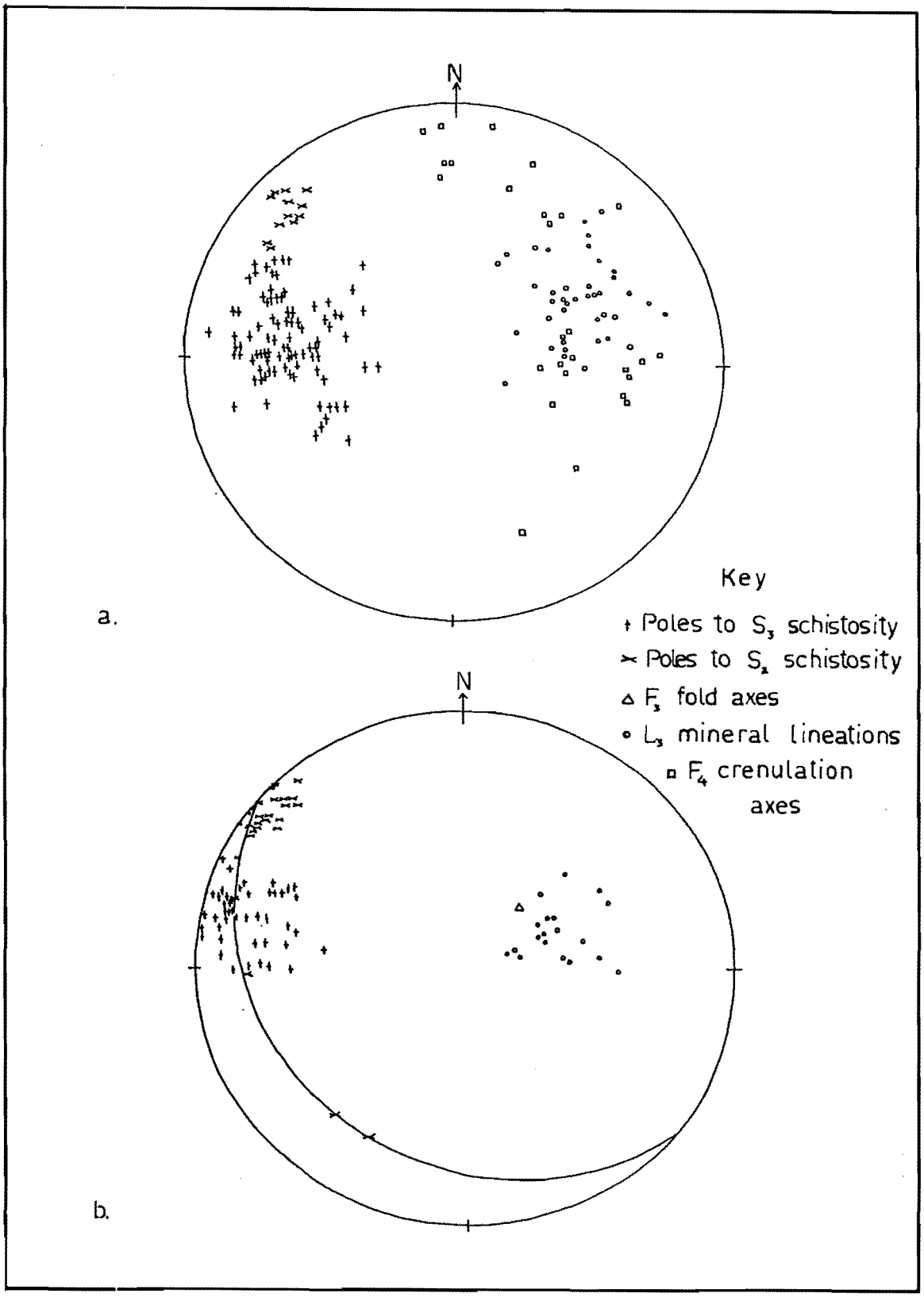

FIG 4.3 Structural Data Equal area progection

a. Middle Glenroy Valley

b. Nardoo Tops

COMMON MICROFABRICS	UC SAMPLE NUMBERS
Ribbon Quartz	10667, 10671, 10674, 10686, 10687, 10689, 10690, 10691, 10708, 10709, 10712, 10720 10721, 10722.
Strong Quartz Crystallographic Preferred Orientation	10632, 10633, 10635, 10668, 10683, 10686, 10687, 10689, 10691, 10696, 10699, 10700 10704, 10705, 10707, 10708, 10709, 10710, 10711, 10720, 10721.
Subgrained Quartz with Grain-Boundary Preferred Orientation Oblique to Schistosity	10631, 10633, 10667, 10668, 10686, 10687, 10690, 10691, 10708.
Shear Bands causing Grainsize Reduction	10641, 10699, 10702, 10705, 10706, 10710, 10712, 10719, 10721.
Deformed Calcite	10636, 10666, 10672, 10673, 10676, 10684, 10701, 10702, 10708, 10709.
Mica "Fish"	10667, 10687, 10704, 10705, 10706, 10707.
Feldspar Porphyroblasts	10631, 10633, 10686, 10689, 10691, 10708, 10709, 10712, 10719.
Epidote Porphyroblasts	10635, 10666, 10678, 10688, 10708, 10709, 10710, 10711, 10719, 10720.
Garnet Porphyroblasts	10667, 10668, 10676, 10683, 10690, 10691, 10694, 10705, 10706, 10707, 10721, 10722.
S_3 Crenulation Cleavage	10634, 10637, 10642, 10645, 10669, 10671, 10677, 10678, 10679, 10680, 10692, 10695 10696, 10698, 10699, 10700, 10703, 10706, 10707, 10715.
Deformed Veins (Including Folding and Boudinage)	10638, 10639, 10640, 10647, 10648, 10653, 10654, 10659, 10665, 10669, 10670, 10671, 10675, 10677, 10678, 10679, 10680, 10682, 10690, 10692, 10693, 10695, 10714, 10715, 10716.
Linking of Quartz Grains through Amalgamation of Pressure Shadows	10644, 10649, 10650, 10651, 10652, 10655, 10656, 10658, 10660, 10661, 10716, 10717, 10718.
Typical Biotite "Cross-Mica" Fabric	10643, 10644, 10647, 10655, 10660, 10662, 10663, 10664, 10697, 10713.

TABLE 1

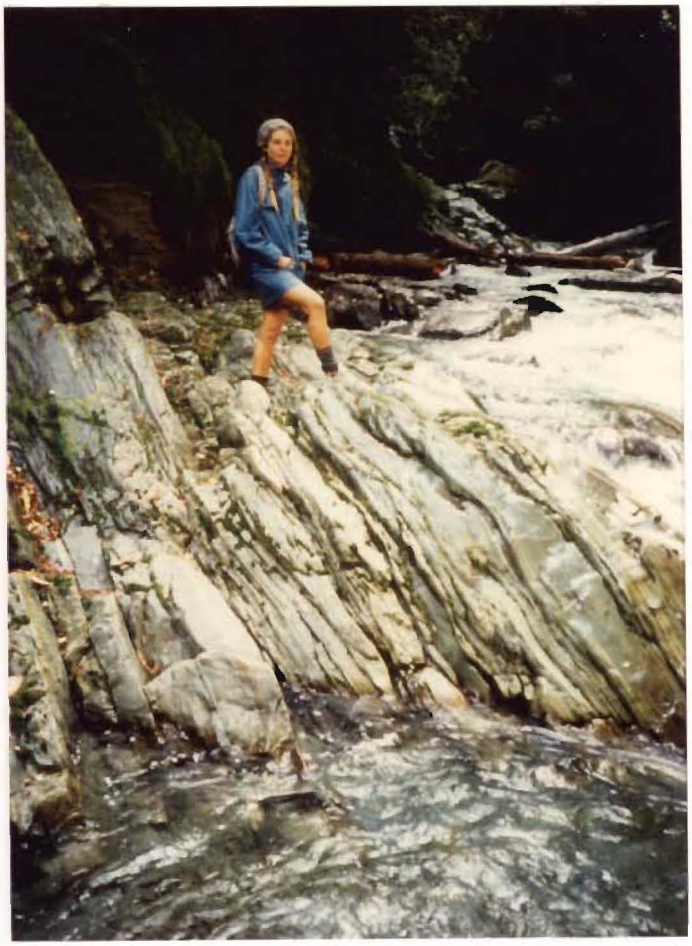

FIG. 4.4
Coarse layering parallels S_3 schistosity in quartz poor greenschist within the Alpine Fault Zone, Branch Creek.

FIG. 4.5
Tight S_3 folds in bedding, S_2 schistosity and early veining. S_3 schistosity/ crenulation cleavage is axial planar to these folds. F_3 folds of similar amplitude and wavelength are common, adjacent to the mylonitic zone between the points at which the Glenroy and Matakitaki Rivers cross the Alpine Fault trace.

FIG. 4.6
Rotated garnets in a boulder of amphibolitic schist, Branch Creek.

FIG. 4.7
S_3 crenulation cleavage approximately 2.5 km east of the mid point of the north-south striking section of the Alpine Fault.

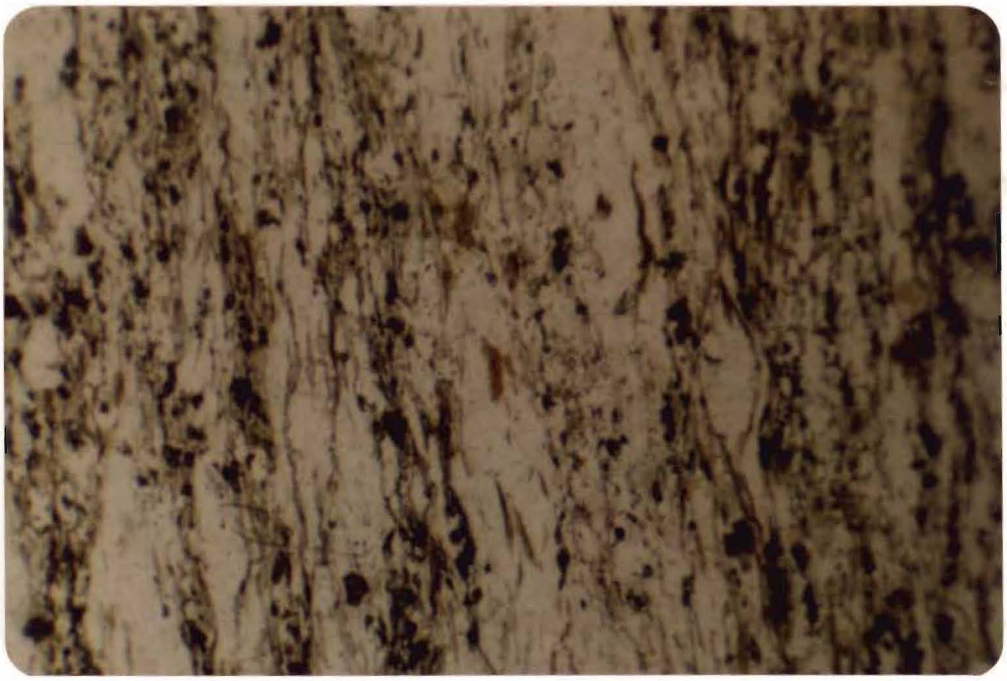

FIG. 4.8 Thin section (UC10669). S_3 crenulation cleavage in quartz-albite-biotite-muscovite schist. The section is cut parallel to the crenulation axes, perpendicular to S_3 (XZ plane of the strain ellipsoid). Micas exhibit a well defined dimensional preferred orientation with long axes parallel to S_3. Quartz has a well defined crystallographic preferred orientation (see Fig. in this sample. Plane polarized light. Field of view 2.5 x 1.7 mm.

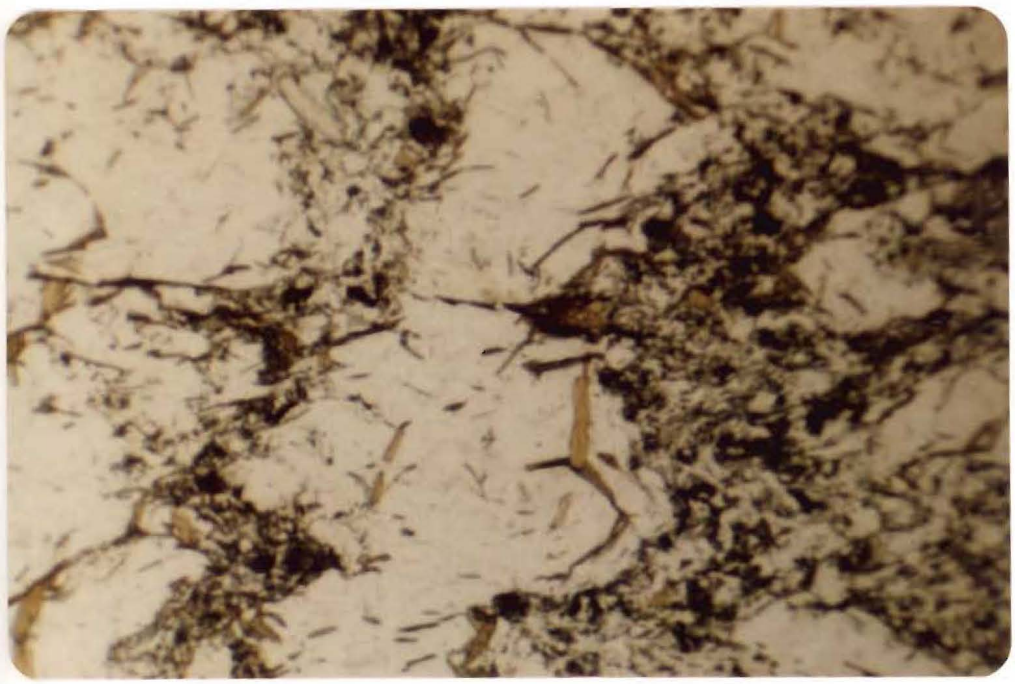

FIG. 4.6 Thin section (UC10669). S_3 crenulation cleavage. This section is cut perpendicular to the crenulation axes and to S_3 (horizontal). The surface being folded is S_2 schistosity. Lines of intersection between S_3 and the basal planes of biotite crystals are statistically parallel to the crenulation axes. Plane polarized light. Field of view 2.5 x 1.7 mm.

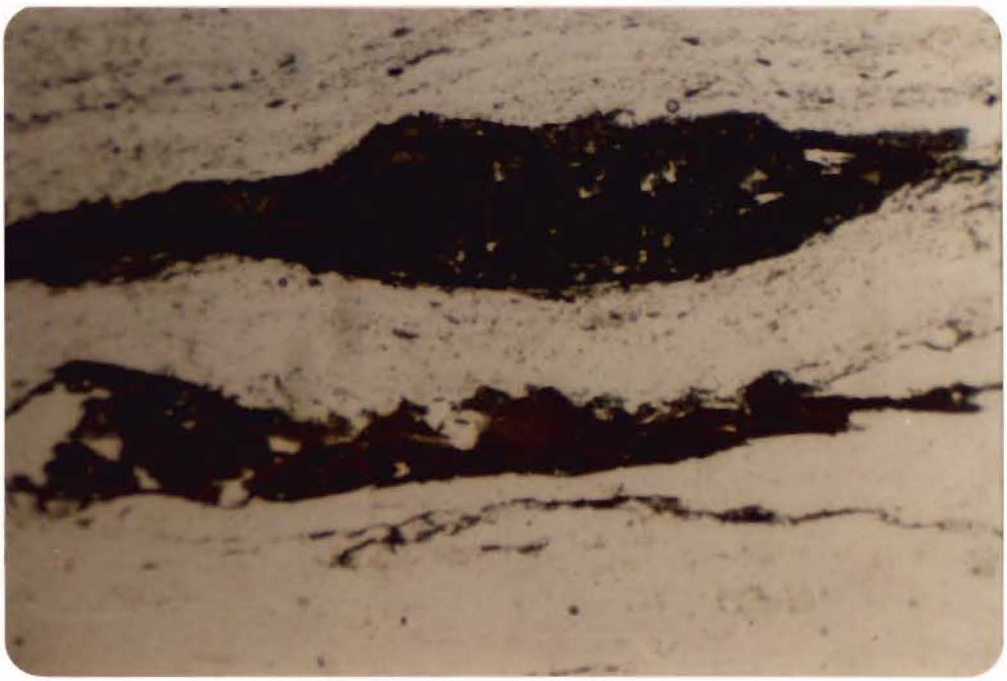

FIG. 4.10 Thin section (UC 10667). Augen mylonite from the Alpine Fault Zone on "Trig. FZ Ridge". Minerals present include garnet, hornblende, biotite, albite, quartz, calcite and retrogressive chlorite replacing biotite. High strain features include ribbon quartz, rotated garnets, biotite and hornblende "fish". Plane polarized light. Field of view 2.5 x 1.7 mm.

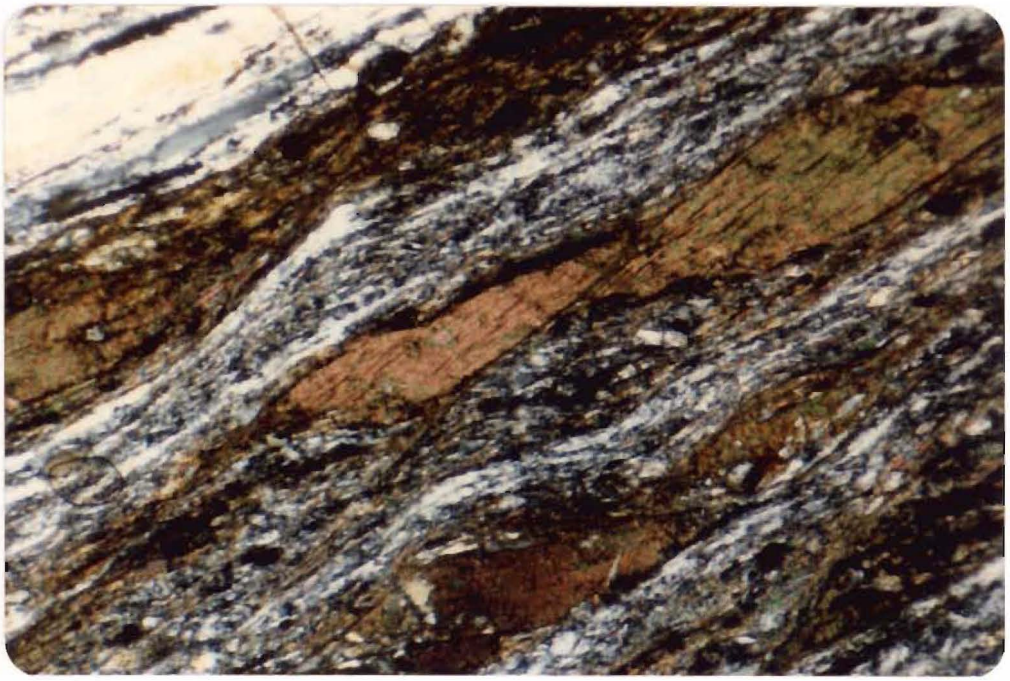

FIG. 4.11 Thin section (UC10707). Garnet-biotite-quartz-albite schist cut parallel to F_3 crenulation axes and perpendicular to S_3 schistosity. A mylonitic fabric is developed in this orientation. Sections cut normal to both S_3 schistosity and crenulation axes display tightly folded S_2 schistosity (grainsize reduction is obvious in sections of this orientation also). Cross-polarized light. Field of view 2.5 x 1.7 mm.

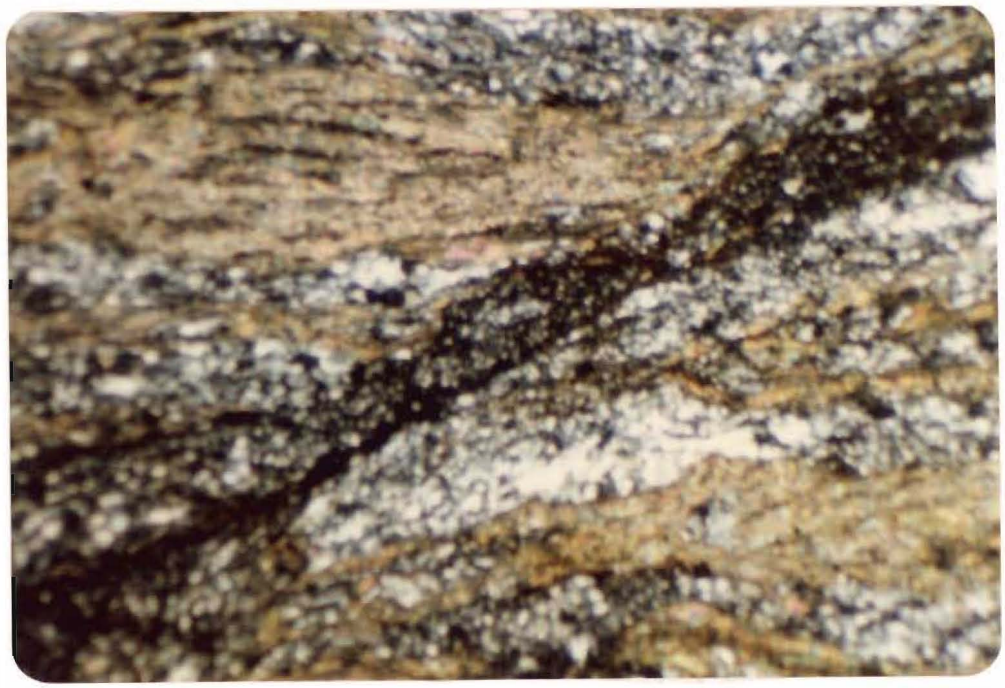

FIG 4.12 Thin section (UC 10704). A shear band cuts S_3 schistosity causing extreme grainsize reduction. This is superimposed on more general grainsize reduction associated with intense F_3 crenulation of S_2 schistosity. This thin section is oriented parallel to the F_3 axes and perpendicular to the S_3 schistosity. Cross polarized light. Field of view 2.5 x 1.7 mm.

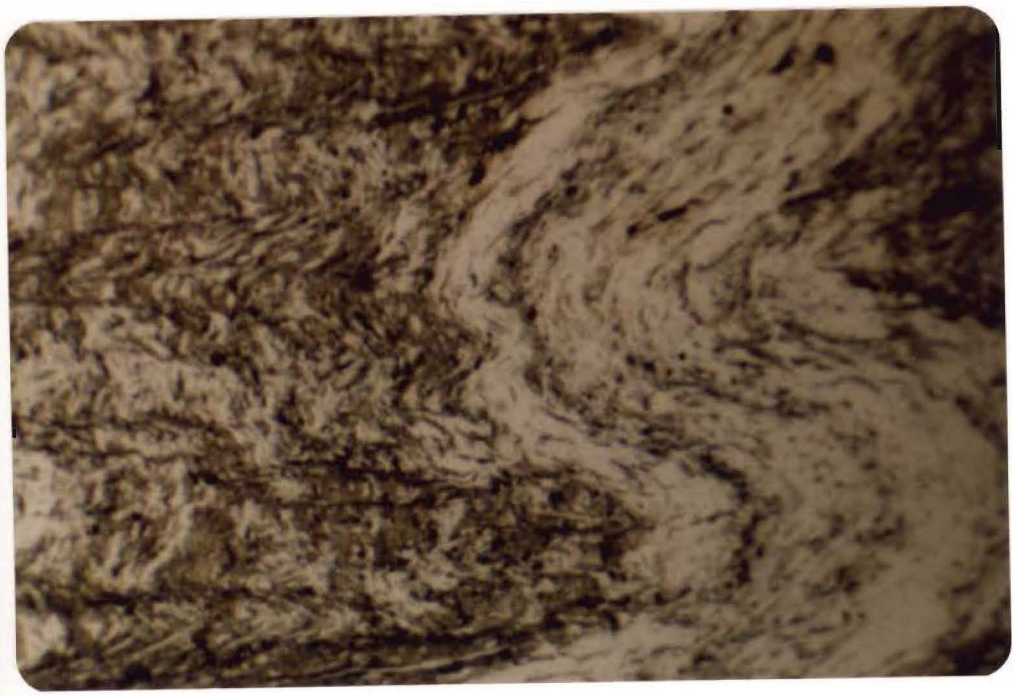

FIG. 4.13 Thin section (UC 10642). F_3 folds and S_3 crenulation cleavage. This section in perpendicular to S_3, and the F_3 fold axes. Plane polarized light. Field of view 2.5 x 1.7 mm.

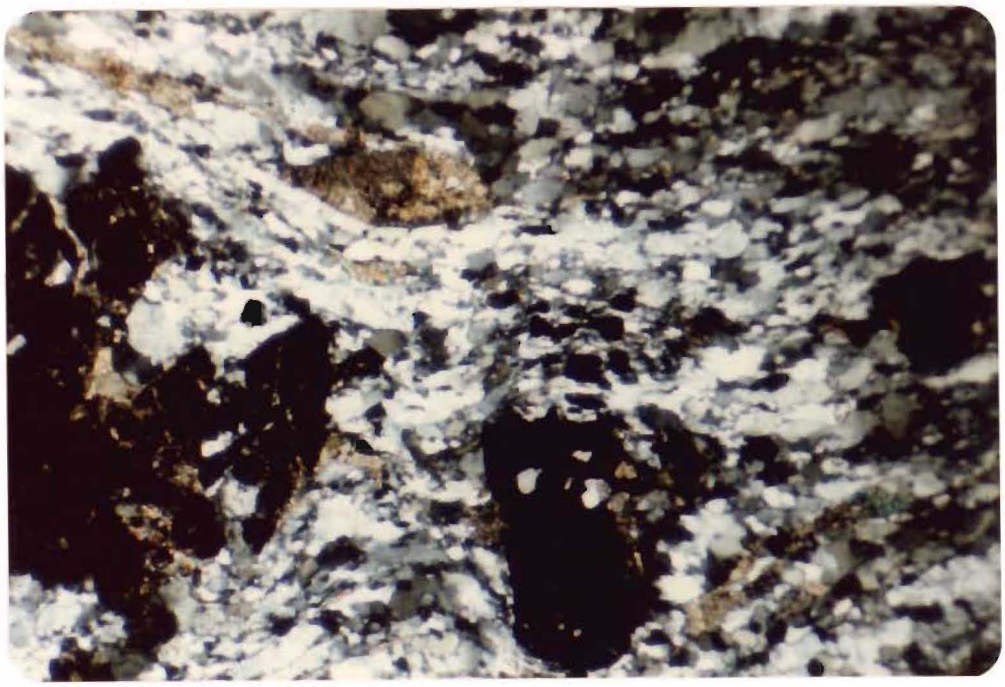

FIG. 4.14 Thin section (UC 10722). Garnet trails, mica "fish", ribbon quartz and recrystallized polygonal quartz in a mylonitic schist from the Alpine Fault Zone, Branch Creek. Cross polarized light. Field of view 2.5 x 1.7 mm.

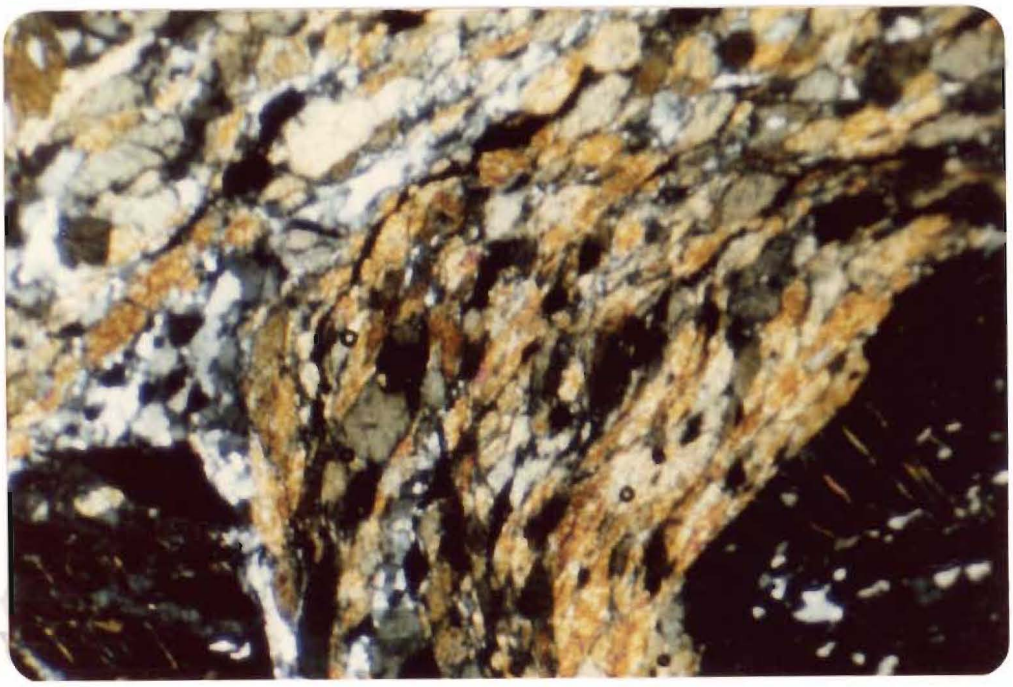

FIG. 4.15 Thin section (UC 10690). Garnet-hornblende schist from the Alpine Fault Zone. Hornblende, quartz and ilmenite are deformed and wrap around resistant garnet porphyroblasts. Cross polarized light. Field of view 2.5 x 1.7mm.

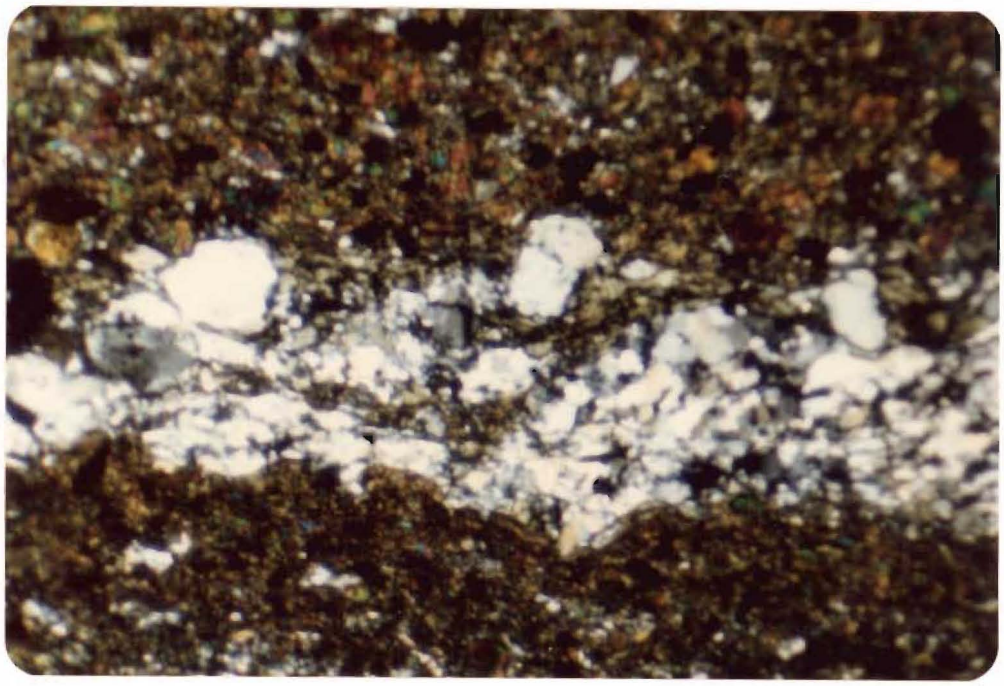

FIG. 4.16 Thin section (UC10711). Chlorite-epidote-quartz-albite greenschist from the Nardoo Tops at the head of Cascade Creek. Cross polarized light. Field of view 2.5 x 1.7 mm.

(d) ribbon quartz.

(e) twinned elongate calcite grains and grain aggregates.

(f) mica and hornblende-actinolite "fish" (of Lister and Snoke, 1984), see figs. 4.10, 4.11, 4.14.

(g) shear bands, see fig. 4.12.

(h) extensional crenulation cleavage (Platt and Vissers, 1979; Platt, 1984; Harris and Cobbold, 1985).

(i) F_3 microfolds and mesoscopic folding, see figs. 4.9, 4.13.

(j) rotated garnets, see fig. 4.6.

These features are consistently developed in similar orientations both with respect to each other, and to a fixed external coordinate system. Lineations and F_3 micro and mesoscopic fold axes lie within the S_3 plane. F_3 folds are most easily observed in the YZ section (as the fold axes parallel X). The remaining features are most easily recognised in the XZ section.

4.2.5 Quartz Microfabric and Crystallographic Preferred Orientation in the Glenroy Valley

Crystallographic preferred orientation of quartz is well developed in many of the M_3 schists sampled (see Table 1). There is a notable correlation between the strength of crystallographic preferred orientation and the extent to which quartz rodding and other mineral lineations are developed. In those samples with high proportions of fine grained phyllosilicate, well defined quartz crystallographic preferred orientation is developed only in phyllosilicate poor regions. These generally represent reoriented and

boudinaged quartz veins, and hinges of folds in veins. A high concentration of fine grained micas tends to inhibit development of strong quartz crystallographic preferred orientation, even though finite strain in phyllosilicate rich domains must be large. Grain boundary sliding, pressure solution of quartz, pinning of quartz grain boundaries by micas and basal slip in the micas are likely contributory factors in suppression of quartz crystallographic preferred orientation in these domains.

Where there is a large grainsize variation of quartz the finer grained zones tend to show considerably weakened crystallographic preferred orientation (e.g. sample UC10637). This is a characteristic property of shear bands and crenulation cleavage zones. Shear bands (Platt and Vissers, 1980; Platt, 1979; Harris and Cobbold, 1984) are narrow zones of very high strain, and in polyphase aggregates they are commonly zones of mixing. Several samples from the Alpine Fault Zone show mixing of quartz, chlorite, muscovite and biotite, and grainsize reduction in shear bands. Shear bands may take on a cherty, almost pseudotachylitic appearance. Here grain boundary sliding, and perhaps superplastic flow may be important (cf. Boullier and Gueguen, 1975). Those samples in which shear bands are developed are listed in Table 1.

Quartz crystallographic preferred orientation, and subgrain-grain boundary preferred orientation are useful in determining the sense of shear in a number of samples (in similar fashion to the Type II C and S surfaces of Lister and Snoke, 1984). All samples which show well defined subgrain-boundary preferred orientation also have strong crystallographic preferred orientation. The shear sense from the subgrain-boundary preferred orientation is invariably dextral reverse parallel to the quartz rodding and F_3 crenulation axes. Preferred orientation of subgrain boundaries is oblique to schistosity with variable angle but consistent vergence.

Most of the samples collected from the Glenroy area are not true mylonites, although some could be labelled protomylonite. High strain schist is perhaps a better description. Well defined C and S surfaces are generally absent. Extensional shear bands are common as is foliation boudinage. Curly schists (Wellman, 1955) occur close to the Alpine Fault from Trig FZ Ridge to Nardoo Trig. Shear bands, extensional crenulation cleavage and foliation boudinage contribute to the undulatory nature of S_3 planes in the curly schists.

4.3 STRAIN IN D_3

4.3.1 S_3 and the Strain Ellipsoid

S_3 appears to represent the approximate position of the XY plane of finite strain, and as such shows a systematic variation across the Alpine Fault Zone. The attitudes of F_3 axial planes swing with increasing finite strain toward the strike of the Alpine Fault. Figs 4.2 and 4.25 are an interpretation of this process and of the structure of the Alpine Fault Zone.

In thin section, microfabrics related to various states of strain are observed. Although S_3 is assumed to approximate the principle plane of the finite strain ellipsoid, quartz ribbon grains, and subgrain boundaries tend to show varying degrees of preferred orientation, usually oblique to S_3. Some of these may indicate intermediate states of strain on the grain or small grain aggregate scale, especially where minerals have recrystallized or are undergoing recrystallization during rotational deformation. In some cases there is evidence of shearing on S_3 indicating that S_3 may not be strictly parallel to the XY plane (cf. Ghosh, 1982), and could represent rotated and attenuated S_2 surfaces.

Towards the Alpine Fault S_3 becomes better defined with good mineral lineation, particularly where the schists

are of highest grade. Some of these rocks take on an amphibolitic appearance. In thin section schistosity is best defined in fine grained rocks.

F_3 fold and S_3 cleavage forming processes are important for any model of the tectonics of this region. These processes involve strain, which is observed on all scales of observation. The roles of F_3 and S_3 in the Alpine Fault Zone are further discussed in Sections 4.4, 4.6.

M_3 overprint of the S_2 surface is progressively more intense towards the Alpine Fault on any east-west traverse. In the east S_2 is dominant, but in the west D_3 strain is such that S_2 is transposed and finally lost in mylonitization at the Alpine Fault. The microfabrics previously described evolve progressively as M_3 intensifies towards the Alpine Fault.

The following Section (4.3.2) is an outline of theory on the development of quarts c-axis fabrics during strain, the uses of quartz fabric diagrams, and conclusions drawn from analysis of such patterns in samples from the Glenroy Valley.

4.3.2 Quartz c-axis Fabrics and Development of Crystallographic Preferred Orientation

(a) Introduction

Quartz is a relatively ductile mineral and is highly deformed in many natural shear zones. In order to better understand strain histories of such areas, considerable research has been directed towards gaining an understanding of the means by which quartz deforms.

(b) Theory

There are several theories, based on different criteria, which can account for the development of crystallographic preferred orientation in quartz aggregates.

One of the most widely quoted is that of Lister, Patterson and Hobbs (1978). This particular example uses the Taylor-Bishop-Hill analysis as a basis for computer modelling of the development of c-axis fabrics in model quartzites, and has frequently been applied to the study of quartz fabrics developed in shear zones.

The Taylor-Bishop-Hill analysis is based on Von Mises criterion which requires a minimum of five active, and linearly independant slip systems at the intragranular scale, before ductile deformation can proceed in a single phase polycrystalline aggregate. Grain boundary sliding and recrystallization are assumed to be insignificant. Each slip system constitutes a uniformly penetrative planar surface on the lattice scale, which can accommodate simple shear in two mutually opposing directions. Slip occurs by increments (Burgers Vector) controlled by lattice spacing. Single slip events are termed dislocations, and occur parallel to the Burgers Vector. Dislocations may climb between two discrete slip planes (dislocation climb). Slip is assumed to be homogeneous on a grain scale.

Lister, Patterson and Hobbs (1978) tested several combinations of slip systems on several model quartzites under a number of strain conditions. They found remarkable similarity between computer generated fabrics and many of those generated in both experimental and natural deformations.

Under conditions of plane strain, quartz aggregates deforming plastically suffer general rotation of c axes towards Z and away from X. c-axis girdles can be either symmetrically or asymmetrically disposed about the XY plane depending on whether strain is coaxial or non-coxial (Lister and Williams, 1979). The sense of asymmetry defines the sense of shear in non-coaxial deformation (Lister and Williams, 1979; Lister and Hobbs, 1978; Behrmann and Platt, 1982; Simpson and Schmid, 1983; Lister and Snoke, 1984).

Quartz responds quickly to imposed deformation and c-axis fabrics reorient with moderate strain under a new or rotated stress field. Coaxial overprint of a non-coxial fabric does not necessarily eliminate evidence of the early phase and a new symmetrical girdle or "skeletal" outline (Lister and Williams, 1979, fig. 13) often retains asymmetrically disposed maxima as a relict. Lister and Williams showed that the fabric "skeleton" is useful in defining girdle type c-axis distributions, and shear sense in non-coaxial deformation. Fabric skeletons are defined by lines connecting the c-axis maxima, and points of maximum curvature of contours on the fabric diagrams.

(c) Quartz c-axis Fabrics and D_3 Strain in the Glenroy Valley

As mentioned in Section 3.4.2 M_2 schists exhibit no strong crystallographic preferred orientation of quartz. Strain in M_2 is moderate to high as seen in a,b,c ratios of deformed conglomerate pebbles (Section 3.5.3). The line delineating the easternmost extent of F_3 folding also marks a westward transition into schists in which crystallographic preferred orientation of quartz is common (but not ubiquitous). Quartz crystallographic preferred orientation becomes better developed towards the Alpine Fault, paralleling the development of F_3 folding, S_3 schistosity and ultimately mylonitization (very close to the Fault). Finite strain in D_3 increases towards the Alpine Fault, and involves ductile deformation (Section 4.3.1).

Quartz c-axis fabrics were analysed using a Leitz Universal Stage on a Swift microscope, and the method of Shelley (1975, pp 57-63). Each sample was oriented so that the spatial orientation of c-axis fabrics can be compared with orientations of other microfabric data.

The strength of c-axis fabric clearly parallels development of mineral lineation, particularly quartz rodding. Where the fabric is well developed (e.g. samples UC10668, UC10633, UC10687) non-coaxial plane strain

(probably including a component of flattening) is indicated. Type I cross girdle fabrics and fabric skeletons (figs. 4.17, 4.18) are asymmetrically oriented about the lineation (approx. 060/50° northeast) and schistosity plane, indicating dextral reverse shear. Lineations appear to represent the transport direction (cf. Sibson et al. 1979, 1981) in a simple shear dominated environment. Other microfabric evidence (Section 4.2.4) also suggests the lineation is close to the axis of maximum extension.

Well defined girdles illustrating plane strain were obtained from UC10668, UC10633, UC10687, UC10669, UC10634, figs 4.17, 4.18, 4.20. More diffuse girdles, probably also produced in plane strain include UC10675, UC10678, UC10676, figs. 4.18(b), 4.19. In each case c-axes cluster about the YZ plane, with c-axis free areas about the X axis.

In order to test the assumption that quartz rodding lineations are equivalent to the X direction, quartz fabrics were analysed from 3 sections taken perpendicular to the lineation, F_3 crenulation axes, and S_3 schistosity. These showed plane strain c-axis distributions (see fig. 4.20). In the case of UC10669 the section parallel lineation and perpendicular schistosity also showed a plane strain pattern.

Sample UC10687 yielded a type 1 cross girdle fabric indicating non-coaxial plane strain with the opposite sense of asymmetry to that expected in dextral reverse shear. The most likely explanation for this discrepancy is that the sample was incorrectly oriented in the field, or during thin section preparation.

With respect to sampling it should be noted that no attempt was made to select quartzites for the purpose of measurement of c-axis fabrics. A number of oriented samples collected are too fine grained to allow reliable optical determination of quartz c-axis fabrics, but nevertheless are clearly highly strained (e.g. UC10698, UC10706). Others are of unsuitable composition. A number of samples which were

not oriented show well developed crystallographic preferred orientation of quartz (see Table 1) and strong mineral lineation. In each case crystallographic preferred orientation is most easily seen, using the sensitive tint plate, in sections parallel lineation and perpendicular schistosity.

Quartz rodding lineations tend to be most obvious in the coarser grained and layered amphibolitic schists. No attempt was made to bias sampling towards schists with strong mineral lineations (infact sampling was biased towards quartz poor greenschist).

In the Alpine Fault Zone there is a considerable variation in the degree to which quartz rodding is developed in any cross strike traverse. This may indicate either variation in shear strain, original grainsize or composition (e.g. metapelite vs metapsammite). Due to the problems outlined in Section 4.2.5 (on S_3 microfabrics) it is not possible to state categorically that rocks with well developed lineations and quartz fabrics are the more highly strained.

Sibson et al. (1979, 1981) argue that shear strain in mylonites of the Alpine Fault Zone can be related to post-Pliocene ductile deformation. They do not comment on whether related strain and general metamorphism, during this period, has affected the Haast Schists further east. For the Glenroy area my structural and fabric analysis shows that ductile strain related to Alpine Fault deformation is not restricted to the zone of mylonites, but extends as far east as the limit of F_3 folding and S_3 schistosity (fig. 3.1).

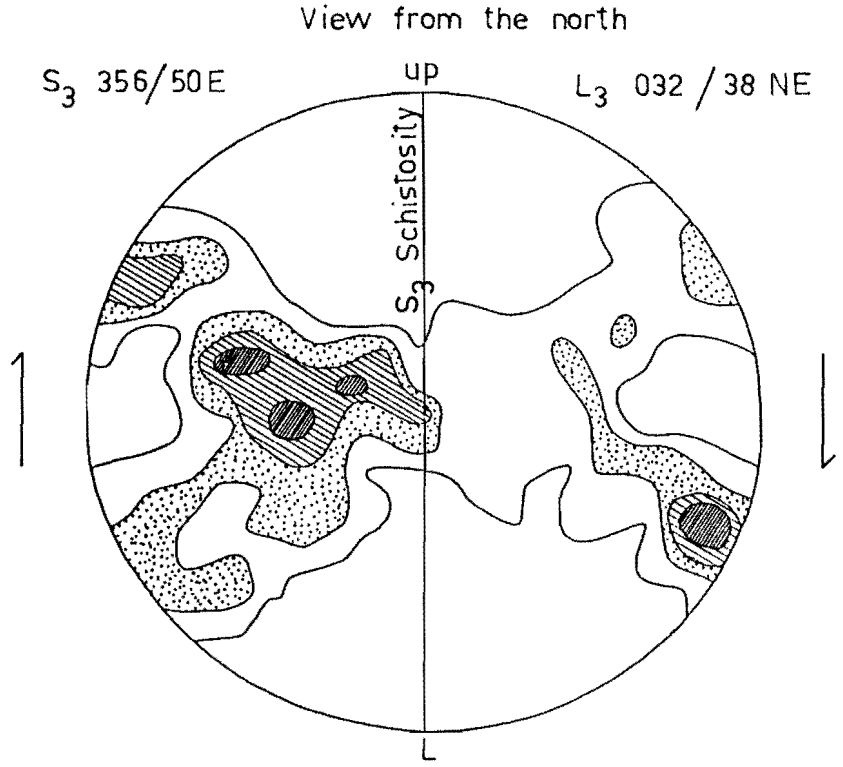

a. UC 10668 400 quartz C axes

Contours 1,2,3,4 % per 1% area

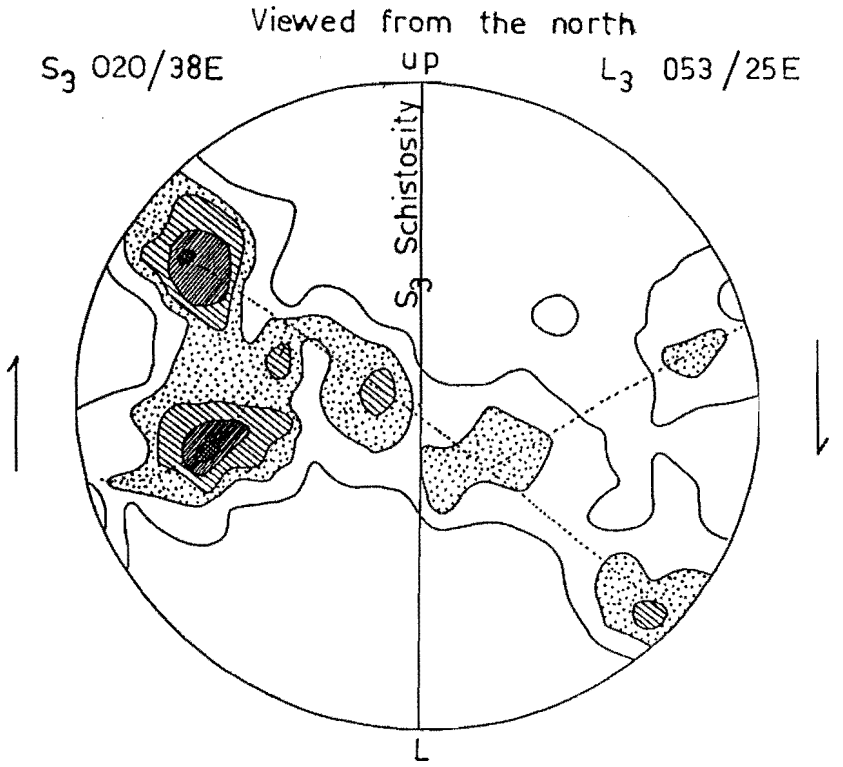

b. UC 10633 400 quartz C axes

Contours 1,2,3,4,5 % per 1 % area

FIG 4.17 Equal area projection

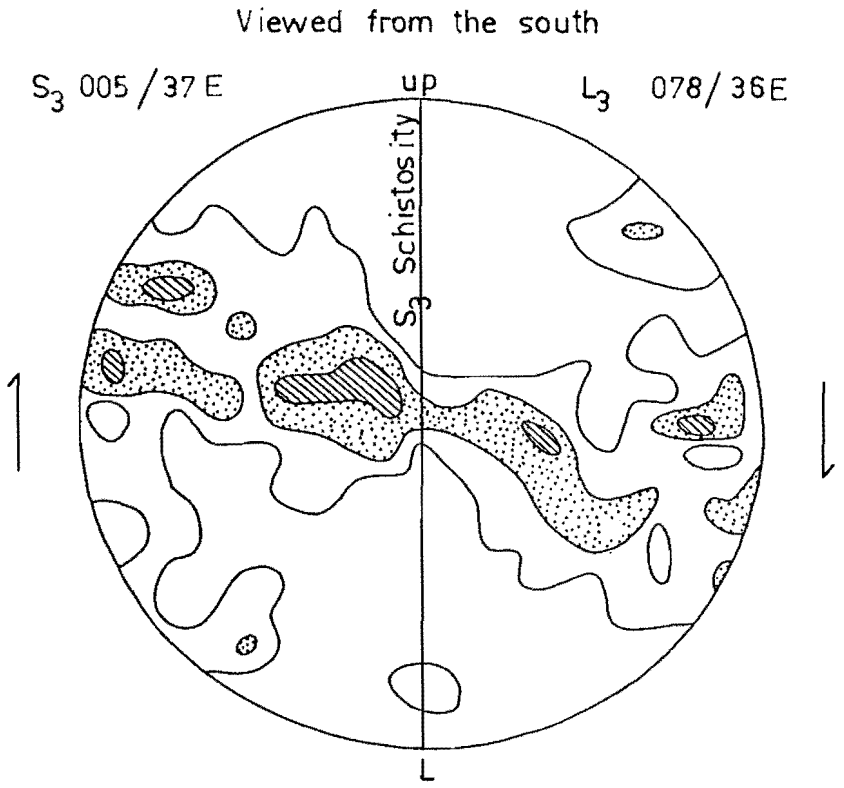

a. UC 10687 400 quartz C axes

Contours 1,2,3 % per 1 % area

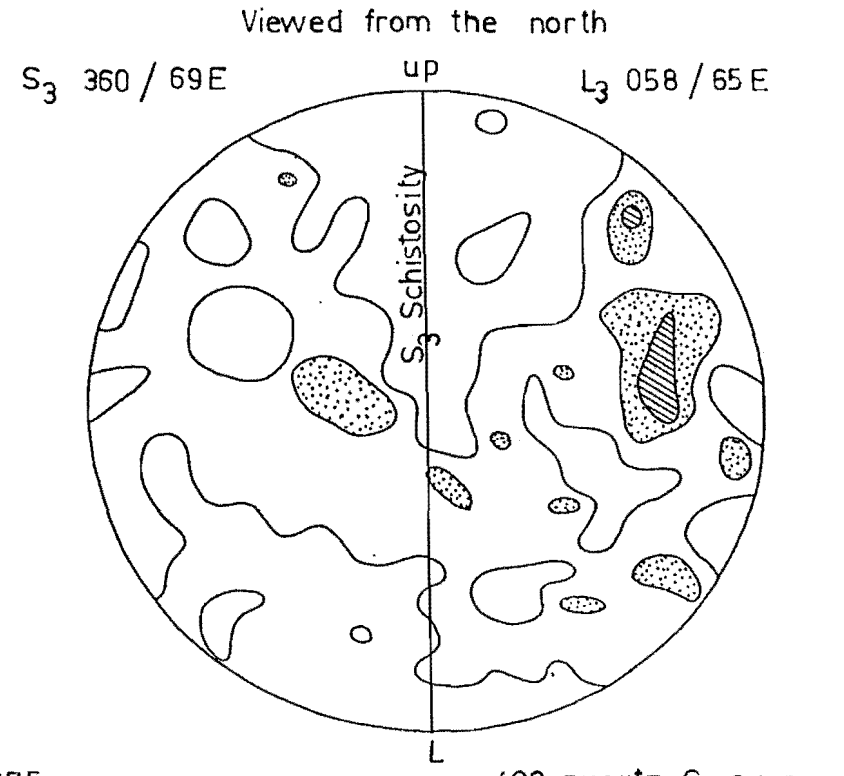

b. UC 10675 400 quartz C axes

Conlours 1,2,3 % per 1 % area

FIG 4.18 Equal area projection

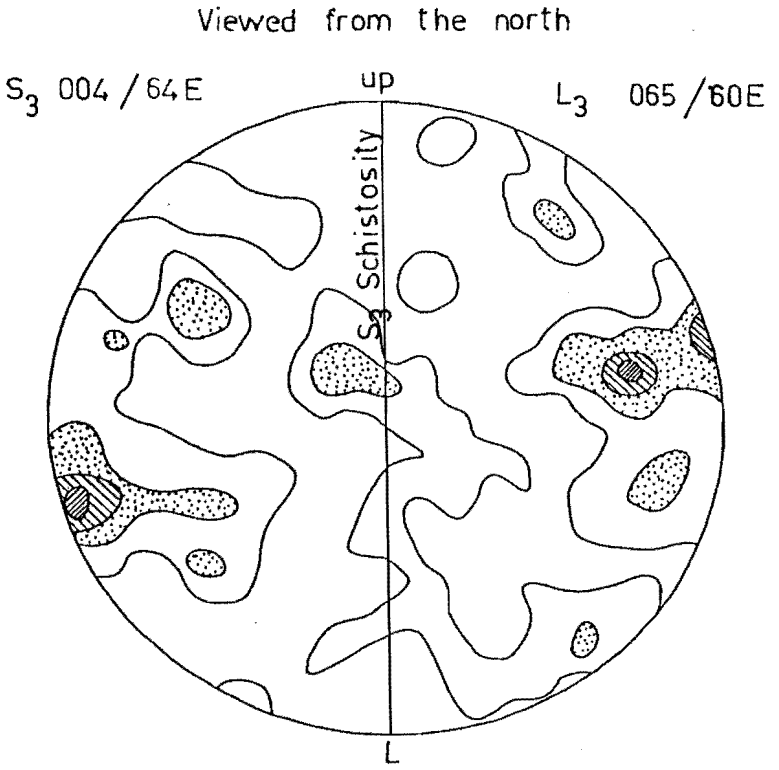

a. UC 10678 400 quartz C axes

Contours 1, 2, 3, 4 % per 1 % area

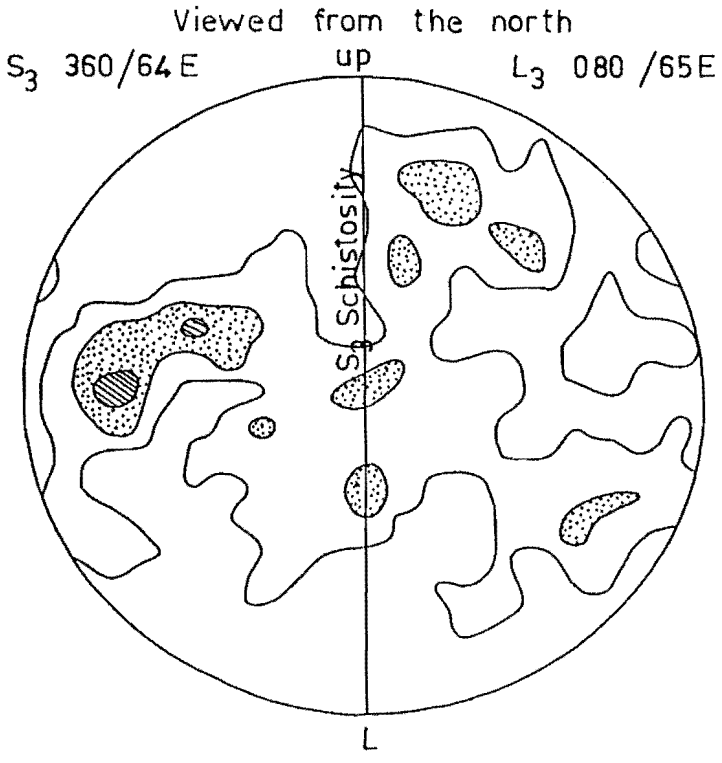

b. UC 10676 400 quartz C axes

Contours 1, 2, 3 % per 1% area

FIG 4.19 Equal area projection

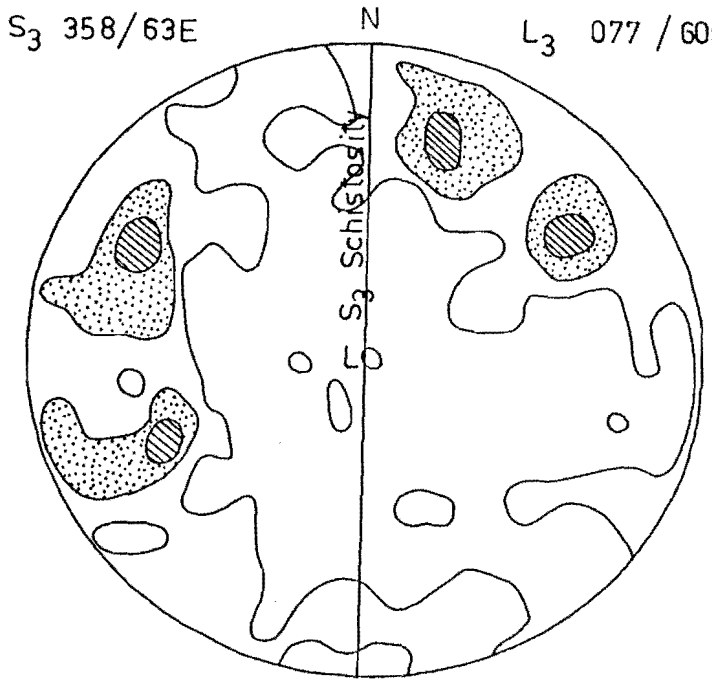

a. UC 10669 400 quartz C axes

Contours 1, 2, 3 % per 1% area

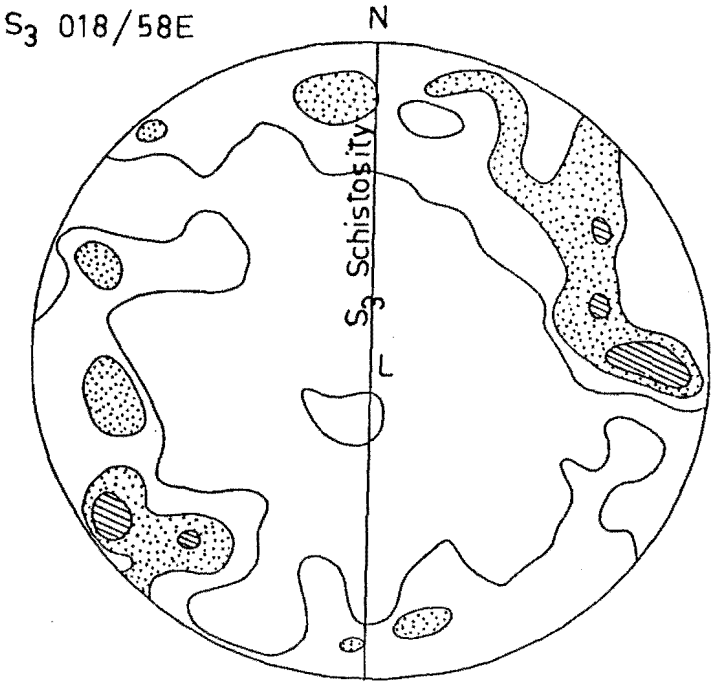

b. UC 10634 300 quartz C axes

Contours 1, 2, 3%per 1 % area

FIG 4.20 Equal area projection

4.4 THE ATTITUDE OF S_3 AND AREAL EXTENT OF D_3

4.4.1 Introduction

In Section 4.2.2 the D_3 structural trend was outlined briefly. Here the attitude of S_3 schistosity is discussed in more detail. Close to the Alpine Fault S_3 strikes between north-northwest and the more common north-south orientation. However towards the eastern margin of the F_3 fold belt S_3 swings toward the northeast, which is a sinistral sense of vergence with respect to the Alpine Fault, if S_3 formed by strain in simple shear. The Alpine Fault is a dextral reverse fault everywhere along its length outside the bends region, and thus it is a logical necessity that it be so between the bends also. Consequently the sinistral vergence of S_3 in the north-south oriented portion of the Alpine Fault Zone demands some discussion.

The reaction of an anisotropic medium to imposed coaxial and non-coaxial strain is discussed in Section 4.4.2. Then in Section 4.4.3 the case of simultaneous superposition of pure and simple shear strain is considered and applied to the problem of a sinistrally verging schistosity developed in a dextral shear zone.

4.4.2 The Reaction of Anisotropic Rock to Superimposed Coaxial and Non-Coaxial Strain

In defining the extent of the D_3 deformation some problems arise from the presence and attitude of the earlier D_2 fabric. If the schistosities of two deformations are coplanar or close to coplanar there can be some difficulty in mapping a line or surface representing the first appearance of the latter event. Such is the case of Trig FZ Ridge in the south of this study area.

In fig. 4.21 S_3 overprints S_2. The line delineating the first appearance of S_3 probably represents a particular finite strain in M_3. In most previously undeformed rocks considerable shortening must take place before folding or

cleavage formation will occur. Thus a line delineating the first appearance of S_3 cleavage will not necessarily coincide with a line indicating the first D_3 strain increment. Where the D_2 and D_3 schistosities are subparallel, the first D_3 strain increment may be accommodated, largely by reactivation of D_2 schistosity. Furthermore D_2 schistosity can be rotated with progressive strain towards a D_3 orientation with no clear cross cutting relationship. Where D_2 and D_3 schistosities are not coplanar D_2 schistosity may still influence the orientation of D_3 schistosity. This means that a strong S_2 anisotropy could effectively mask low finite strain S_3 overprint, particularly if the angle of obliquity is small.

If strain in D_3 is non-coaxial and one assumes that schistosity forms parallel the XY plane of the strain ellipsoid, S_3 will then be variable in orientation, depending on the value of strain at any given position. An example of this would be strain in simple shear within the Alpine Fault Zone. Here S_2 and S_3 strike subparallel for the most part, but differ in dip and dip direction (cf. fig. 4.22). Non-coaxial D_3 deformation can produce low strain S_3 coplanar with S_2, even though the transport direction in D_3 is at a high angle to S_2.

In an initially homogeneous medium the angle β will reflect the shear sense in the fault zone, and will be at a maximum in sections parallel the transport direction and perpendicular to the shear zone. Any other section (e.g. the horizontal profile through an oblique reverse fault) will give an apparent angle for β.

Where the medium is cut by a penetrative anisotropy (in this case S_2) development of the S_3 shear strain related schistosity will be influenced by the pre-existing weakness. Providing strain occurs by ductile means (e.g. crystallization-recrystallization, grain boundary sliding, translation glide etc.) then I would suggest several likely consequences:

(a) Sections with S_2 parallel to the shear plane will develop S_3 parallel to S_2 regardless of the attitude of the slip vector with respect to that section.

(b) In sections with S_2 parallel the shear plane incremental strain in D_3 at the boundaries of the shear zone will be represented by microscopic fabrics oblique to, but not necessarily cross cutting S_2 (e.g. new subgrain preferred orientations in quartz). Strain in this section will act to enhance the S_2 anisotropy. The S_2 strain ellipse is in the same orientation as that of a future S_3 ellipse should deformation continue (cf. fig. 4.23).

(c) In a closed anhydrous system there need be no change in mineralogy even where S_2 and S_3 have evolved under different pressure/temperature conditions.

(d) Different shear zones will each have special characteristics depending on variables such as pressure, temperature, strain rate, bulk chemistry of the surrounding rocks (including the presence or absence of water), the attitudes of pre-existing layering with respect (i) to the shear plane, (ii) the principal stress and (iii) the slip vector, and the mechanical properties of the pre-existing layering. These last two points have particular relevance to the Glenroy Valley where S_2 and S_3 are oblique to each other, to the Alpine Fault plane and to the direction of principal horizontal stress.

Problems in identifying the schistosities of two separate deformational events are compounded when one or both are the result of combined non-coaxial and coaxial deformation. This is a potential problem with respect to the Alpine Fault Zone and is discussed in Section 4.4.3.

FIG. 4.21

Two schistosities (S_2 and S_3) intersect obliquely. S_3 was formed during the D_3 deformation and becomes more penetrative towards the left. Initial strain in D_3 is accomodated, at least in part, by reactivation of S_2.

FIG. 4.22

Diagrammatic cross-section through a reverse fault which post-dates S_2 schistosity. The presence or absence of a cross-cutting relationship between S_3 (shear related) and S_2 schistosities depends on the orientation of S_2 with respect to the kinematic framework of simple shear. Here S_2 has a sinistral vergence sense with respect to the shear zone and a cross-cutting relationship does not necessarily develop.

FIG. 4.23

Plan view of a dextral shear zone which post-dates S_2 schistosity. If S_2 is oriented parallel to, or with a dextral sense of vergence with respect to the shear zone, then a cross-cutting relationship between S_3 (shear related) and S_2 schistosities will be inhibited.

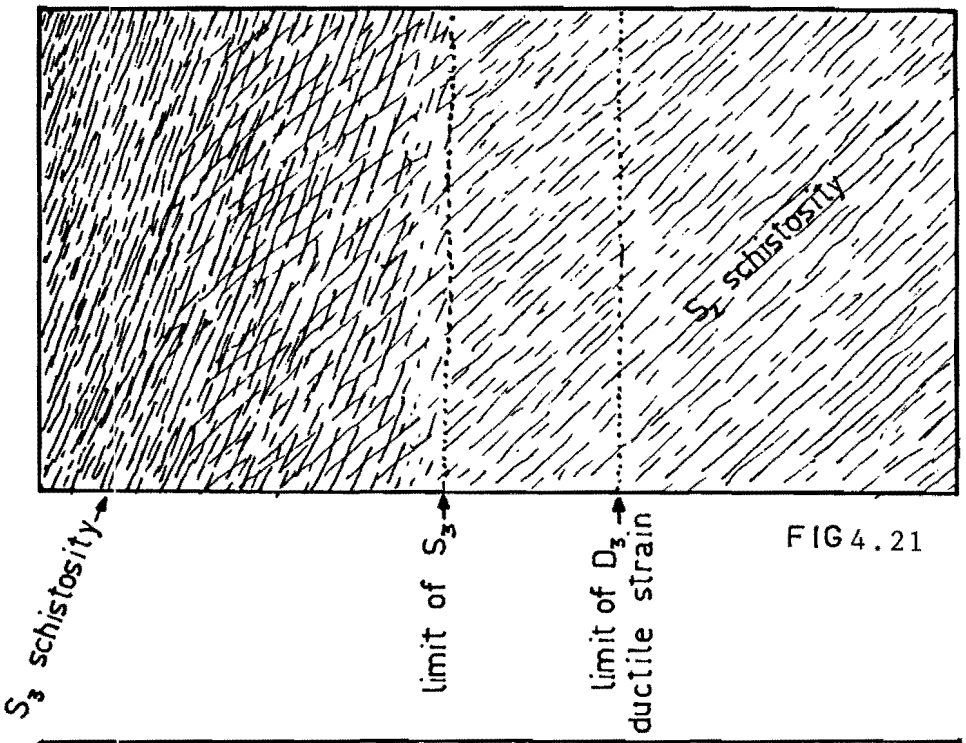

FIG 4.21

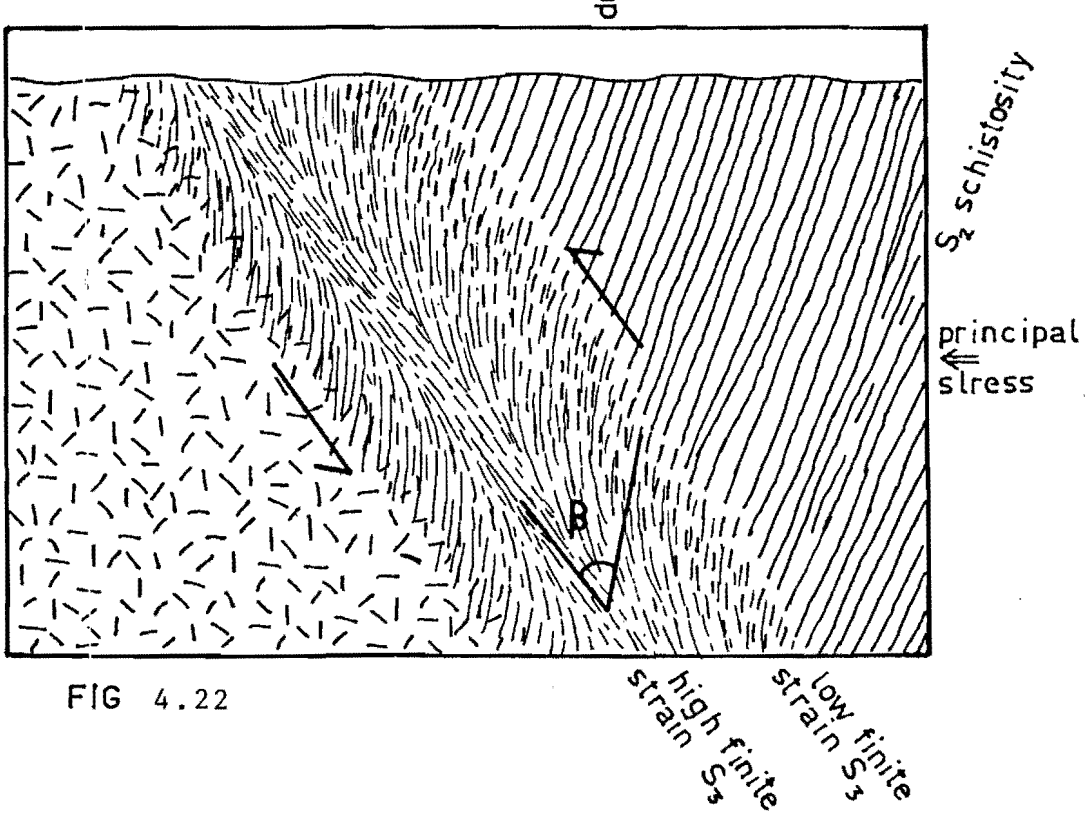

FIG 4.22

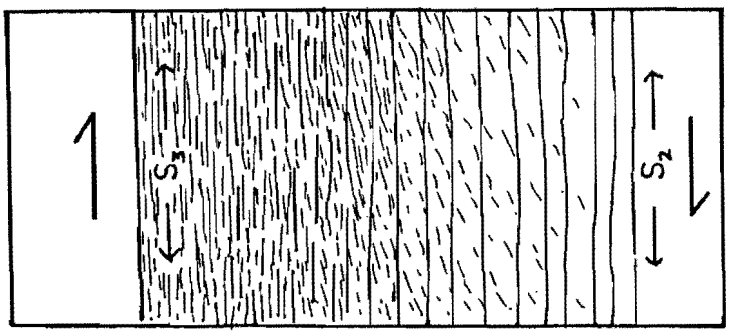

FIG 4.23

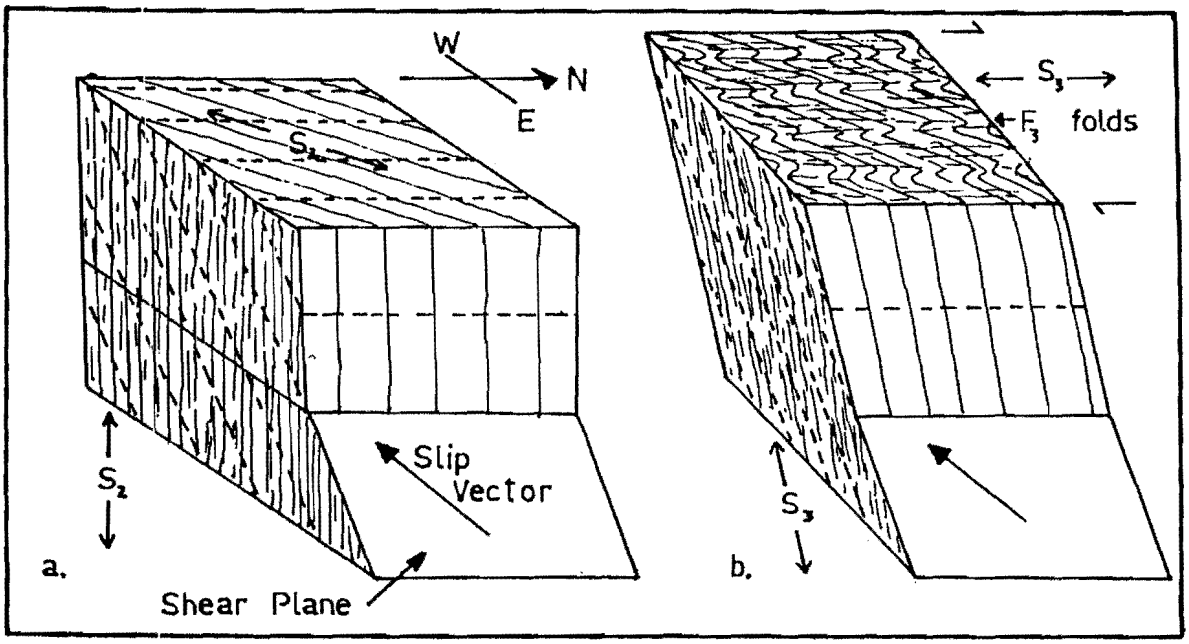

FIG 4.24 Development of F_3 folds and S_3 schistosity in non-coaxial plane strain.

cf. Cosgrove (1976), plate 2 a,b,c ,
Cobbold et al. (1971), fig 7 ,
Patterson and Weiss (1966) , fig 11,

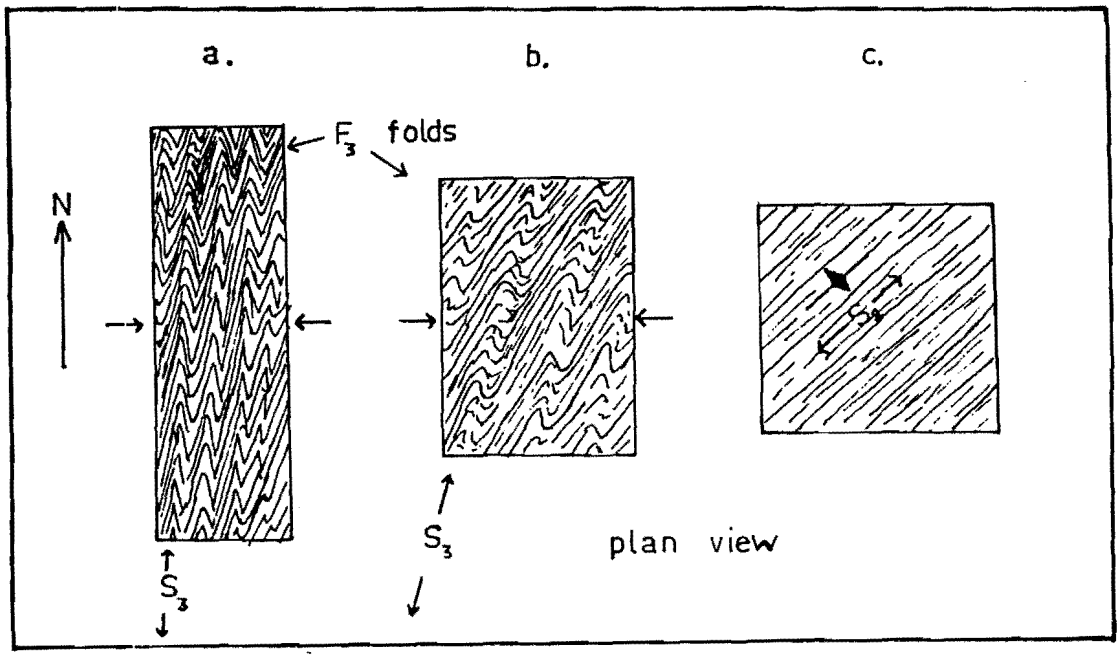

FIG 4.25 Development of F_3 folds and S_3 schistosity in pure shear.

cf. Manz and Wickham (1978), figs 2 and 3,
Gosh (1966), figs 9, 10 and 12

4.4.3 Simultaneous Superposition of Pure and Simple Shear in an Anisotropic Medium

(a) Introduction

In Section 4.4.2 some ideas on the development of a new schistosity in an anisotropic medium were outlined. If D_3 deformation is due solely to non-coaxial plane strain then it may be possible to explain the attitude of S_3 schistosity via the arguments of Section 4.4.2. Analysis of quartz fabric diagrams and microtextures from within $1^1/_2$ km of the Alpine Fault suggests non-coaxial plane strain was important, at least in the latter stages of D_3. However further east where D_3 is less intense the evidence for non-coaxial plane strain diminishes. Thus it is potentially useful to consider the effects of a systematically variable combination of coaxial and non-coaxial components in D_3.

For the purposes of this discussion the Alpine Fault Zone and the adjacent Haast Schists are subdivided into two domains, these being the Trig FZ and Glenroy-Nardoo domains (see fig. 4.27).

(b) Trig FZ Domain

Throughout the Trig FZ domain S_2 and S_3 are essentially coplanar. Here F_3 mesoscopic folds are rare, and smaller in amplitude than in the Glenroy-Nardoo domain. S_3 develops largely through reactivation and subsequent textural enhancement of S_2. There is no mapped surface separating schists which exhibit only S_2 schistosity from those also influenced by M_3. Close to the Alpine Fault M_3 schists exhibit features consistent with non-coaxial strain, including an asymmetric quartz c-axis girdle (sample UC10633, fig. 4.17(b)). Four kilometres from the Alpine Fault there is no evidence of non-coaxial strain (in hand specimen or thin section). Here the schists are still biotite grade, and display a well developed "cross mica" fabric (see Section 3.4.3). Also at approximately 4 km from

the Alpine Fault there is a reversal or fanning in the dip direction of schistosity. The schists steepen in dip on both sides of the fan axis and pass through vertical at this axis. Just what causes the fanning is not known but rotation of S_2 in low strain M_3 overprint is a possibility. A cross cutting schistosity is not developed due to the low angle between the principal axes of S_2 and S_3 strain.

In a large shear zone such as the Alpine Fault, strain is unlikely to occur solely through simple shear. Rather, strain in D_3 is more likely to be a combination of pure and simple shear components. The relative proportions of each will vary within the shear zone but quantification of these components may not be possible in many cases. Ramberg (1975) outlined the likely particle paths for various combinations of pure and simple shear. Figs. 4.26, 4.28 are an adaption of the particle paths of Ramberg. In fig. 4.26 the principal axes of pure shear are equivalent to the regional principal axes of horizontal stress. The orientation of simple shear is that of the horizontal dextral component of the slip vector. Superposition of pure and simple shear is simultaneous. If the proportions of pure and simple shear are varied, the directions of combined compression and extension will rotate toward the principal axes of the dominant component of strain. In fig. 4.26(a) the combined extension direction is approximately parallel the strike of S_2 schistosity. Strain ellipses representing various states of D_3 strain are slightly oblique to S_2 but as outlined in Section 4.4.2, are unlikely to cause a new cross cutting cleavage.

The effect of a component of pure shear is to reduce the angle between the principal axes of D_3 incremental and finite strain as compared to the case of simple shear alone. As the horizontal profile is oblique to the east-northeast plunging axis of the non-coaxial strain ellipsoid this angle (β) will be even further reduced. If the above discussion is valid then S_2 must lie within the extensional field of D_3 strain, and so F_3 folding of S_2 will be inhibited.

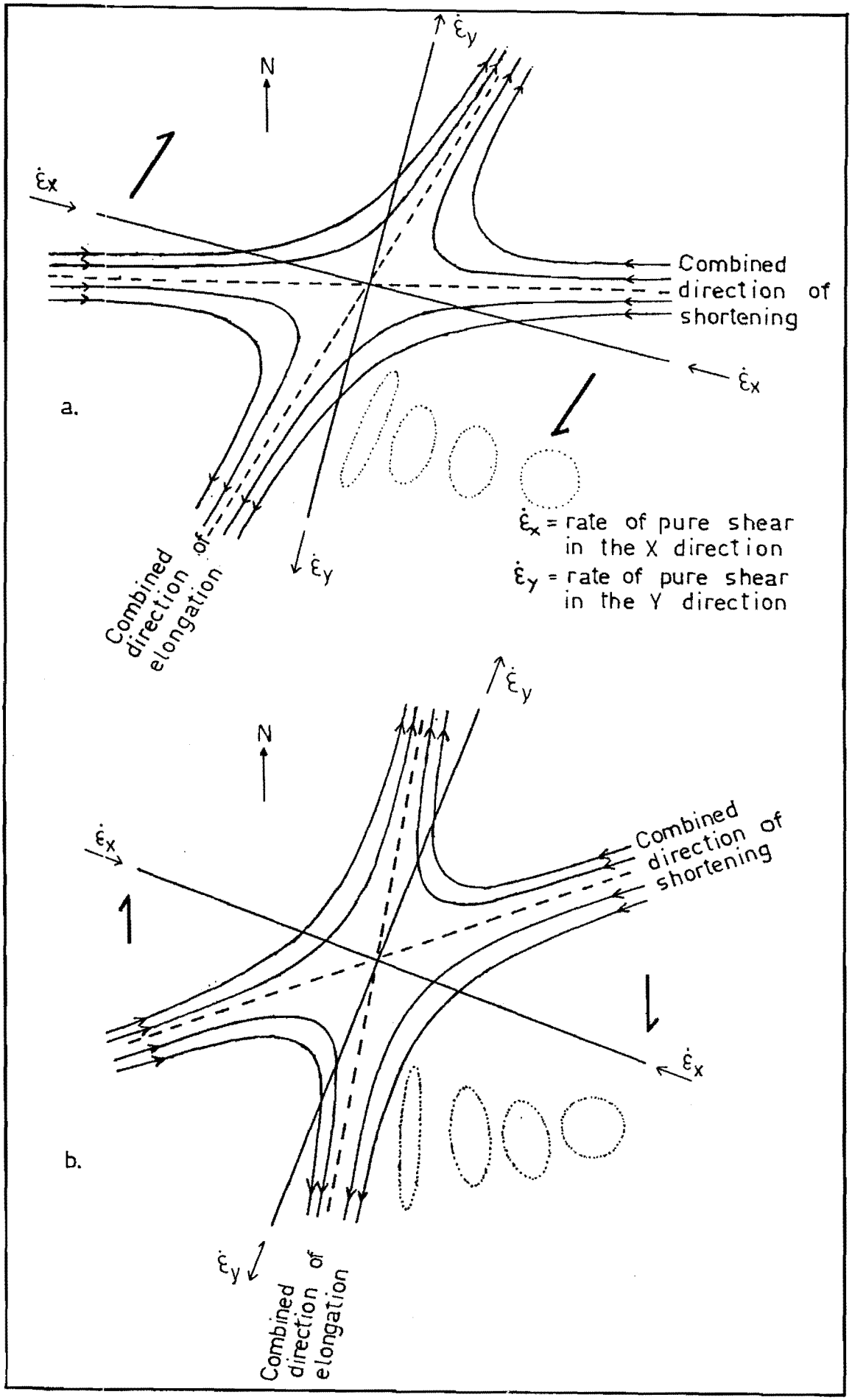

FIG 4.26 Simultaneous superposition of pure and simple shear. Plan profile.

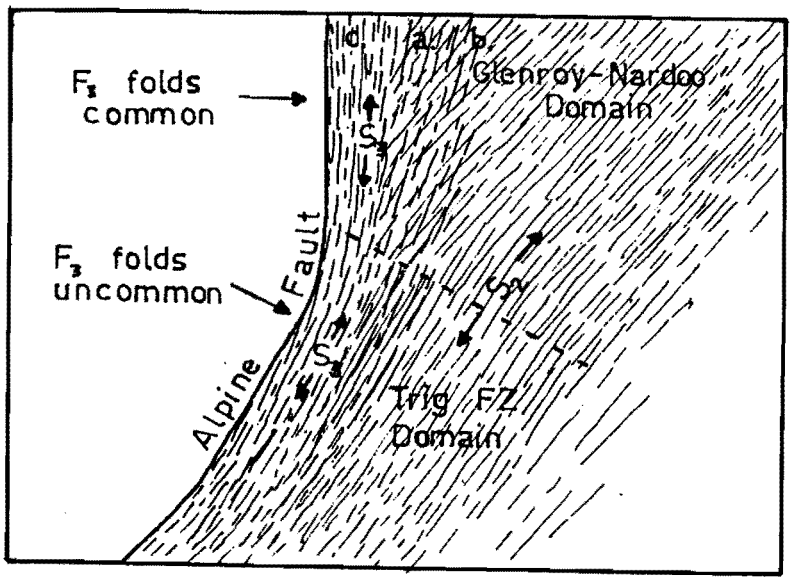

FIG 4.27 Refer to text - section 4.4.3

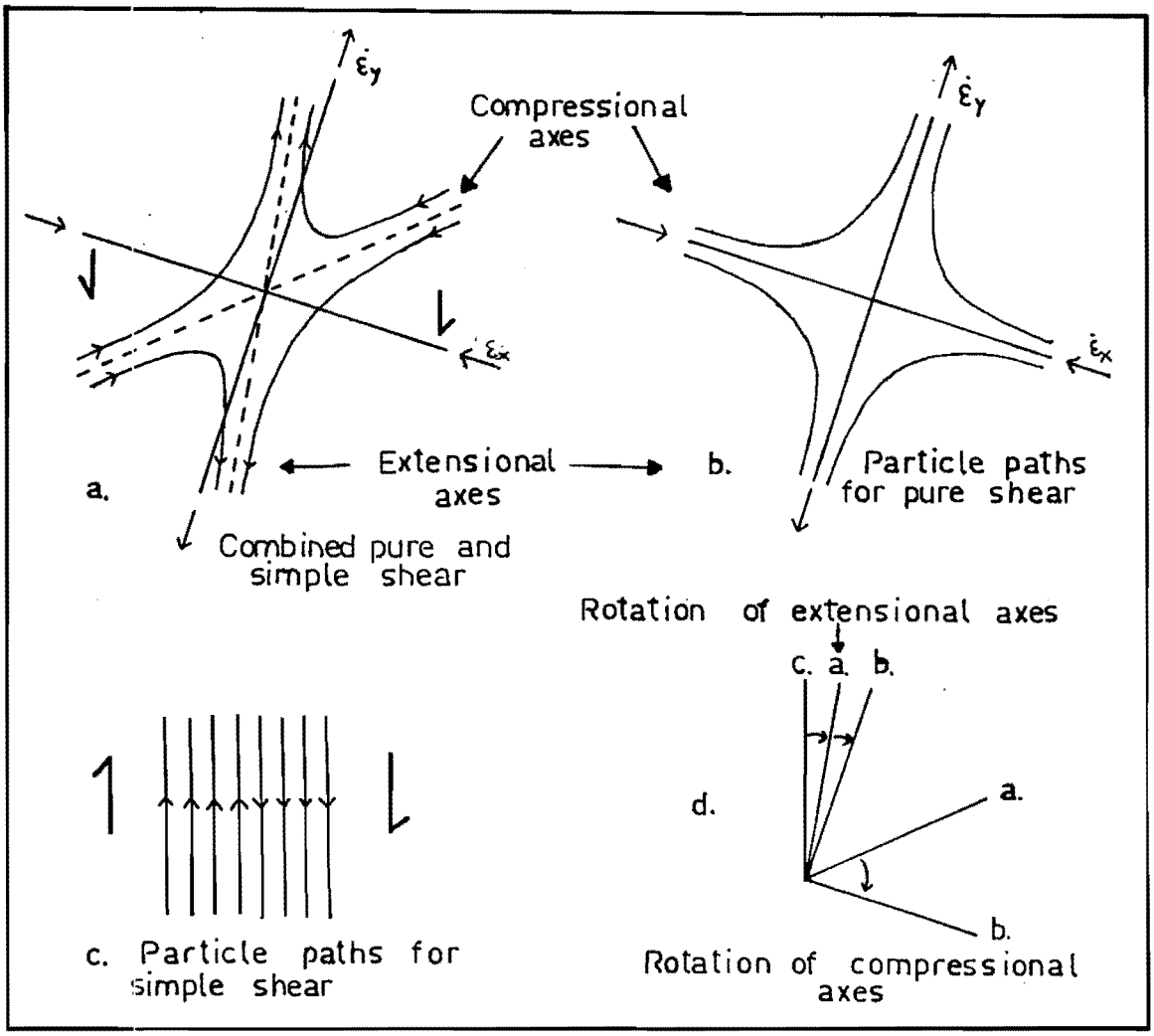

FIG 4.28 Progressive rotation of compressional and extensional axes in deformation with systematically variable proportions of simple and pure shear Positions of a. b. and c. are marked on fig NB. these positions are speculative.

(c) Glenroy-Nardoo Domain

In the Glenroy-Nardoo domain, structural relationships are such that the strike of S_2 is oblique to that of S_3, the Alpine Fault, the isograds and isotects, the D_3 slip vector, and the principal horizontal stress (principal stress directions are discussed in Section 5.2). The attitude of S_3 is variable, striking subparallel the Alpine Fault close to the active trace, but fanning clockwise through an angle of approximately 25^o towards the eastern limit of detection.

Figs. 4.24 and 4.25 represent the extremes in which strain is either entirely coaxial or non-coaxial. Such extremes are unlikely in the case of Alpine Fault metamorphism and strain. Deformation is more likely to result from combined coaxial and non-coaxial deformation. Whatever the strain path followed, the S_2 anisotropy will influence the attitude of S_3 schistosity and F_3 folds. In order to access the consequences of superimposed pure and simple shear in the Glenroy-Nardoo domain particle path diagrams are analysed (figs. 4.26(b), 4.28).

Figs 4.26(b) and 4.28 represent strain in the horizontal profile only. The attitude of the combined shortening and elongation directions depends on the difference in attitude between the principal axes of pure and simple shear, and the ratio of pure to simple shear. In fig.4.26(b) the combined shortening direction is approximately 070^o and thus crosses S_2 at an acute angle if applied to the Glenroy-Nardoo domain, putting S_2 in the compressional field. The combined elongation direction is 010^o sub-parallel the Alpine Fault and the high strain S_3 surface.

If the ratio of pure to simple shear is increased the combined extensional and compressional directions will rotate counterclockwise. This rotation is illustrated in fig. 4.28, and is sufficient to explain the sinistral vergence of S_3 with respect to the Alpine Fault for a

mechanically isotropic medium. In the Glenroy-Nardoo domain the presence of a penetrative S_2 anisotropy is likely to mask the effects of a low strain pure shear deformation. The principal axes of finite strain in pure shear will be close to those of the S_2 strain ellipse in the horizontal profile. Therefore by the arguments of Section 4.4.2 a new cross-cutting cleavage will not necessarily result, strain being accommodated by reactivation of S_2. Such a situation is relevant with respect to the biotite "cross mica" fabric described in Section 3.4.3. This fabric may have been generated during M_3 overprint of M_2 schists.

Northeast of Branch Creek S_3 schistosity no longer parallels the Alpine Fault, even close to the Fault. Here the sense of vergence is dextral as the strike of the Alpine Fault has rotated to the northeast. It should be noted that northward along the Alpine Fault the horizontal profile probably represents a progressively shallower cross section through the ductile zone. Secondly the S_2 schistosity strikes subparallel the Alpine Fault north of Nardoo Basin. If simple shear dominated then S_3 would parallel S_2 (by the argument of Section 4.4.2). However if pure shear dominated then S_3 would be oblique to S_2 and to the Alpine Fault. A northward increase in the ratio of pure to simple shear is consistent with northward decrease in D_3 finite strain, in the width of the F_3 fold belt, and the decrease in metamorphic grade.

(d) Conclusion

The swing in strike of S_3 and its divergence from the strike of S_2 around the curve of the Alpine Fault (particularly the southern bend) can be explained by rotation of the principal horizontal axis of non-coaxial strain. Sinistrally verging S_3 schistosity can be explained by variation in the ratio of pure to simple shear across the Alpine Fault Zone and/or the influence of S_2 schistosity on the developing S_3 surface.

Variation in the proportions of pure and simple shear is not unrealistic. Ramberg (1975) described several cases where such variations were likely. These include spreading ice sheets, tectonic nappes and folding. Sanderson et al. (1980) present several case studies from the Irish Caledonoides where superposition of coaxial and non-coaxial strain is invoked to explain observed strain and strain variation.

Although the application of particle paths to the problem of S_2, S_3 and F_3 orientations is somewhat speculative, the results do not conflict with field data for the areas in question.

4.5 LINEAR FABRIC WITHIN THE ALPINE FAULT ZONE

L_3 linear features within the Alpine Fault Zone include F_3 fold axes, the LS_3/S_2 intersection lineation, quartz rodding lineations and preferred elongation directions of biotite, epidote and hornblende. Although these were not measured with the same frequency, they appear to be parallel, and to have been generated by the same strain. The trend and plunge of L_3 lineations is east-northeast at moderate to steep angles depending on the dip of S_3 schistosity (L_3 lineations lie within the plane of S_3 schistosity). The swing in strike of S_3 (see Section 4.4.1) is not accompanied by a demonstrable swing in the trend of L_3 lineations (see fig. 4.29). If the fanning of S_3 is due to an external rotation then the L_3 lineations must be parallel or subparallel to the axis rotation. However the changing attitude of S_3 can be explained by other means (see Sections 4.4.2, 4.4.3). It is most likely that the L_3 lineations form parallel to the long axis of D_3 finite strain ellipsoid, which is more or less constant in attitude across the Alpine Fault Zone.

This broad consistancy in attitude of L_3 lineations, and the systematically variable strike and dip of S_3 schistosity indicates that large scale outward collapse of

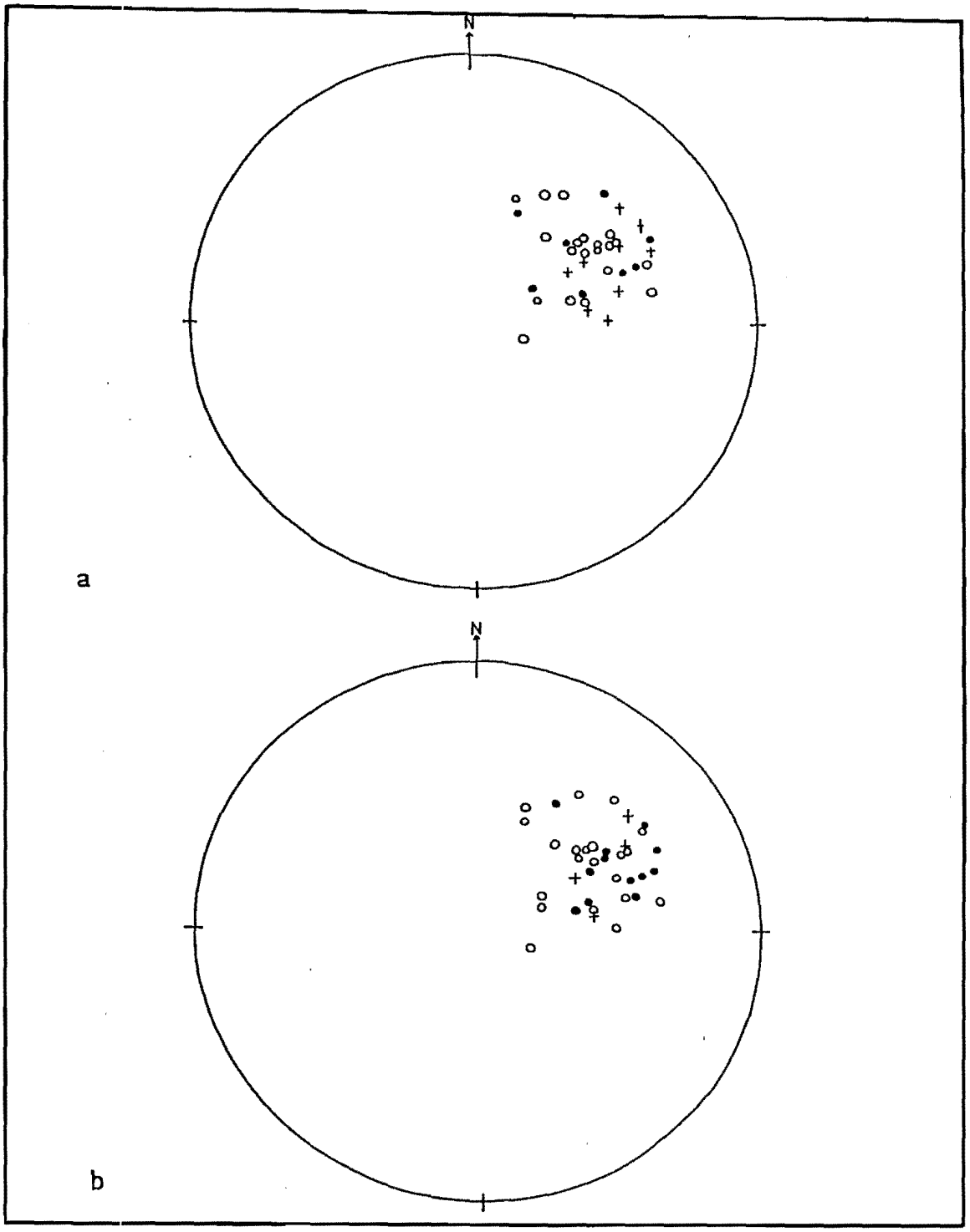

FIG 4.29 Quartz rodding liniations from the zone of M_3 metamorphism in the Glenroy Valley

a: Strike of S_3 schistosity which bears the lineation
- o From 340 to 000
- • From 001 to 010
- + From 011 to 030

b: Distance of each locality from the Alpine Fault
- o Within 1km of the Alpine fault
- • Between 1 and $1\frac{3}{4}$ km from the Alpine Fault
- + Between 1 and 3km the Alpine Fault

FIG. 4.30 Slope instability on the northeast flank of "Trig FZ Ridge". The upper 15m of garnet grade schistose mylonite is unstable at this locality and is collapsing under the influence of gravity. Mylonitic schistosity strikes subparallel to the oversteepened face of an actively eroding gully which drains towards the northeast (left). Metric grid reference M31 4570 8846.

FIG. 4.31 Slope instability. An oversteepened slope, lack of lateral support across schistosity ahd active erosion by the stream (a tributary of the Glenroy River) contribute to slope collapse. Note the in situ outcrop in the foreground in which bedding and schistosity are subvertical. Metric grid reference M31 4595 8843.

schists across the Alpine Fault (cf. Wellman, 1955) is unlikely in the Glenroy Valley. Therefore generation of the M_3 schists and the attitude of M_3 structures is best explained by a model similar to that of Sibson et al. (1979, 1981).

Some variation in the attitude of L_3 lineations is inherent since the S_2-S_o anisotropy which is overprinted by S_3 exhibits some variability in attitude as does S_3 schistosity at the mesoscopic scale. Small rotations across brittle shear surfaces in the Alpine Fault Zone also contribute to the variation in L_3 attitudes.

In combination S_3/L_3 and S_2/L_2 attitudes from outcrops representing deep seated structure indicate stability within the schistose massif. However many slopes, particularly those lacking lateral support across schistosity and bedding, have an outwardly collapsing surficial "skin" of weathered and shattered schist. The collapsing schist retains its layered appearance but is internally broken, often with a block and matrix type texture. Examples of collapse under gravity are shown in figs. 4.30 and 4.31. The thickness of collapsed schist varies from zero to perhaps fifty metres. Ridge rents (small gravitational collapse faults with apparent upthrow on the downhill side) are common in areas where there is a collapse skin, run parallel the ridge crests and contribute to downslope wasting under the influence of gravity.

4.6 THE ALPINE FAULT DUCTILE ZONE

4.6.1 Introduction

The Alpine Fault Ductile Zone is defined as that body of rock which has suffered strain associated with shear on the Alpine Fault, by processes other than brittle fracture. Discussion here is limited to processes occurring at and below the brittle-ductile transition zone of Johnston and White (1983).

In areal extent the Alpine Fault Ductile Zone is at least as wide as the zone of F_3 folding, although intense transposition takes place only within 3 km of the fault. Exposure of the Alpine Fault Ductile Zone is controlled by uplift, which decreases northeastward along the Wairau section of the Alpine Fault. This is assumed to be the reason for the termination of the Alpine Fault Ductile Zone in the vicinity of the D'Urville River.

Ductile processes cause strain in M_3 metamorphism, with S_3 schistosity being approximately parallel the XY plane of the finite strain ellipsoid. Mylonitic schistosity in those rocks immediately adjacent to the Alpine Fault trace is assumed to reflect the attitude of the Alpine Fault Ductile Zone at depth (cf. Sibson et al., 1979). The fault zone is curviplanar on a regional scale. Linear and planar features such as F_3 fold axes, mineral lineations, and S_3 schistosity indicate that shear is dextral reverse with convergence from approximately 060°. In the Glenroy Valley the Alpine Fault strikes north-south and dips at approximately 50-60° to the east. North of Branch Creek the fault swings to a northeast strike and probably steepens to a dip of around 70° beyond Nardoo Trig. The Haast Schists are being thrust over the Western Province with the vector direction and rate of movement remaining relatively constant at all points around the curve of the Alpine Fault Ductile Zone. The relative proportions of displacement expressed as components of horizontal strike slip parallel to the Alpine Fault and horizontal movement normal to the fault are a function of the convergence vector, and the attitude of the fault plane. The convergence vector between the bends is not equivalent to the regional principal horizontal stress.

4.6.2 Shear Heating and Metamorphism in the Alpine Fault Zone

(a) Introduction

Although a number of authors have suggested the possibility of shear heating in the Alpine Fault Ductile Zone the extent to which this process has been active is as yet uncertain. Therefore it is pertinent to background current theoretical models of shear heating in major fault zones as a prelude to discussion of this effect in the Alpine Fault Ductile Zone.

(b) Theoretical Aspects

Shear or strain heating is caused by the conversion of mechanical energy into heat during deformation. If the rate of energy dissipated exceeds the rate of heat loss by conduction then the temperature will rise, causing a thermal anomaly. Fleitout and Froidevaux (1980) present mathematically derived thermal profiles across shear zones in a variety of litholigies and of variable initial width, background temperature, strain rate and stress level. They came to several conclusions concerning the deep ductile portion of large fault zones including the following:

(1) Initiation of a ductile shear zone proceeds by the rapid buildup of a thermal peak and by concentration of strain.

(2) The maximum temperature does not vary much with time once the shear zone is established, but is dependent upon lithology. Temperature is at a maximum in the centre of the zone.

(3) The hot zone (and consequently the shear zone also) widens due to thermal conduction. Widening is proportional to the square root of time.

(4) In homogeneous rocks softening, but not melting, will result from the shear heating process.

(5) Since the lithosphere has an isothermal upper boundary, widening of the thermal anomaly will be ultimately inhibited. Three of the profiles shown by Fleitout and Froidevaux are across hypothetical transcurrent shear zones comparable with the Alpine Fault in width and strain rate. These examples have not reached thermal equilibrium (where heat generation balances heat loss) 10 Ma after initiation.

(6) The sheared region is much narrower than the thermal anomaly.

Brun and Cobbold (1980) reviewed the literature on the subject of shear heating and came to several conclusions including:

(1) That temperature rises of several hundred degrees can be expected in major shear zones and that such temperatures must be significant in localizing deformation.

(2) A rise in temperature of 100K is sufficient to localize 90% of the deformation in the hotter zone.

Assuming the above theory to be valid, then there are several likely consequences of the slow rate of heat conduction in crustal rocks. During the initiation of a shear zone, and for some time afterward, the thermal anomaly is restricted to an area close to the heat source. If there is no relative uplift then the rocks more distant from the shear zone will undergo a prolonged gradual warming phase until thermal equilibrium is reached. If heat generation were to stop, cooling would be initiated in the centre of the zone. However if thermal equilibrium had not been reached, the stored heat could be sufficient to continue the

warming trend at points more distant from the shear zone (equivalent to post-deformational thermal metamorphism). When differential uplift begins across a shear zone in which thermal equilibrium has been achieved, then low conductivity is likely to result in pronounced disequilibrium, and unusually high geothermal gradients above the thermal anomaly (and beyond if the uplift is widespread).

Where the shear zone is inclined, with uplift on the hanging wall, an asymmetric thermal anomaly is likely to be created (a situation which is relevant to the Alpine Fault Ductile Zone). The consequences of an asymmetric thermal anomaly (see fig. 4.32) include:

(1) A maximum geothermal gradient some distance from the surface expression of the fault (on the down dip side).

(2) Maximum uplift rates need not coincide with the area of highest geothermal gradient. N.B. uplift occurs along a significantly non-vertical path.

(3) Across any horizontal profile the highest temperatures will have been suffered by rocks at the zone of maximum shear strain (rather than at the point with the highest geothermal gradient).

(4) The youngest cooling ages will occur above the area of highest geothermal gradient, rather than in the area of maximum uplift rate.

(5) Uplift in the hanging wall will result in a contraction of the isotherms i.e. the isotherms will move relative to the rock mass, inward towards the area of maximum geothermal gradient. Such a contraction would cause a pattern of decreasing cooling ages towards the area of maximum geothermal gradient.

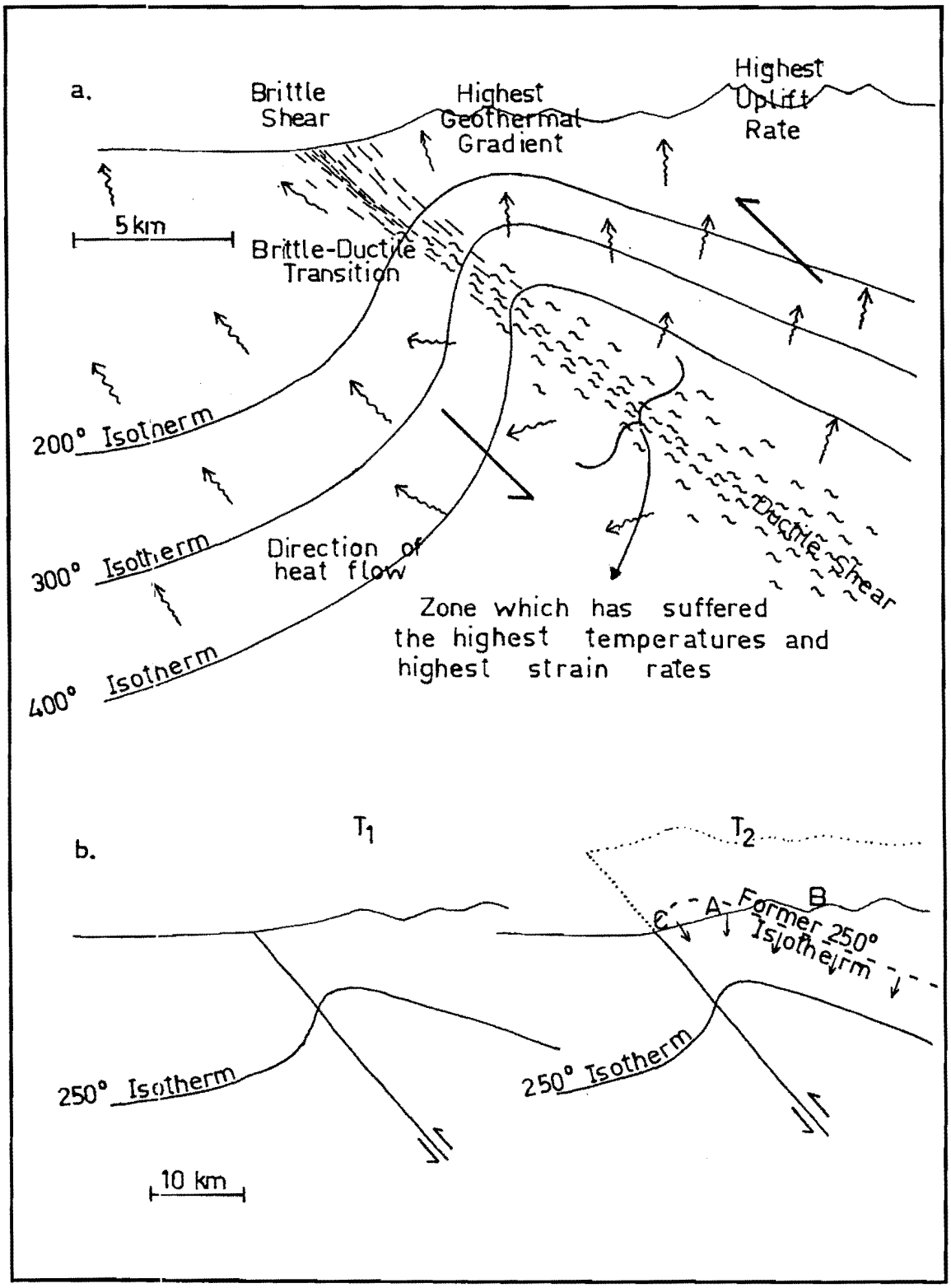

FIG 4.32 a. Cross section and diagramatic thermal profile through a reverse shear zone
b. Migration of rocks through the isotherms in uplift on a reverse fault. Cooling ages are a minimum at A and increase towards B and C.

(6) In a steady state situation with constant heat generation and uplift which is in balance with erosion, the cooling age pattern (e.g. K-Ar isotopic ages) across the ground surface profile will be constant in time. Again the youngest ages occur above the area of highest geothermal gradient, but do not vary with time. Therefore a K-Ar age pattern with a concentration of young dates does not necessarily reflect a heating event of short duration (cf. Adams, 1981). In the case of a shear zone which cuts across an older metamorphic terrane is of interest. The increase of K-Ar ages outward from a linear zone separate from but parallel to the fault may indicate genuine cooling ages for some distance perpendicular to the fault, rather than simply partial degassing of the rocks of the older terrane.

(c) Application to the Alpine Fault Ductile Zone

The above discussion is relevant to the Alpine Fault and the adjacent Haast Schists as a number of authors have suggested shear heating occurs in association with strain in the Alpine Fault Ductile Zone. These include Sheppard et al. (1975), Sibson et al. (1979), Adams (1981) and Johnston and White (1983). The evidence which supports this reasoning includes high finite strain and high strain rates associated with the zone of mylonites. Secondly Fe-Mg partitioning between garnet and biotite pairs indicates a period of elevated temperature (Johnston and White, 1983). Thirdly the K-Ar isotopic age pattern observed by Mason (1961), Hurley et al. (1962), Sheppard et al. (1975), Adams (1981) and Adams and Gabites (1985) has been attributed to limited shear heating, and partial degassing of older Rangitata phase schists.

The current view appears to be that a shear heating event occurred during a change in slip direction within the Alpine Fault Zone about 5 million years ago (Sibson et al.,

1979, 1981; Adams, 1981; Adams and Gabites, 1985; Johnston and White, 1983). Sibson et al. (1979) suggest that mylonitic lineations from within the ductile zone reflect slip which has occurred since the onset of strong uplift. As no earlier mylonitic structures were observed these lineations are regarded as dating a period of shear heating. This period was seen to be short and to have occurred during rapid reorientation of the slip direction coincident with a migration of the pole of rotation in the Pacific Plate. In view of the theory outlined in Section 4.6.2(b) it is likely that the zone of intense shear (inlcuding mylonitization) progressively widened to encompass schists which were previously unaffected. Therefore at the extremities of the zone of transposed schist, only the most recent kinematic framework will be represented. Towards the centre of the shear zone deformation is sufficiently rapid to reorient older fabrics. Most plate tectonic reconstructions illustrate a progressive but gradual migration of the pole of rotation in the Pacific Plate (e.g. Molnar et al., 1975) rather than the sudden change Sibson et al. (1979) suggest.

Johnston and White (1983) suggest a base temperature of 400-450°C for amphibolite facies schists close to the Alpine Fault prior to mylonitization. More importantly Johnston and White suggest the mineral assemblage of the schistose mylonites formed coeval with amphibolite facies schists. Assuming a geothermal gradient of 20°C/km they favour a depth of formation for the schistose mylonites of 25-30 km. By similar reasoning transition zone and green mylonites are thought to originate at 12-15 km depth in the Alpine Fault Zone. Uplift rates in the Southern Alps are thought to be at a maximum some distance southeast of the Alpine Fault (Wellman, 1979; Walcott, 1979). Sibson et al. (1979) show that the maximum strain rates occur within the Alpine Fault Zone. If, as is suggested by Johnston and White (1983), the amphibolite facies schists at the Alpine Fault have suffered 25 km of uplift then it would follow by the reasoning of Wellman (1979) that the schists some distance southeast of the Alpine Fault have suffered even greater uplift. Adams (1981) estimated a maximum uplift of

only 10 km for the Haast Schists since the early Pliocene, based on the distribution of K-Ar ages. This is a more realistic figure than that of Johnston and White (1983) and is based on a geothermal gradient of 50°/km. Allis (1981) estimated the geothermal gradient in the central Southern Alps at 60°/km.

Johnston and White (1983) estimated a rise in temperature of approximately 100°C within the Haast Schists adjacent to the Alpine Fault Zone based on garnet-biotite geothermometry, and attribute this to shear heating. Adams (1981) suggests this thermal aureol may have extended as far back as 15 km into the Haast Schists causing outfassing of argon and the observed distribution of K-Ar ages. If the arguments of Section 4.6.2(b) are valid then the distribution of K-Ar ages may reflect a period of heating more prolonged and more intense than that envisaged by Adams (1981).

The mineralogy of the schist derived mylonites is still to be explained if the total uplift during Cenozoic times is as low as 10 km. Mylonitization at shallow depths and retrogressive temperatures will not necessarily cause a change in the mineralogy of a metastable assemblage. Secondly, if the rocks were buried at a depth of 10 km prior to mylonitization they may have been close to the argon retention limit. Shear heating producing a 100° rise in temperature (conservative estimate) would then subject these rocks to greenschist facies conditions at the very least. I argue on the basis of structure and petrology, that amphibolite and greenschist facies conditions have influenced the Haast Schists of the Glenroy Valley during late Cenozoic times. This does not conflict with the observed K-Ar age profiles of Sheppard et al. (1975) or the garnet-biotite geothermometry of Johnston and White (1983). In the Glenroy Valley M_3 metamorphism is related to strain associated with movement on the Alpine Fault. Mapping by McLean (1986) indicates that this zone of deformation extends at least as far south as the Maruia River.

The observations that M_3 schists have suffered an extended period of elevated temperature and high strain rates are compatible with a prolonged shear heating event. This event is likely to be in progress still, and will continue so long as the shear strain rates at the Alpine Fault are maintained at the current level.

4.6.3 Drag on the Alpine Fault

(a) Introduction

Ductile shear in the Alpine Fault Zone is responsible for a large proportion of the total offset recorded at those localities where mylonitic rocks are exposed. In Section 4.6.2(c) it is proposed that Alpine Fault related ductile shear may occur throughout the zone of M_3 metamorphism in this study area. Assuming this to be true then structures which pre-date ductile shear should show evidence of rotational strain, particularly those which were once continuous across this zone. The S_o-S_2 structural trend is such a feature. As this trend is continuous on a regional scale, and not deflected with the changing orientation of the Alpine Fault, it provides a unique opportunity to examine drag on the Alpine Fault. The effects of ductile shear on individual passive markers is considered, then discussed with repect to angular relationships between surfaces in the Glenroy area.

(b) Ductile Shear in Two Dimensions

A two dimensional model is discussed here to aid conceptualization of the three dimensional case. Motion in the ductile shear zone (fig. 4.33) is traced by defining displacement vectors relative to a line normal to the zone. The maximum displacement vectors are equal in magnitude and symmetrically opposed on the margins of the zone. Vectors of opposing direction are separated by a "stationary line" relative to which both margins have been displaced by the shearing process. This line need not be centrally located in real shear zones, as strain will not necessarily vary

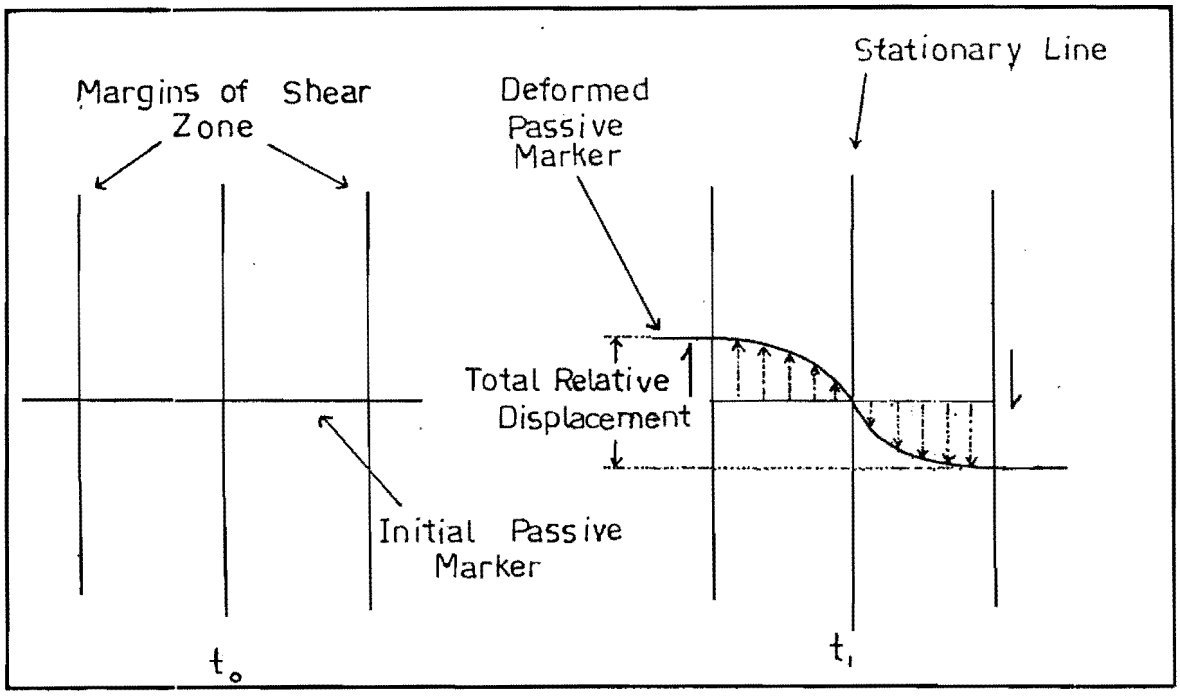

FIG 4.33 Rotation of a passive marker in simple shear (two dimensional case).

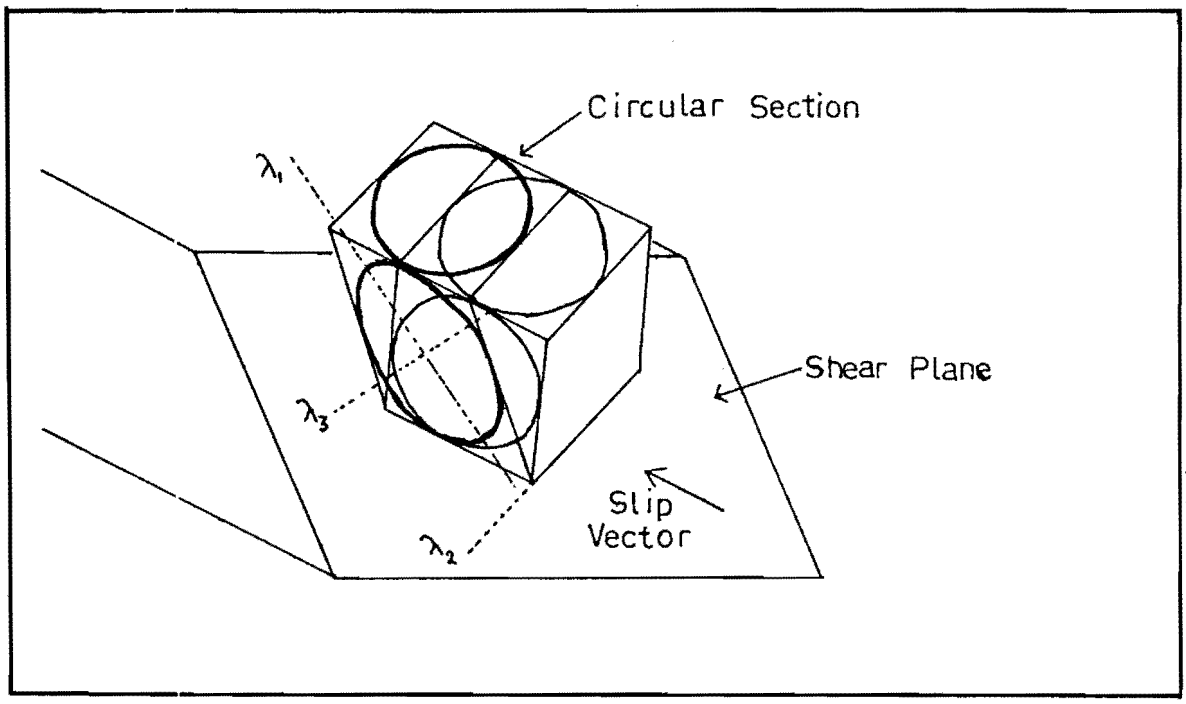

FIG 4.34 Orientation of the strain ellipsoid in dextral oblique reverse slip within an inclined shear zone.

linearly across the zone.

The relative displacement (or velocity) between any two bounding points on a deforming passive marker (fig. 4.33) is the sum of relative movement (infinetesimal increments between the continuum of points) between "subpoints" representing finer divisions on the marker. All displacements are given a positive value. In the limit the relative motion between bounding points tends towards zero as the distance (perpendicular the shear zone margins) between these points tends towards zero. Likewise the relative motion between bounding points tends towards zero as the time interval approaches zero.

(c) Ductile Shear in Three Dimensions

In this section ductile shear is discussed with respect to the general three dimensional situation. An illustrative technique for prediciton of the rotation of planar surfaces is outlined. This method is similar to that of Skjernaa (1980), which allows quantitative prediction of the rotation of lines and planes in simple shear.

Here passive marker planes are deformed in shear zones of known width and slip direction. For each of the examples outlined the time interval (t_n) during which shear takes place, and the cumulative movement rate across the shear zone as a whole are unspecified. Flow rates are heterogeneous across the shear zone but symmetrically arranged with respect to the "stationary plane" (equivalent of the stationary line in fig. 4.33). Any line within the "stationary plane" is a stationary line. For example the line of intersection between the passive marker and the "stationary plane". In order that this discussion might be applied directly to the Alpine Fault, each of the diagrams (figs. 4.34, 4.35, 4.36, 4.37) represents a oblique-dextral-reverse shear zone.

At low to moderate finite strain (see fig. 4.34) the long axis (λ_1) of the strain ellipsoid is oblique to the

plane of shear, and the slip vector. Only at high finite strain does λ_1 rotate into near parallelism with the plane of shear. Schistosity formed in simple shear deformation is assumed to parallel the $\lambda_1\lambda_2$ or XY plane of finite strain, rather than the plane of shear.

Fig. 4.35 shows the effect of oblique-dextral-reverse ductile shear on a passive marker which strikes parallel the margins of the shear zone. During shear the strike of this marker remains the same, irrespective of the attitude of the slip vector.

Figs. 4.35, 4.36, 4.37 show that in oblique-dextral-reverse shear passive markers with strike oblique to that of the slip vector and the shear zone will rotate in map view. The sense of rotation depends on the vergence of the slip vector with respect to the line of intersection between the passive marker and the shear plane. Thus it can be demonstrated that counterclockwise rotation of passive markers is possible in oblique-dextral-reverse ductile shear. Applying the method of Skjernaa (1980) to the geometry of fig. 4.36 produces the same sense of rotation for the passive marker in both the horizontal and vertical section.

Fig. 4.37 illustrates the sense of rotation seen in the horizontal profile, as determined from figs. 4.34, 4.35, 4.36, and applied to the Alpine Fault. The orientation of the Alpine Fault in fig. 4.38 a,b,c is similar to that seen near Trig FZ at the southern end of the thesis area. Fig. 4.38b shows a passive marker which can be equated with the S_2-S_o anisotropy on Trig FZ Ridge (see also Section 4.4.3(b)). Fig. 4.38d can be compared directly with the oblique angle of intersection between the S_2-S_o anisotropy and the north-south (Glenroy) section of the Alpine Fault (see also Section 4.4.3(c)).

Discussion of shear in three dimensions has so far been simplified by the initial assumption that the shear zones should be symmetrical. A note of caution must be

sounded though. The full width of the Alpine Fault Ductile Zone is not necessarily represented in horizontal profile at the ground surface. Relative uplift across the Alpine Fault tends to expose the eastern half of the ductile zone in preference to the western half.

Deformation within the Alpine Fault Zone is not necessarily spatially symmetrical at depth. Contrast in lithology across the shear zone may produce strain localization close to the western margin. Velocity profiles (with respect to the stationary plane) are almost certainly asymmetric both at the surface and at depth. This is likely to be true of ductile, brittle-ductile, and brittle shear. It cannot be assumed that the "stationary plane" coincides with the lithologic boundary. The "instantaneous" stationary plane need not coincide with the "finite" stationary plane. Here the terms instantaneous and finite are analogous to their usage in general strain theory.

Passive marker planes rotate in the manner outlined here regardless of the symmetry of the shear zone, so long as the slip vector and shear zone are constant in orientation.

Rotation of passive markers in simple shear within the bends region is limited to the zone of M_3 metamorphism. The maximum width of the rotational zone within the Haast Schists is approximately 5-6 km and intense transposition occurs only within 3 km of the active fault trace. Further east within the main mass of the Haast Schists ductile rotation in Alpine Fault related deformation is relatively insignificant. In this context ductile shear also includes the penetrative brittle shear fabric outlined in Sections 4.7.3 and 4.7.4.

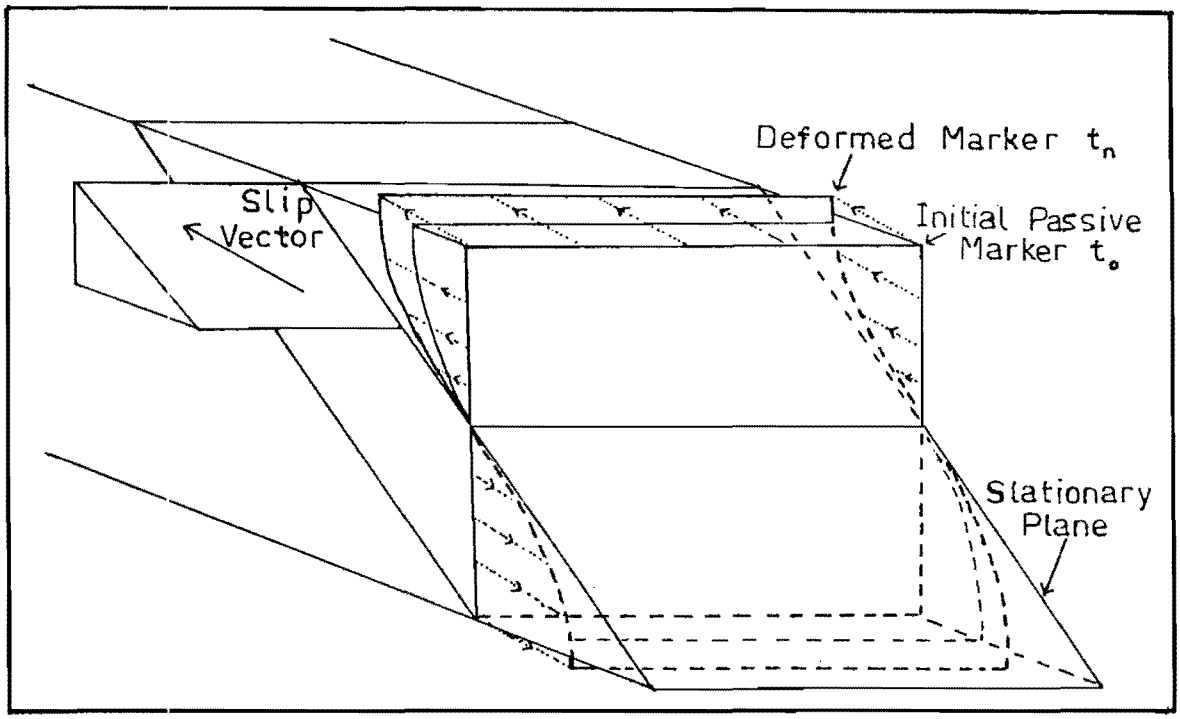

FIG 4.35 Ductile drag of a vertical passive marker which is initially parallel to the strike of an inclined dextral oblique reverse shear zone. The passive marker is also oblique to the slip vector

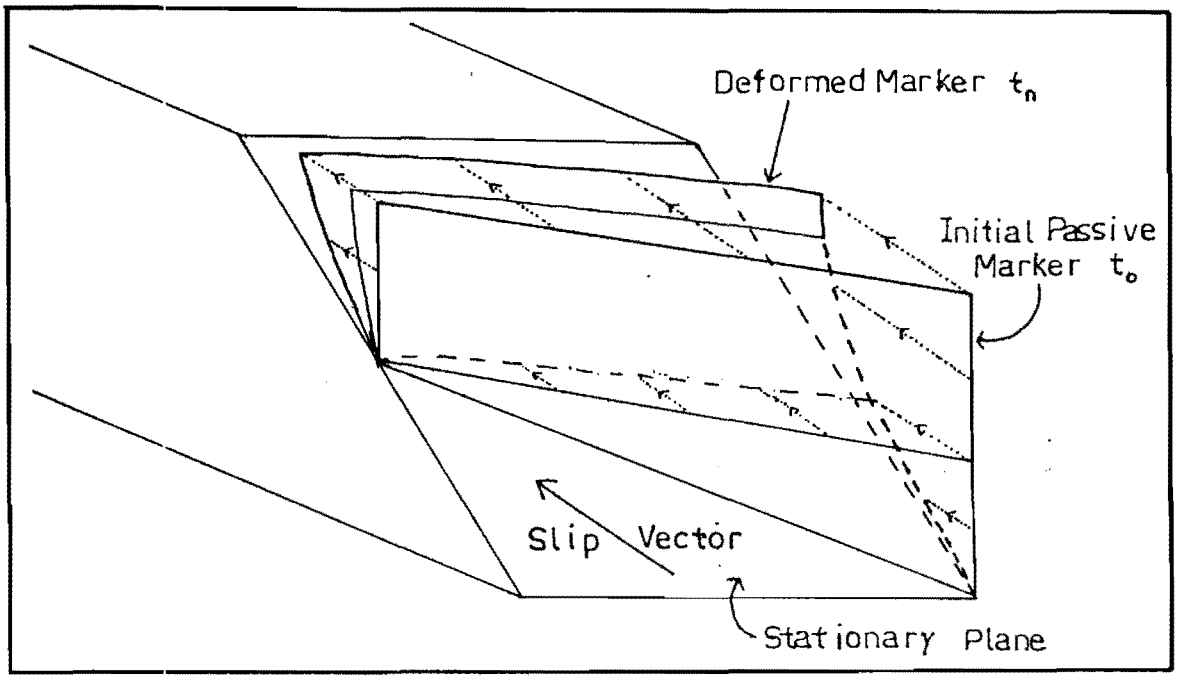

FIG 4.36 Ductile drag of a vertical passive marker initially oriented such that it approximatly bisects the angle between the slip vector and the strike of the inclined oblique dextral reverse shear zone

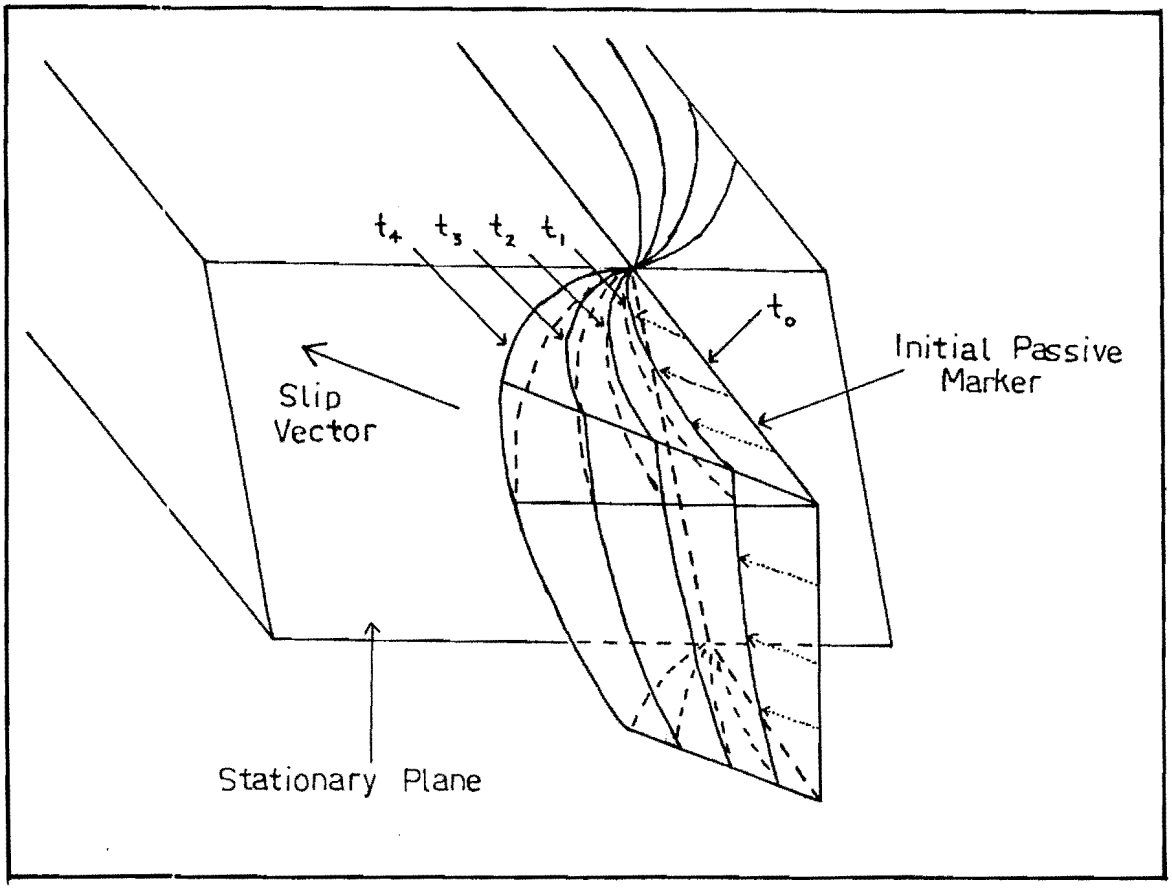

FIG 4.37 Ductile drag of a passive marker initially oriented perpendicular to the stationary plane (see text) and at a high angle to the slip vector of a dextral oblique reverse fault.

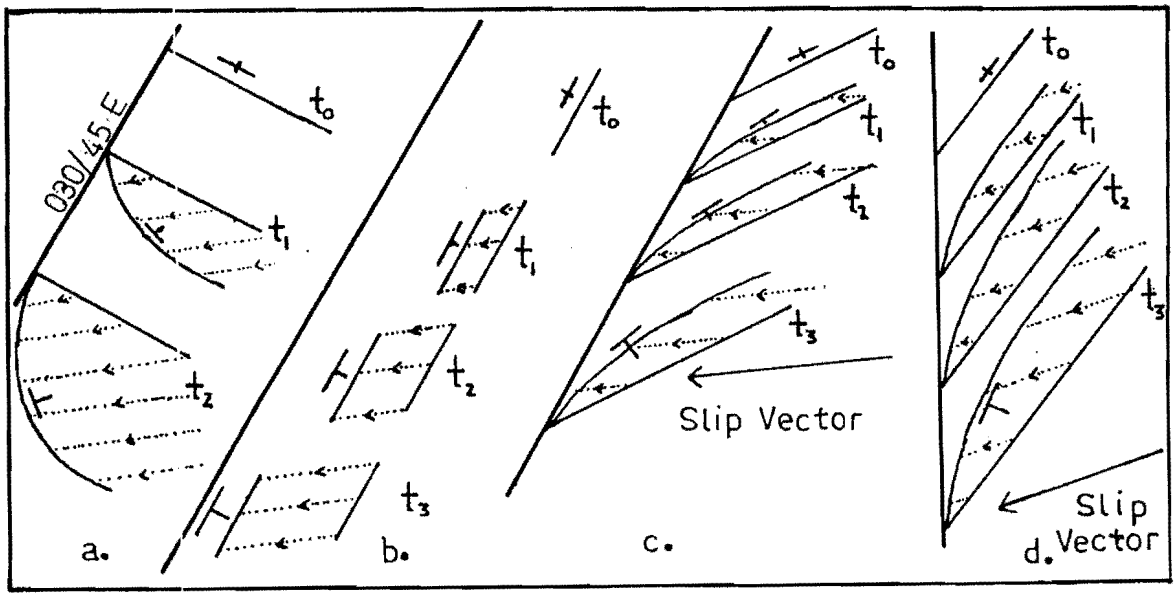

FIG 4.38 a.,b. and c. are plan profiles of figs 4.6.6, 4.6.5, and 4.6.4 and show the sense of rotation for the passive marker of each. The geometry of d. is essentially the same as that of c. but can more readily be compared with the N-S section of the Alpine Fault. A different passive marker is illustrated for each time period (t_n).

$t_4 > t_3 > t_2 > t_1$

4.7 BRITTLE SHEAR IN THE HAAST SCHISTS OF THE BENDS REGION

4.7.1 Introduction

When dealing with a large feature such as the Alpine Fault it is unrealistic to dissociate brittle and ductile shear processes. Often the distinction is a matter of scale only. For the purposes of this discussion ductility includes: folding, brittle and brittle-ductile microshears and metamorphic processes operating on the scale of a few grains. Brittle shear includes planar or anastomosing shear systems operating at outcrop (>1 m) or larger scales. Therefore this discussion is concerned with joints and faults. Distinction between these is arbitrary as they form by brittle fracture in the same stress field, and many joints show small offsets as a consequence of reactivation.

4.7.2 Collection of Data

Collection of data involved the measurement of planar fracture surfaces (excluding schistosity and bedding) from a selection of localities. Selection of localities was rather random (ie. there was no predetermined pattern of sampling). Data collated from any single locality included at least one fracture orientation for each of the major sets seen in that outcrop, as well as a selection of the least common orientations. It was hoped that when collated only the major regional sets would show as clusters in equal area projection plots. The thesis area is divided into domains within which data was collected and then collated for comparison. Where possible the shear sense was noted. Slickensides on joints are uncommon.

Shear sets as defined by stereographic projection of poles to joints, are anastomosing planes which vary in attitude about an average value.

The domains in which fracture data were collated are divided into two groupings. Firstly those which lie within the Alpine Fault Zone, and secondly those which lie east of

the Alpine Fault Zone.

4.7.3 Brittle Shear in the Alpine Fault Zone

(a) Introduction

The term Alpine Fault Zone was coined by Kupfer (1964) and refers to the "wide zone of intense faulting, slicing, and brecciation" in a zone with arbitrary boundaries. Brittle and brittle-ductile processes are related to structural level within the Alpine Fault Zone. Discussion here is essentially limited to those processes occurring at or above the brittle-ductile transition zone of White and White (1983).

Within the zone influenced by ductile processes (which include M_3 metamorphism, mylonitization and F_3 folding) brittle shear postdates ductile shear. Uplift in the Alpine Fault Zone causes unroofing and cooling in the ductile zone. Subsequent to this shear takes place by brittle fracture mechanisms. Brittle offset within the Alpine Fault Zone is largely concentrated about the upward projection of the zone of most rapid ductile shear.

Shear in the Alpine Fault Zone is penetrative on a macroscopic scale, and in a regional context brittle shear planes are most numerous in the broad zone also influenced by ductile shear. M_3 structure within this zone is still largely intact in its original spatial orientation. Intense crushing is limited to a zone as narrow as 20 m south of the Matakitaki River. However in Mole Stream and Bull Creek the crush zone is up to 300 m wide with no well defined boundaries. Here the original hardrock structure is largely obliterated.

(b) Recent Traces of the Alpine Fault

Several relatively fresh fault scarps cross the Trig FZ Ridge at its junction with the Mt Cann Range. These show dextral reverse movement sense. The displacement of two

such traces (the largest ones) were paced out. Approximate horizontal displacements were 50 m and 10 m and vertical displacements were 12 m and 4 m respectively. These give horizontal:vertical ratios of 4.2 and 2.5. The scarps strike at approximately 060° across a glaciated face with a dip of approximately 20° and dip direction 060°. As the two traces run parallel to and above an oversteeped northwest facing slope there could be some associated gravity collapse.

(c) Orientation of Shear Planes in the Alpine Fault Zone

The dominant shear patterns in the north-south (Glenroy) section of the Alpine Fault Zone are illustrated in fig. 4.39(a), patterns at the northern bend (Nardoo) in fig. 4.39(b) and further northeast at Matakitaki Base Hut fig. 4.41(a), the Mole Tops fig. 4.40(a) and Mt Misery fig. 4.40(b). In each case data were gathered immediately east of the zone of intense crushing. These five stereoplots have two main features in common. Each shows a domain defining a northeast striking shear set, although the dip and dip direction is variable. Offset on this set is invariably sinistral. Secondly there is a north-south striking shear set common to each, although the dip and dip direction is again variable. In the Glenroy Valley the northeast striking set swings to east-northeast.

Fig. 4.39(a) showing shear sets in the Glenroy Valley is of particular interest. Here the north-south westward dipping shear set is better developed than elsewhere in the study area. Crenulation of S_3 schistosity by this shear set reveals a dominantly reverse movement sense. These fractures are therefore considered to be antithetic to the Alpine Fault. Sampling was biased such that fractures parallel east dipping S_3 schistosity were not generally measured. However there are numerous planes subparallel S_2 on which brittle failure has occurred. These shears are assumed to be reverse and constitute a set sympathetic with the Alpine Fault. The sympathetic and antithetic sets form

via stress relief in the body of coherent schist which is overiding the Alpine Fault crush zone. Figs. 4.39(a), 4.44, 4.45, and 4.46 illustrate this interpretation.

Although many shear planes have a breccia or gouge infilling there is little evidence of large displacement on any single surface. In some cases, particularly shear planes which strike northeast (e.g. fig. 4.47), and those of the antithetic set, considerable brecciation and gouge zones up to 10 cm thick lead to displacement of individual marker layers by only a few metres. Some such shear planes are continuous for hundreds of metres along strike.

A post glacial river terrace located in the acute angle formed by the junction of the Matakitaki River and Nardoo Creek is offset by a recent fault trace. This locality was examined by Berryman (1975). The single dextral offset of 9.0 m horizontal and 2.2 m vertical is not preserved on the northeast bank of the Matakitaki River. However, directly southwest along strike and beyond Nardoo Creek a more substantial trace runs obliquely across the northern extension of Nardoo Trig Ridge. On this slope, which is inclined at approximately 30^{o} east the fault has a vertical offset of 5-8 m. Here the scarp appears to be a composite of at least two discreet movements and strikes at 045^{o}.

Along the north-south section of the Alpine Fault the active trace is constrained to run under a series of large fans supplied by streams running from the mountain front to the east of the fault trace. High rates of sediment supply from the Alpine Fault Zone (across which these streams flow) has caused burial of any evidence of recent displacement in the Glenroy Valley floor.

A large landslide from the Mt Cann Range 1,000 yds north of Sub A covers the area where the Alpine Fault is projected to cross the Glenroy River. This landslide appears to have dammed the river for a time, allowing accumulation of an undetermined thickness of sediment on the

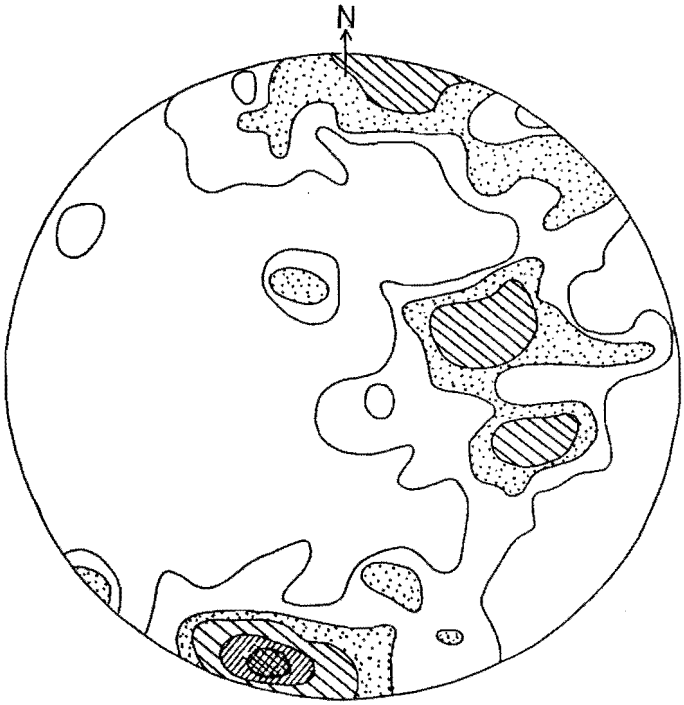

a. Middle Glenroy Valley 294 poles

Contours 1,2,3,5,7 % per 1 % area

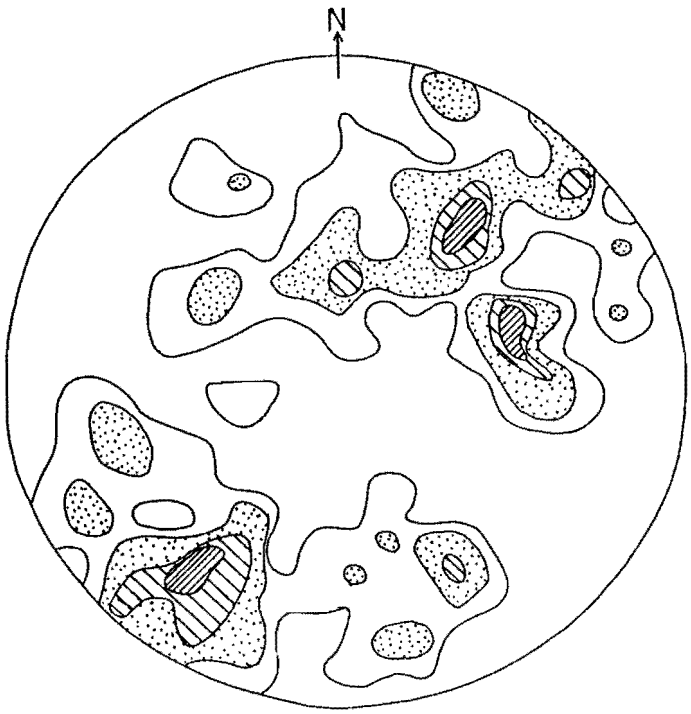

b. Nardoo Tops 200 poles

Contours 1,2,3,4 % per 1% area

FIG 4.39 Poles to Joints Equal area projection

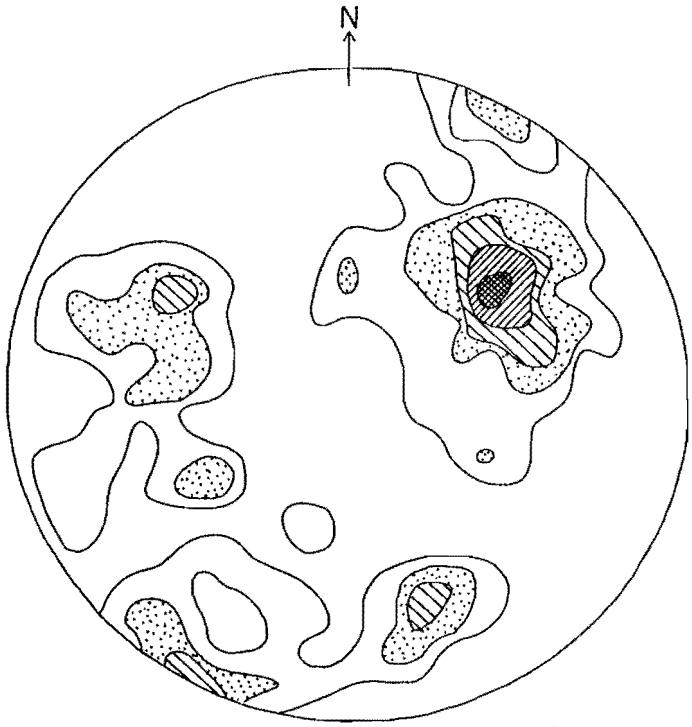

a. Mole Tops 200 poles

Contours 1,2,3,4,5 % per 1% area

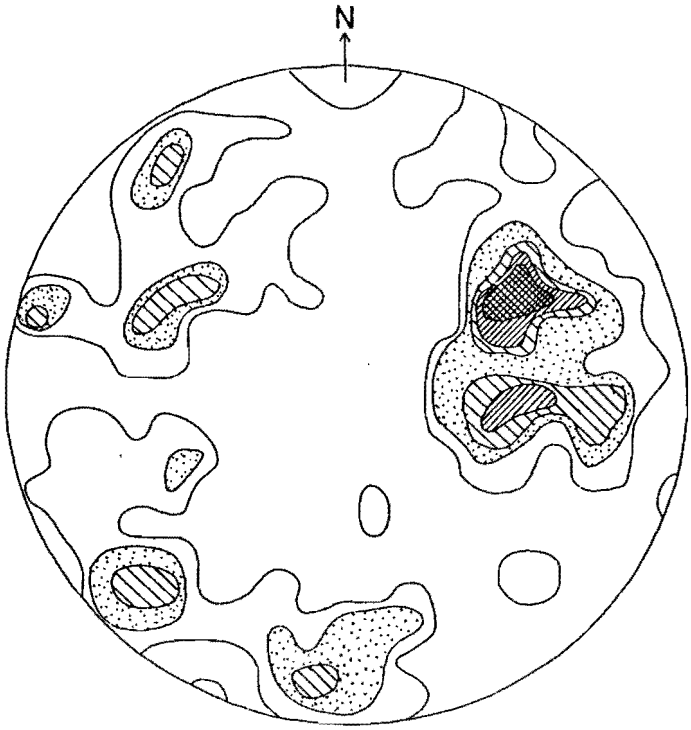

b. Mt Misery 150 poles

Contours 1,2,3,4,5 % per 1 % area

FIG 4.40 Poles to Joints Equal area projection

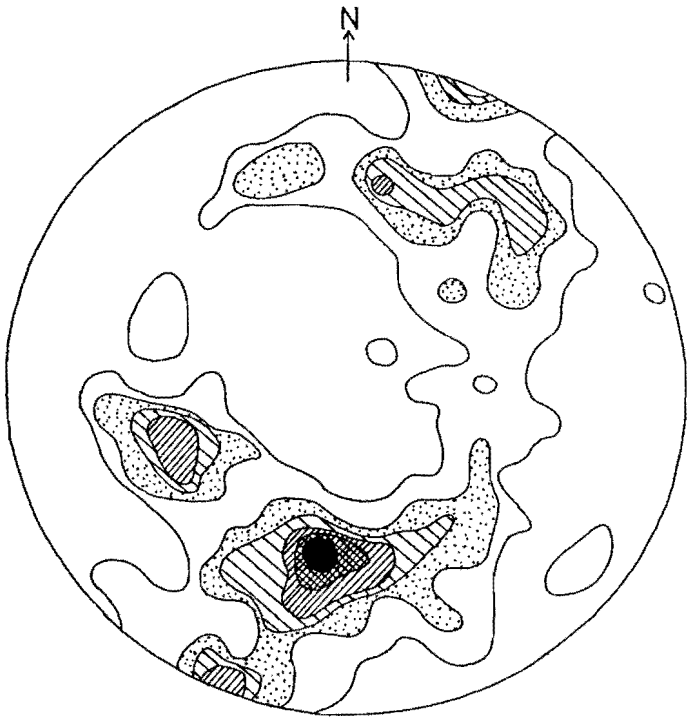

a. Matakitaki Base Hut 175 poles

Contours 1,2,3,4,5,6 % per 1% area

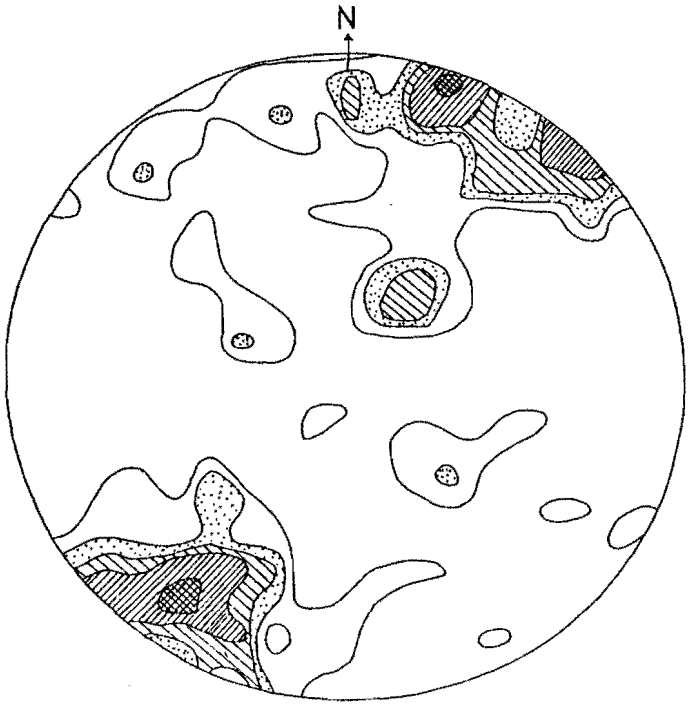

b. Burn Creek and Sunset Valley 196 poles

Contours 1,2,3,4,6 % per 1% area

FIG 4.41 Poles to Joints Equal area projection

a Upper Glenroy Valley, Spenser Mts west of Gloriana Peak, and Trig F Z Ridge. 430 poles

Contour intervals 1,2,3,5, and 7 percent per 1 percent area

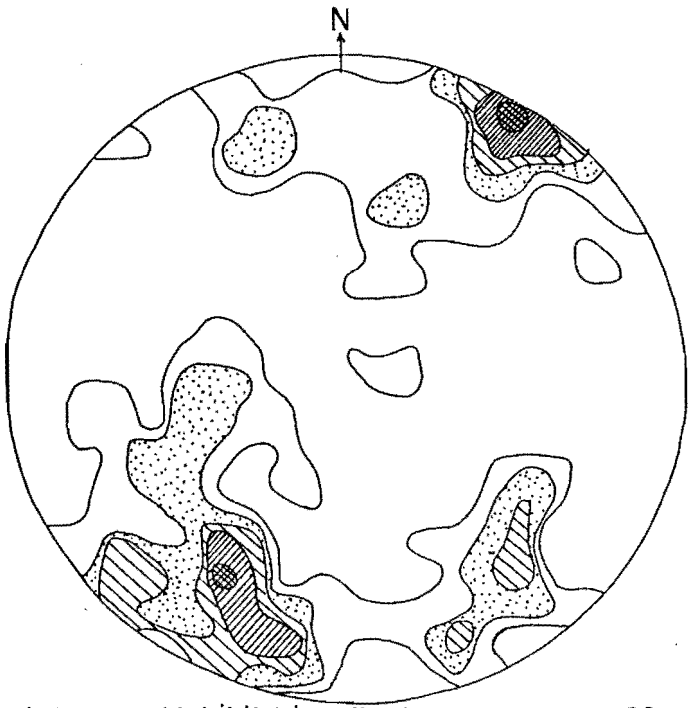

b. Bobs Hut (Upper Matakitaki Valley). 200 poles

Contours 1,2,3,4,5 % per 1% area

FIG 4.42 Poles to Joints Equal area projection

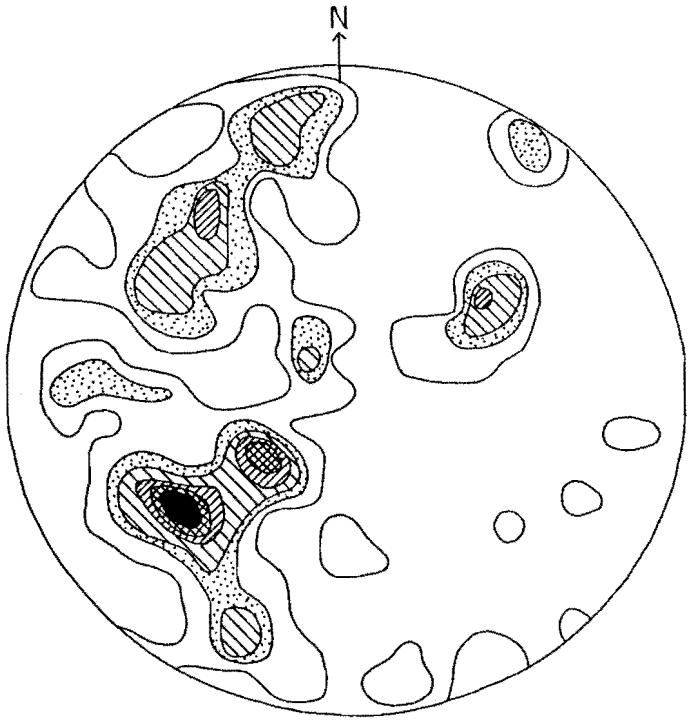

Ella Range between Mt Ella and Mt Watson 150 poles

Contours 1,2,3,4,5,6 % per 1% area

FIG 4.43 Poles to Joints Equal area projection

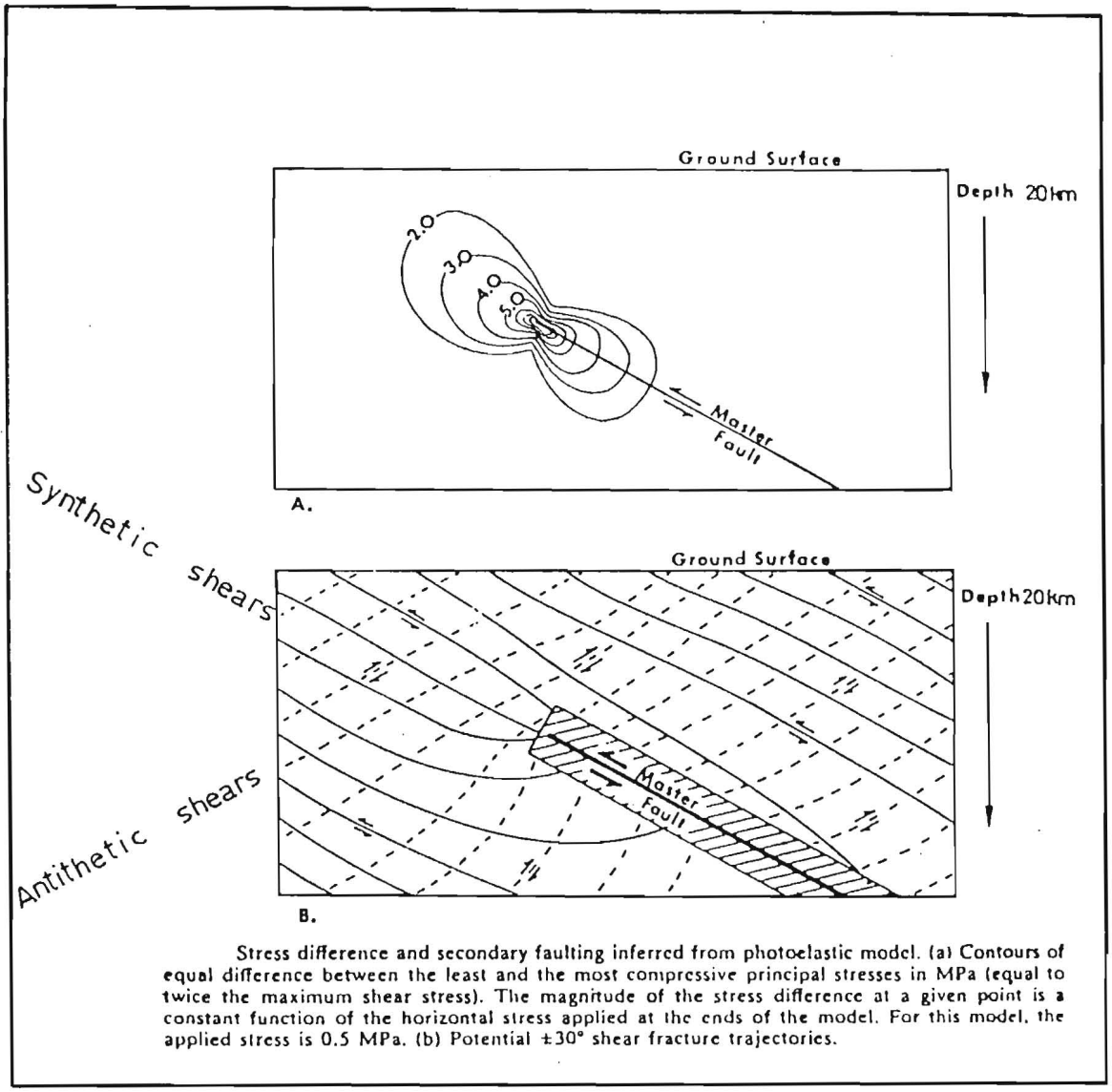

Stress difference and secondary faulting inferred from photoelastic model. (a) Contours of equal difference between the least and the most compressive principal stresses in MPa (equal to twice the maximum shear stress). The magnitude of the stress difference at a given point is a constant function of the horizontal stress applied at the ends of the model. For this model, the applied stress is 0.5 MPa. (b) Potential ±30° shear fracture trajectories.

FIG. 4.44 Figure 6 of Rogers and Rizer (1981).

FIG. 4.45 Eastern slopes of the Glenroy Valley. The Alpine Fault runs north to south through the valley (middle distance) and dips towards the east (left). Note the synthetic-antithetic shear pattern in the foreground.

FIG. 4.46 Alpine Fault Zone, Mole Tops. The scree slopes face northwest towards Mole Stream, through which the Alpine Fault runs. Bedrock structure is progressively disruped towards the Fault by brittle shear processes. Surficial gravitational collapse and freeze and thaw action accentuates the brecciated appearance of the outcrops in the foregraound.

FIG. 4.47 A brittle shear zone oriented subparallel to bedding and S_2 schistosity in mudstone-siltstone association. The direction of view is northeast into Junction Creek from the ridge dividing Burn and Junction Creeks. Metric grid reference M30 4657 8955.

upstream side where the fault is also projected. A stream flowing from the eastern side of the valley appears to be deflected by the landslide debris. The landslide could concievable have been triggered by a seismic event, although such an event would not necessarily be associated with the Alpine Fault. Forest cover over the landslide surface gives a minimum age although this was not estimated.

4.7.4 Brittle Shear East of the Alpine Fault Zone

In the area between the Glenroy and Matakitaki Rivers, excluding the Alpine Fault Zone, there is extraordinary consistancy in orientation of the major joint/shear set. This set (see figs. 4.41(b), 4.42, 4.43) strikes at 125-135^{o} on average, and dips steeply northeast or southwest, often as a conjugate set. Topographically shear in this orientation has had a strong impact, with numerous ice scoured valleys running northwest-southeast. Valley and joint orientations swing in attitude within the Alpine Fault Zone toward east-west. This is probably due, at least in part to the swing in strike of schistosity. Brittle offsets and F_4 crenulations of schistosity and bedding are invariably sinistral on this shear set. The cumulative regional offset is not known. Structural markers such as the large northeast striking metapelites are not noticably offset, and have the same regional trend as bedding in outcrop.

A second shear set which is not represented in figs. 4.41(b), 4.42, 4.43, strikes subparallel to bedding and S_2 schistosity. Shear planes are much more widely spaced than those of the northwest-southeast set and are most common in thick mudstone-siltstone association metasediments. Several gouge zones of up to 20 cm thichness with associated breccia are continuous for over 300 m in both horizontal and vertical profile. The combination of bedding, schistosity and shear plane anisotropies has a strong topographic expression with many ice scoured valleys (e.g. Nardoo and Junction Creeks) trending northeast-southwest. Total cumulative offset on this shear set is unknown as no marker

horizons are displaced.

Shear planes which strike at 070-080° with variable dip and dip direction are common. Such planes often offset bedding by up to 3 m in a dextral sense. Again the cumulative regional offset is not known. One such fault may significantly offset the isotects in the Upper Glenroy Valley. Several tributories of the Upper Glenroy River, Mt Maling Creek and two sections of the Matakitaki River's West Branch follow this trend. Shear planes in this orientation parallel the Awatere Fault.

In the lower textural grade schists east of the Matakitaki River the topographic expression of the above shear sets is less pronounced. Fig. 4.43 which defines shear sets on the Ella Range also shows a breakdown of the regular pattern.

4.7.5 F_4 Folds

F_4 folds include open mesoscopic folds and small crenulations of schistosity (see figs. 4.48, 4.49). The axial planes of F_4 folds are invariably parallel to one or other of the major regional shear sets. Such folds are most commonly associated with the sinistral northwest-southeast striking shear set, and are often cored by brittle shear planes. Morphologically F_4 folds, particularly the small crenulations, are angular asymmetric or monoclinal kink bands. Fold axes are parallel to the intersection of the axial plane and general attitude of schistosity. Offset of schistosity and bedding is always the same as that of discrete brittle shear on the corresponding shear sets. Joints with brittle offset often pass directly along strike into F_4 crenulations with axial planes in the same orientation. F_4 crenulation axes from the Glenroy Valley are plotted on fig. 4.3.9. These fall into two domains, one representing the sinistral northeast-southwest shear set, and one representing the antithetic north-south shear set.

4.7.6 Pseudotachylyte

Pseudotachylyte (glassy frictional melt rock) was observed at one locality within the Alpine Fault Zone. A large boulder in a tributary stream of the Glenroy River at metric grid ref 4590 8891 (see fig. 4.50) contained numerous pseudotachylyte "veins". These "veins" are axial planar to F_4 crenulations which have associated brittle shear offset. Fig. 4.50 shows two such shear planes which have a thin layer of pseudotachylyte. Smaller subsidiary planes appear to be "blind" thrusts and not directly connected with the main shear planes. Discrete pseudotachylyte cored shear planes may pass into, and out of F_4 crenulations along strike (fig. 4.51).

FIG. 4.48 Joints and F_4 crenulations in metapelite on Mt Burn. Schistosity is subvertical and strikes normal to the direction of view. Axial planes of the crenulations are parallel to the orientation of the joint set and the direction of view.

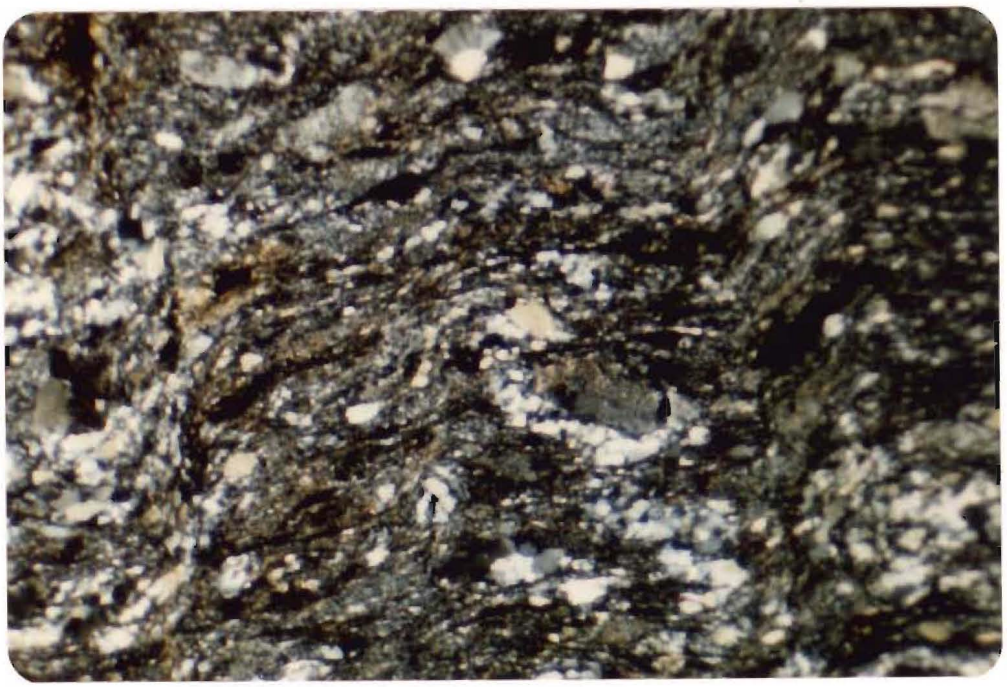

FIG. 4.49 Thin section (UC10650). F_4 crenulations of schistosity in quartzofeldspathic metapsammites of TZ IIA. Within any single specimen crenulations with the same axial plane invariably exhibit the same sense of shear. Cross polarized light. Field of view 2.5 x 1.7 mm.

FIG 4.50 Pseudotachylytes and F_4 crenulations in a large boulder (metric grid ref. 4590 8891)

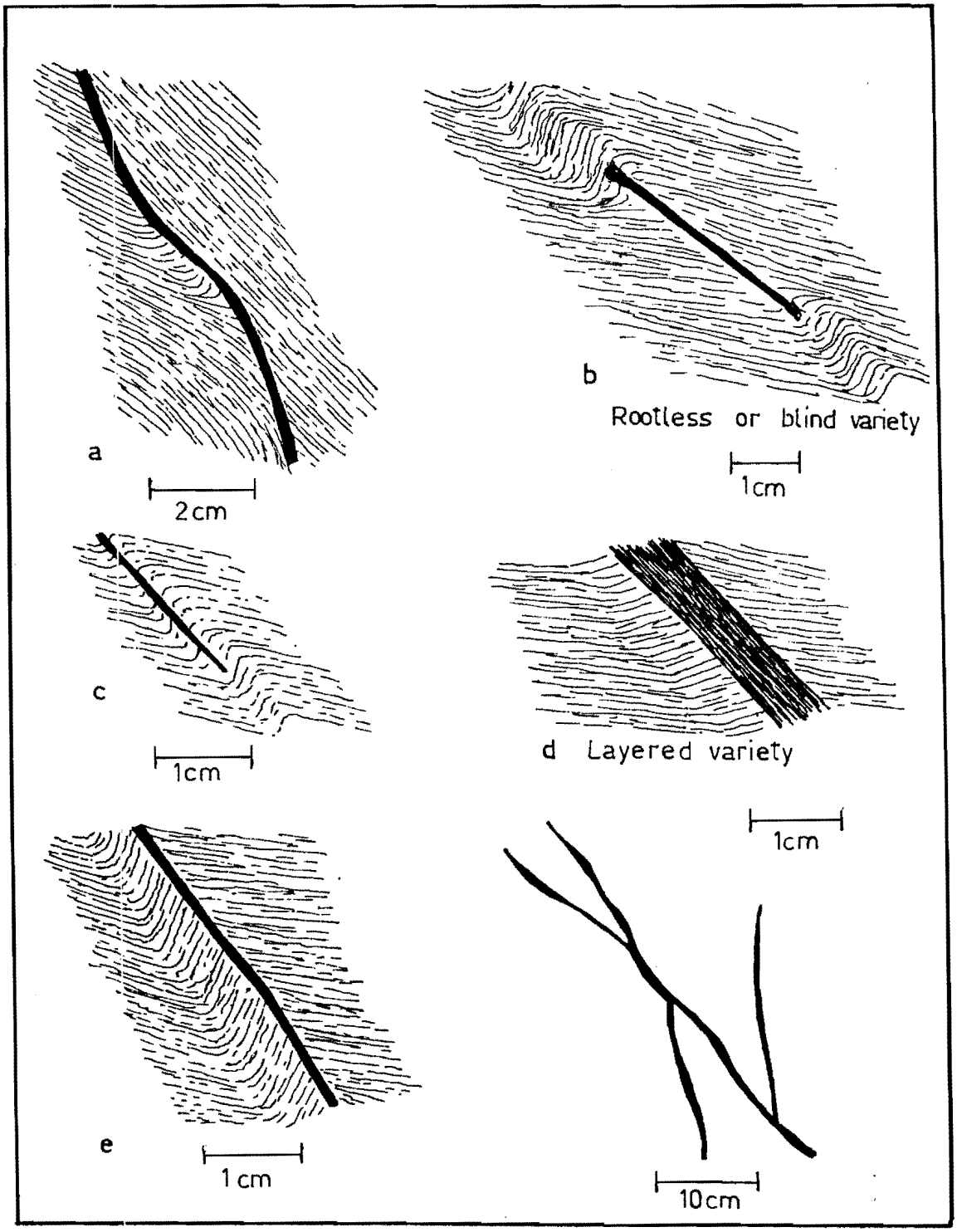

FIG 4.51 Pseudotachylyles and F_4 crenulations

CHAPTER FIVE

SYNTHESIS

5.1 INTRODUCTION

In Chapters two, three and four the geology of the bends region is outlined in some detail. Section 5.2 covers origins for the Alpine Fault Bends and draws in part on the information presented in the preceeding Chapters. General theory from the geological literature is also utilized in this discussion.

In Section 5.3 the current tectonics and the geological history of the bends region and the Haast Schists in particular are outlined. The findings of this study have some implications for the broader history of the South Island and these are also outlined briefly.

5.2 THE ORIGIN OF THE ALPINE FAULT BENDS

One of the most interesting problems associated with the Alpine Fault is the question as to the origin of the Alpine Fault bends. A number of hypotheses have been advanced, notably Walcott (1978), and Suggate (1979). Neither of these was based on a detailed knowledge of the geological structure immediately adjacent to the Alpine Fault in the bends area. Both hypotheses require that the Haast Schists have flexured on a regional scale in order to form the bends (Suggate 1979, fig. 7) and allow the schists to "flow" around the bends. D_2 structures and the D_2 structural trend have not been deformed in this manner. Curvature of the isograds and isotects in this region is a composite effect of the regional uplift pattern, and of the M_3 metamorphic overprint.

Suggate suggests four possible origins for the bends (illustrated in fig. 4, pp 69, Suggate, 1979). These are:

"(a) the Alpine Fault was bent from the start;

(b) it has been offset by a north-trending transcurrent fault;

(c) the north trending section is part of a pre-existing fault that was, as it were, "adopted" as part of the Alpine Fault; or

(d) that the Alpine Fault was substantially straight after the Permian belts were situated on opposite sides of the bends, and it has indeed since been bent."

Origin (c) is adopted by Suggate and discussed in some detail. However this model is in conflict with the geological structure mapped by Cutten (1976, 1979) and Campbell, Cutten and Tulloch (in prep). Suggate's model requires the north-south "Glenroy" section of the Alpine Fault to have been generated as part of a pre-existing Fault (probably the Waimea Fault), the northern extension of which has subsequently been offset to the north-east. Thus the basement block immediately west of the Glenroy River must be Rotoroa Complex (Suggate, 1979, figs. 5 and 6). Campbell, Cutten, and Tulloch show this is not the case. These rocks are almost certainly correlatives of the Mt Arthur Suite of rocks, which run in a discontinuous belt from Springs Junction to Collingwood.

An assumption implicit in Suggate's model is that the bends are now fixed with respect to the Western Province (or Indian Plate). Structure in the Haast Schists demands that the bend is fixed, with respect to, and at the leading edge of, the Wairau Block (that area between the Alpine-Wairau and Awatere Faults). Furthermore the Wairau Block must act as a more or less rigid wedge (c.f. Mackie, 1968). If the

bend is fixed in this manner then the question as to its age is still open. I would suggest, on the grounds of structure within the Alpine Fault Zone, that the north-south section of the Alpine Fault is at least as old as earliest Pliocene (ie. as old, or older than M_3 metamorphism). If offset during subsequent millenia is restored this places the bends in a region where the rocks on both sides of the Alpine Fault are either Torlesse or Haast Schist lithologies. Therefore the origin of the bends would not have involved the Western Foreland of the Nelson Province.

A number of authors have illustrated means by which faults may be generated with non-linear traces. These include: Chinnery (1966a, 1966b), Wilcox et al. (1973), Tchalenko (1970), Ramsay (1980), and Bahat (1983). My proposal regarding the mechanics of evolution of the Alpine Fault bends is based on the ideas of Ramsey (1980) and Chinnery (1966a, 1966b). Two possibilities are considered. Firstly that illustrated in fig. 5.2 (after fig. 18, Ramsay, 1980). Two faults of the same shear sense which propagate towards each other share a mutual dipole-dipole like attraction. As the faults propagate the independant stress fields at each fault tip are superimposed producing a pattern of stress trajectories resulting in refraction of their propagation directions. Thus the merging of faults can produce a single curved trace.

The second possibility is illustrated in figs. 5.1, 5.3 (after Chinnery, 1966b, fig. 5). Individual faults have a tendency to alter their direction of propagation in regional pure or uniaxial compressive stress. Here stress trajectories are based on the residual stress remaining after large magnitude seismic relief on the main linear section of the fault. Chinnery (1966, pp183) states: "once a secondary fault has occurred the stress distribution in its vicinity will be changed into a rather complex form. A large secondary fault may well give rise to new subsidiary faults, although there are few cases where these are clear. Usually it seems that when a secondary fault prop agates out of the region of influence of the master fault it is

controlled by the initial stress distribution and curves around until it is parallel to the approximate complementary shear direction." In this way, a major fault propagates along a secondary orientation before returning to its original trend.

The model of Chinnery (1966a, 1966b) assumes a mechanically isotropic medium through which a single fault propagates. The angle between the fault and the principal stress is 30° (an average value for most experimental and natural transcurrent systems). Chinnery (1966a) and Hafner (1951) both state that stress must be regarded as a tensor rather than a vector quantity. Only the shear stress components are relieved in discrete slip events. Consequently the direction and magnitude of the principal stresses relate to the seismic release of shear stress. If stress is treated in this fashion then the model of wrench fault tectonics proposed by Moody and Hill (1956)is invalid, as is the method of determination of principal horizontal stress proposed by Lensen (1958). The method of Lensen has been used more recently by Berryman (1979). Means (1963) also dismisses Moody and Hill (1956) and Lensen (1958) on the basis of their assumptions which include: (1) that the Earth's crust can be considered mechanically isotropic; (2) that transcurrent faults are necessarily steeply dipping; (3) that transcurrent faults are generated at 45° to the principal horizontal stress; and (4) that the maximum principal stress is necessarily horizontal.

The propagation direction of a fault is likely to be influenced by pre-existing mechanical anisotropies (eg. schistosity and bedding in the Haast Schist and Torlesse Zones) and by an inherent tendency for faults to change direction during propagation, even where the medium is mechanically isotropic (see Chinnery, 1966). Thus it is my contention that the Alpine Fault bends were created during propagation of the Alpine Fault. This is not contradictory to any known structural features within the Haast Schists of southeast Nelson.

The D_2 structural trend swings in sympathy with the southern bend between Pell Stream and the Glenroy River but diverges from this trend and that of the Alpine Fault Zone north of the Glenroy River. This swing is illustrated in figs. 3.1, 4.2, 4.27, 5.4. Although the swing could reflect rotational strain there is no reason why it should not be regarded as a primary feature of the Haast Schists. In this context a "Chinnery" or "Ramsay" type model of the origin of the bends becomes more likely. Such a swing in the orientation of the D_2 mechanical anisotropy could cause a sympathetic swing in the propagation direction. Having diverged from its original direction of propagation the fault is then more likely to diverge further along a direction of secondary faulting.

Once a transcurrent fault has formed, the relative motion between the rocks to each side will be complicated if the trace is curved. It is proposed that the Alpine Fault bends are able to move with respect to the Indian Plate. This is achieved largely through stress relief by plastic and brittle deformation west of the Alpine Fault, as proposed by Mackie (1968), as well as uplift and genuine westwardly directed thrusting along the Alpine Fault.

Mackie's proposal is stated thus: "Suppose, for the sake of argument, that the rocks on the north-west side of the fault were stationary and those on the south-east side, within a western protuberance formed by the bends in question, were moving to the south-west, the protuberance moving with them. The compression of the rocks on the north-west side of the fault caused by the passage of the protuberance would be manifested in the form of shortening with possible fracturing along roughly north-south lines; plastic yielding would accommodate some of the strain, but not all. This fracturing would extend progressively towards the south-west as the protuberance moved in that direction." This proposal leads directly into the examination of the structure and tectonics of the bends region.

FIG 5.1 After Chinnery (1966a), Figures 4, 5 and 6.

a and d Contours of equal shear stress at the ground surface after faulting has occurred:
a) for faulting under pure shear and
d) for faulting under uniaxial compression.
Contour values are in units of 10^5 dynes/cm^2.

b and e Trajectories showing the direction of maximum shear stress at each point on the ground surface after faulting has occurred:
b) for faulting under pure shear and
e) for faulting under a uniaxial compression.

c and f Typical likely directions for secondary faulting:
c) for faulting under pure shear and
f) faulting under a uniaxial compression.
Solid lines show most likely locations, broken lines show less likely locations.

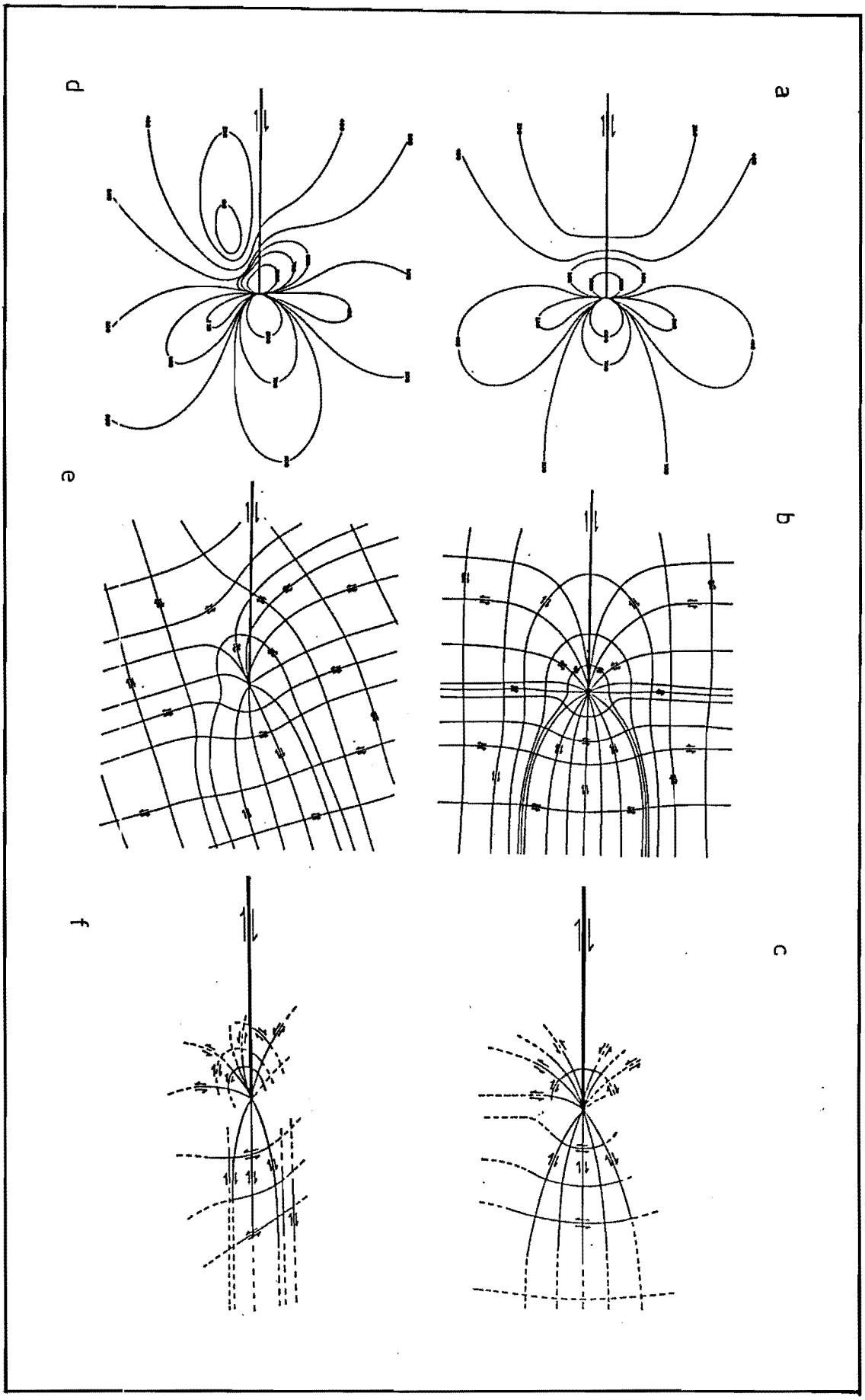

FIG 5.1 Scale 25 km

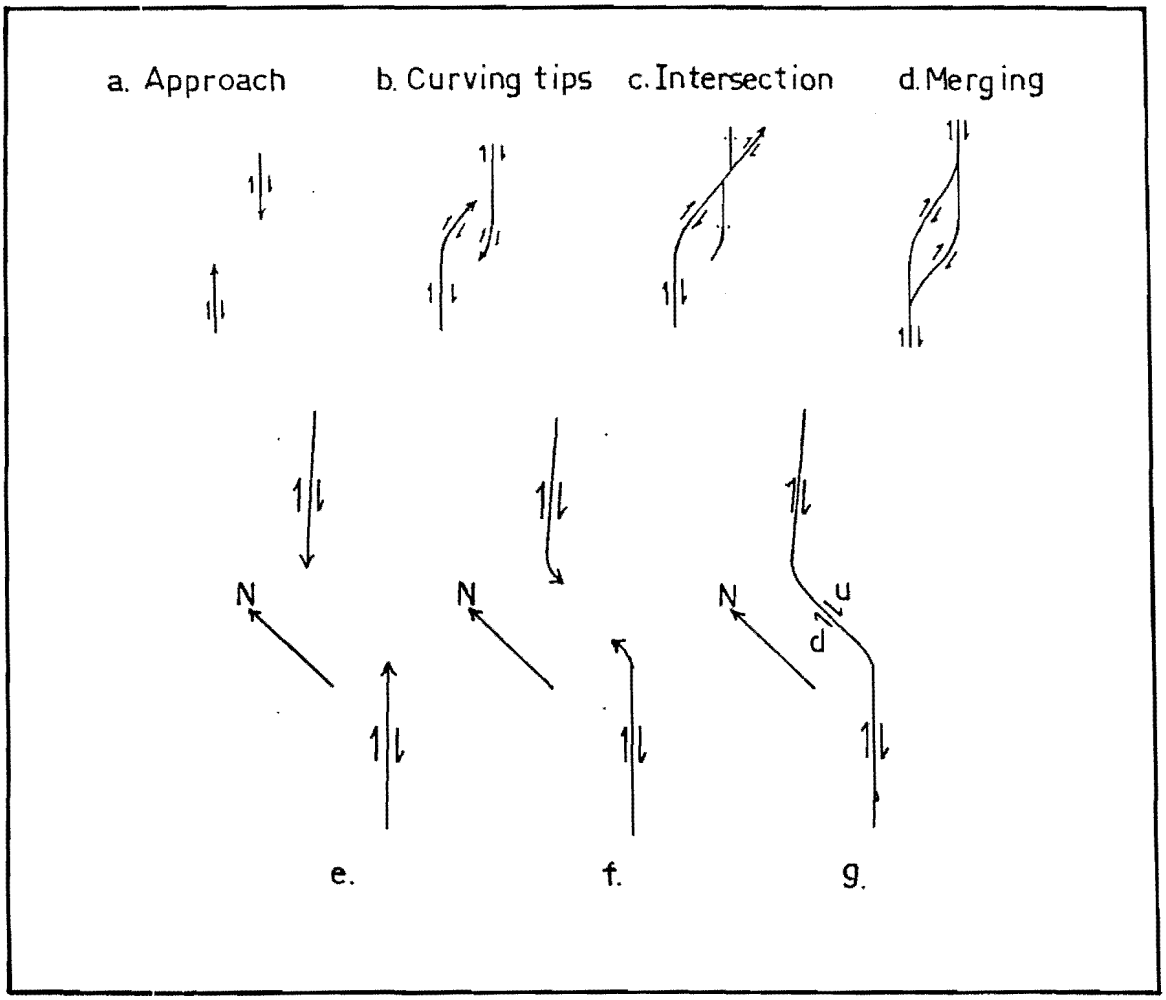

FIG 5.2 Curving and merging of faults during propagation (after Ramsay,1980,fig 18)

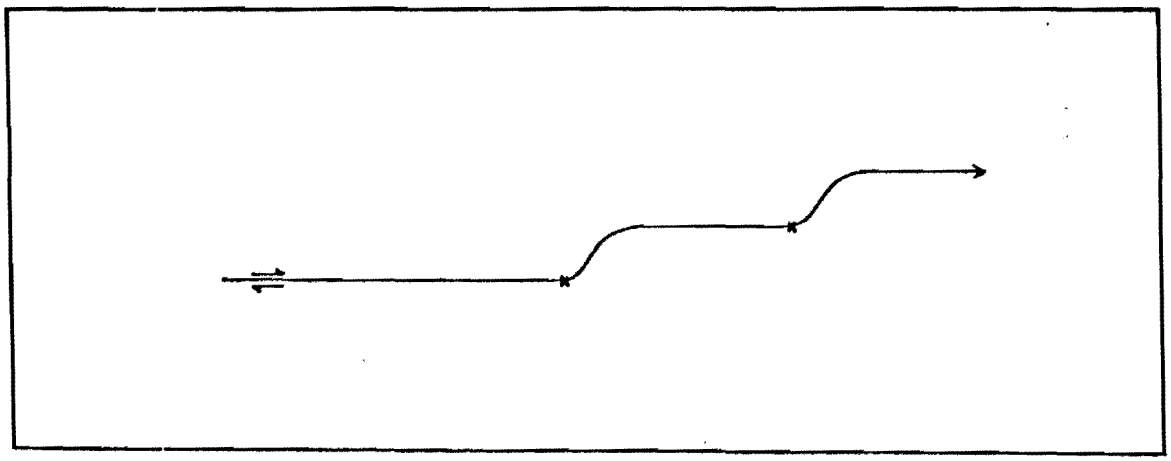

FIG 5.3 (after Chinnery 1966b,fig 5.) A fault that once ended at the point marked by a cross will tend to extend itself along a curve as shown. (for the case of uniaxial compression).

5.3 TECTONICS OF THE BENDS REGION

5.3.1 An Overview

Any model which is designed to explain the tectonics of a particular area must be in accord with the geological field relationships. The following is a summary of improtant features within the bends region with which a tectonic model should be compatible.

(1) The Alpine Fault is the major tectonic lineament in this region. This zone dips at around 50-60° towards the east in the Glenroy Valley, and 70° southeast between the Matakitaki River and Lake Rotoroa. Uplift rates increase dramatically from west to east across the Alpine Fault Zone. Consequently mylonites, and M_2 schists of amphibolite and greenschist faceies have been exposed immediately east of the Alpine Fault trace. Lineations (L_3), which probably reflect the slip vector during strain in mylonitization and M_3 metamrphism, plunge at moderate angles to the east and northeast (see Sections 4.2.5, 4.5). Microtexture, microfabric and mesoscopic structures suggest that ductile shear was oblique-dextral-reverse in nature. Mechanisms of ductile and brittle shear within the Alpine Fault Zone are significant in terms of the regional history. These include crystallization-recrystallization processes, intergranular slip (grain boundary sliding, shear banding), intragranular slip (twinning, dislocation glide), and pressure solution (see Sections 4.2.5, 4.5).

(2) Within the zone of M_3 metamorphism variation in the attitude of S_3 schistosity can be related to strain in oblique-dextral-reverse shear (Section 4.4). The distribution of F_3 folds is related to the angle between S_2 and S_3 schistosities, and thus is a consequence of curvature of the Alpine Fault.

(3) A tectonic model should account for the types of drag seen in the Alpine Fault Zone. The D_2 structural trend provides a penetrative marker fabric which can be used to

identify the sense of rotation in ductile shear. It is suggested (Section 4.4.3) that the strike of S_2 schistosity will either remain the same or rotate counterclockwise depending on the sense of vergence with the Alpine Fault Zone. In cross section S_2 will also rotate counterclockwise towards parallelism with S_3, and ultimately the Alpine Fault.

(4) Early structures such as bedding, S_2 schistosity, L_2 lineations, and F_2 fold axis (Section 3.3.1) are remarkably consistent in attitude over the region as a whole. This indicates that the main mass of Haast Schist has not suffered internal rotation. Furthermore these structures have much the same orientation for at least 20 km southeast of the bends (McLean, 1986). Therefore the bend in the Alpine Fault cannot have formed through an external rotation of the Haast Schists. Nor can the Haast Schsts be "flowing" around a fixed bend in any simple fashion. Brittle shear on closely spaced fractures will not allow flow without rotation of the major structural markers (Section 4.7.4). The oblique angle of the Alpine Fault is unlikely to be coincidental, and probably dates from the origin of the bends (Section 5.2).

(5) Stress levels are (on average through time) likely to be higher outside the Alpine Fault Zone than within. Relief of stress in seismic slip tends to be limited to the immediate neighbourhood of a fault (Hafner, 1951, pp383). Therefore active deformation can be expected to the west of the Alpine Fault. The swing in attitude of the Alpine Fault Zone probably results in increased resistance to dextral shear in this part of the plate boundary zone, and to an anomalously large principal stress. Deformation immediately west of the bends includes westward directed imbricate thrusting and associated folding (see fig. 4.10, 5.4), producing signigicant crustal shortening (cf. Murata and Weber, 1983). Anticlines have steep to overturned western limbs, and axial planes which dip towards the east. Thrusting and folding affect both the crystalline basement (including amphibolites, granulites, granites and slates)

and the overlying sedimentary strata (mainly Miocene to Pleistocene) (see Cutten, 1976; Campbell and Cutten, 1985; Campbell, Cutten and Tulloch, in prep.). Further west folding is more open (Cutten, 1976), faulting is reverse with uplift to the east, and a sinistral horizontal component on north to north-northeast striking planes (Walcott, 1978).

(6) That area bounded by the Alpine Fault, the Glenroy River and the Matakitaki River is occupied in part by an allochthonous slice of the East Nelson Permian sequence. The allochthon is internally telescoped such that, although many of the distinctive East Nelson units are present, the sequence is drastically reduced in thickness. Lithologies include a number of formations from the Maitai Group, the Dun Mountain Ophiolite, the Rai Sandstone, granite (probably Separation Point), marine Whaingaroan Maitai derived sediments and possibly some Pelorous Group sandstones. Surrounding and underlying the allochthon on three of four sides are a selection of amphibolitic gneisses, granulites and Miocene sedimentary strata (Campbell and Cutten, 1985; Campbell, Cutten and Tulloch, in prep.). Along the fourth side (Alpine Fault) the allochthon is bounded by greenschist facies Haast Schists.

There are a number of possible mechanisms whereby the allochthon could have been emplaced. Firstly that of Suggate (1979) in which the origin is as a fault sliver from the Tophouse termination of the Nelson Permian sequence. This is in conflict with mapping by Campbell, Cutten and Tulloch (in prep.). Secondly the allochthon could be a transcurrent sliver from the South Westland termination of the Permian sequence. Thirdly (and my preferred mechanism) the allochthon could have been thrust west to southwest in bulldozer-like fashion by an advancing Wairau block, from an original position probably now beneath the Wairau block.

(7) The curvature of metamorphic isograds and isotects within the Haast Schists is in contrast with the linear trends of schistosity and bedding. An anomalously

high uplift rate (cf. Wellman, 1979) and a north-south oriented axis of tilting (in sympathy with the swing in strike of the Alpine Fault) could produce curved isograds and isotects without rotating the strike of schistosity appreciably. Secondly the Alpine Fault generated M_3 metamorphic overprint does parallel the Fault and causes the garnet isograd and the TZ-IIB/IIIA isotect to swing rather sharply, particularly about the southern bend.

5.3.2 Summary and Conclusions

Together the various features outlined above suggest that the bends are unlikely to be fixed with respect to the Indian Plate. It is envisaged that the Haast Schists are being thrust obliquely across the eastern edge of the Indian Plate, with the vector direction and rate of movement remaining relatively constant at all points around the curve. In effect this is the same model as that proposed by Mackie (1968) (see Section 5.2). The bend in the Alpine Fault is fixed to the leading edge of the Wairau block. This model is viable proviede crustal shortening west of the Alpine Fault has been sufficient to allow the bends to move southwest with respect to the Indian Plate.

Geological structure within the Haast Schist is consistent with an origin for the bends during the formation of the Alpine Fault itself. Currently slip vectors in the fault zone are oblique. However several authors (e.g. Sibson et al., 1979; Walcott, 1979; Molnar et al., 1975) suggest that convergence and uplift were much less pronounced during the early movement history of the Alpine Fault. Thus southwest displacement of the Wairau block would have been more easily achieved at this time.

Faults which follow the trend of D_2 structures are oriented such that dextral shear along them can potentially eliminate the bends. When extended downward these planes must intersect the Alpine Fault Zone (cf. Wellman, 1979, fig. 4) but are unlikely to penetrate through this zone. Brittle shear within the Haast Schist of the bends region is

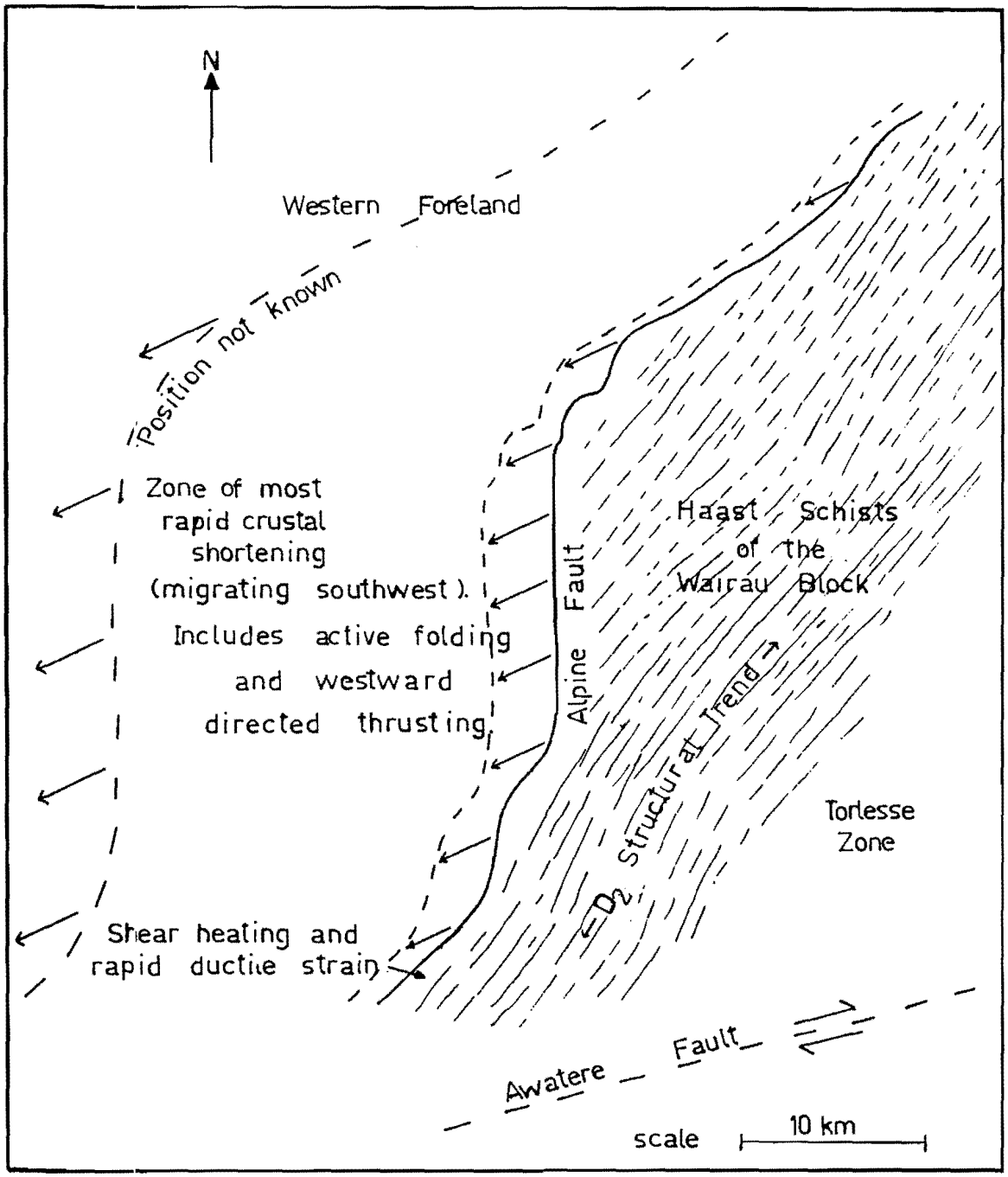

FIG 5.4 The Haast Schists are being thrust obliquely across the Western Foreland with the vector direction and rate of movement of the rock mass remaining relatively constant at all points around the curve of the Alpine Fault. West of the Alpine Fault the zone of crustal shortening migrates relative to the rocks of the Western Foreland.

probably subsidiary to the dominant zone of ductile shear at the base of the schists, and may be related to internal adjustments within the Wairau block. Therefore faults which run parallel to D_2 structures are not assumed to contribute a large cumulative dextral offset.

5.4 GEOLOGICAL HISTORY OF THE HAAST SCHIST AND TORLESSE ZONES OF THE BENDS REGION

The Haast Schist and Torlesse Zone metasediments were derived from a continental granite bearing source, probably to the east of the present New Zealand continental landmass (cf. Andrews et al., 1976). Deposition probably occurred in a submarine fan setting with mass flow as an important transport mechanism. Paleontologic evidence from the Torlesse Zone in adjacent areas suggests that local deposition occurred during the late Triassic.

Metamorphism (M_2) responsible for development of the Haast Schists occurred subsequent to shortening and structural stacking of the Torlesse stratigraphy (Rangitata I orogeny of Bradshaw et al., 1980) during lower Jurassic times. The reason for the timing of M_2 in D_2 deformation appears to be that the thermal effects of D_2 reached a peak subsequent to the main phase of structural stacking.

The M_2 schists of southeast Nelson are unlike those of Marlborough and Otago in a number of aspects. Firstly the structural histories are markedly different. The Otago Schists are part of an Orogenic belt which had been multiply deformed and unroofed by the mid-Cretaceous. In contrast the M_2 schists of southeast Nelson appear to have suffered only one main phase of deformation, and although uplifted by as much as 10 km (Sheppard et al., 1975) and cooled through the argon retention level by the mid-Cretaceous they were not exposed. Reed (1958) noted on petrographic grounds that the schists of Otago and Marlborough were unlike those of southeast Nelson. At equivalent mineralogic grade and degree of chemical reconstitution the schists of southeast

Nelson have less well developed schistosity and mineralogic segregation. As a consequence primary sedimentary structures are better preserved at equivalent mineralogic grade in southeast Nelson. The regionally consistent northeast strike of S_2 schistosity, and the lack of evidence for rotation of D_2 structure in simple shear strain within this region are arguments in favour of a primary difference in orientation of structures in Otago and southeast Nelson.

During early Miocene times the Alpine Fault propagated through the Torlesse and Haast Schist Zones of the bends region. The bends may have formed at this time. Rapid strain in the Alpine Fault Zone generated a curvilinear thermal anomaly by shear heating and resulted in M_3 metamorphism in and adjacent to the fault zone. In combination structural, strain and thermal softening allowed continued strain localization and contributed to preservation of curvature in the Alpine Fault Zone (the bends).

The establishment of M_3 as an Alpine Fault related event may be important outside this region. If M_3 extends southward towards Haast and if the M_2 schists are fundamentally different from the Otago Schists then it may be incorrect to show them as a continuation of the Otago Schist belt. In this context it becomes unrealistic to regard the Haast Schists of southeast Nelson as having been attenuated in extreme drag and shear rotation as is implicit in many traditional tectonic interpretations e.g. Kingma (1974), Walcott (1978), Norris (1979).

A migrating rotational pole in the Pacific plate (Molnar et al., 1975) caused an increasingly compressional component across the Alpine Fault resulting in uplift and unroofing of both M_2 and M_3 schists during Miocene to Recent times. In the bends region the north-south section of the Alpine Fault is oriented such that the thrust and uplift components of displacement have been substantially higher than elsewhere. Several authors including Sheppard et al. (1975), Adams (1981) and Johnston and White (1983) suggest

restricted shear heating occurred at the Alpine Fault raising temperatures by as much as 100°C. These authors consider shear heating occurred over a relatively short period of time. However if the reorientation of convergence was gradual then shear heating was probably a longer lived event, as is necessary for the development of D_3 structures between the bends.

Repeated glaciation during Pleistocene to Recent times has moulded the topography, valleys being excavated along penetrative anisotropies within the Haast Schists.

ACKNOWLEDGEMENTS

This study was made possible by a research grant from the Department of Lands and Survey. Numerous people were involved at various stages during this project. I wish to thank the staff of the Department of Lands and Survey and in particular Mr B. Mannix, for their interest and active involvement. The New Zealand Forest Service were of assistance in providing accommodation and transport.

Mrs J.K. Campbell supervised the project. Her help and encouragement is gratefully acknowledged.

Dr D. Shelley provided useful discussion and reviewed parts of the draft.

Andrew Donaldson, Ingrid Meister, Phillip Simpson, Bruce Horner and Allister McRae provided company during the long excursions necessary to complete the mapping for this study.

The staff of Canterbury Mountain Radio Service kindly maintained communications between ourselves and the outside world during field work.

Mr A. Downing helped in the preparation of photographic prints.

A large number of thin sections were made by Mr D. MacDonald.

The one true cross section presented here was draughted by Miss L. Leonard.

Andrea Lobb and Nigel Campbell typed the manuscript under considerable pressure of time. Andrea's concern over the details and quality of presentation was invaluable.

Mike Stewart is thanked for checking various parts of the draft.

REFERENCES

Adams, C.J. 1981: Uplift rates and thermal structure in the Alpine Fault Zone and Alpine Schists, Southern Alps, New Zealand. In: McClay, K.R.; Price N.J. ed.: Thrust and Nappe Tectonics. Geological Society of London: 211-222.

Adams, C.J.; Gabites J.E. 1985: Age of metamorphism and uplift at Haast Pass, Lake Wanaka, and Lake Hawea, South Island, New Zealand. New Zealand Journal of Geology and Geophysics 28: 85-96.

Adamson, J.K. 1964: The Alpine-Wairau and Waimea Fault System in the Lake Rotoiti area. Unpublished M.Sc. thesis lodged in the Library, University of Canterbury, Christchurch, New Zealand.

Adamson, R.G. 1966: Stratigraphy and structure in the northern part of the area between the Glenroy and Matakitaki Rivers, South Nelson, New Zealand. Unpublished M.Sc. thesis, lodged in the Library, University of Canterbury, Christchurch, New Zealand.

Allis, R.G. 1981: Continental underthrusting beneath the Southern Alps of New Zealand. Geology 9: 303-307.

Allis, R.G.; Henly, R.W.; Carman, A.F. 1979: The thermal structure beneath the Southern Alps. In: Walcott, R.I Cresswell, M.M. ed. The Origin of the Southern Alps. Royal Society of New Zealand Bulletin 18: 79-85.

Andrews, P.B. 1974: Deltaic sediments, Upper Triassic Torlesse Supergroup, Broken River, North Canterbury.New Zealand Journal of Geology and Geophysics 17: 881-905.

Andrews, P.B.; Speden, I.G.; Bradshaw, J.D. 1976: Lithological and paleontological content of the Carboniferous - Jurassic Canterbury Suite, South Island, New Zealand. New Zealand Journal of Geology and Geophysics 19: 792-819.

Arabasz, W.J.; Robinson, R. 1976: Microseismicity and geologic structure in the Northern South Island, New Zealand. New Zealand Journal of Geology and Geophysics 19: 569-601.

Bahat, D. 1983: New aspects of rhomb structures. Journal of Structural Geology 5: 591-602.

Beggs, J.M. 1980: Sedimentology and paleogeography of some Kaihikuan Torlesse rocks in mid Canterbury. New Zealand Journal of Geology and Geophysics 23: 437-445.

Bell, J.M.; Fraser, C. 1906: The geology of the Hokitika Sheet, North Westland Quadrangle. New Zealand Geological Survey Bulletin 1 n.s.

Berryman, K.R. 1975: Earth deformation studies reconnaissance of the Alpine Fault. New Zealand Geological Survey E.D.S. report 30: 25 p.

Berryman, K.R. 1979: Active faulting and derived PHS directions in the South Island, New Zealand. In: Walcott, R.I.; Cresswell, M.M. eds.: Origin of the Southern Alps. Royal Society of New Zealand Bulletin 18: 29-34.

Berryman, K.R. 1980: Late Quaternary movement on the White Creek Fault, South Island, New Zealand. New Zealand Journal of Geology and Geophysics 23: 93-101.

Bibby, H.M. 1975: Crustal strain from triangulation in Marlborough, New Zealand. Tectonophysics 29: 529-540.

Bibby, H.M. 1976: Crustal strain across the Marlborough Faults. New Zealand Journal of Geology and Geophysics 19: 407-426.

Bishop, D.G. 1972: Progressive metamorphism from prehnite - pumpellyite to greenschist facies in the Dansey Pass area, Otago, New Zealand. Geological Society of America Bulletin 83: 3177-3197.

Bishop, D.G. 1976: Sheet 126, Mt Ida (1st Edition) Geological Map of New Zealand 1:63 360 Department of Scientific and Industrial Research, Wellington, New Zealand.

Bishop, D.G. 1978: Isotects - Reply New Zealand Geological Society Newsletter 46: 43-44

Bowen, F.E. 1964: Sheet 15, Buller (1st ed.) Geological Map of New Zealand 1:250 000. Department of Scientific and Industrial Research.

Bradshaw, J.D. 1972: Stratigraphy and structure of the Torlesse Supergroup (Triassic - Jurassic) in the foothills of the Southern Alps near Hawarden, Canterbury, New Zealand. New Zealand Journal of Geology and Geophysics 15: 71-87.

Bradshaw, J.D. 1980: Torlesse Terrane excursion: The Esk Head Melange. Field Trip Guide, Christchurch Conference, Geological Society of New Zealand Miscellaneous Publication.

Bradshaw, J.D.; Adams, C.J. & Andrews, P.B. 1980: Carboniferous to Cretaceous on the Pacific Margin of Gondwanna: The Rangitata phase of New Zealand.In: Cresswell, M.M.; Vella, P. ed. Proceedings of the Fifth International Gondwanna Symposium: 217-221.

Brun, J.P.; Cobbold, P.R. 1980: Strain heating and thermal softening in continental shear zones: a review. Journal of Structural Geology 2: 149-158.

Campbell, J.K.; Cutten, H.N.C. 1985: Foreland structure west of the Alpine Fault in the region of the Glenroy Valley, South Nelson. Programme and Abstracts Christchurch Conference, Geological Society of New Zealand Miscellaneous Publications 32 A: 28.

Campbell, J.K.; McLean, G.W. 1985: The structure of the Torlesse rocks adjacent to the Alpine Fault between the Sabine River and Lake Rotoiti. Programme and Abstracts Christchurch Conference, Geological Society of New Zealand Miscellaneous Publications 32 A: 29.

Carter, R.M.; Landis, C.A.; Norris, R.J.; Bishop, D.J. 1974: Suggestions towards a high - level nomenclature for New Zealand rocks. Journal of the Royal Society of New Zealand 4: 5-18.

Carter R.M.; Norris, R.J.; Turnbull, I.M. 1978: Sedimentation patterns in an ancient arc-trench basin complex: Carboniferous to Jurassic Rangitata Orogeny, New Zealand. In: Stanley, D.J. & Kelling, G. ed.: Sedimentation in Submarine Canyons, Fans and Trenches: 340-361.

Chinnery, M.A. 1966: Secondary faulting 1. Theoretical aspects Canadian Journal of Earth Sciences 3: 163-174.

Chinnery, M.A. 1966b: Secondary faulting 2. Geological aspects. Canadian Journal of Earth Sciences 3: 175-190.

Cobbold, P.R.; Cosgrove, J.W.; Summers, J.M. 1971: Development of internal structures in deformed anisotropic rocks. Tectonophysics 12: 23-53.

Cosgrove, J.W. 1976: The formation of crenulation cleavage. Journal of the Geological Society of London 132: 155-178.

Cox, H.S. 1884: On the district between the Maruia and Buller Rivers. Report on the Geological Exploration of the Colonial Museum and Geological Survey of New Zealand 16: 1-10.

Cutten, H.N.C. 1976: The Rappahannock Group: Late Cenozoic sedimentation and tectonics in the Alpine Fault Zone in Southeast Nelson. Unpublished M.Sc. thesis, lodged in the Library, University of Canterbury.

Cutten, H.N.C. 1979: Rappahannock Group: Late Cenozoic sedimentation and tectonics contemporaneous with Alpine Fault movement. New Zealand Journal of Geology and Geophysics 23: 535-553.

Davey, F.J.; Broadbent, M. 1980: Seismic refraction measurements in Fiordland, southwest New Zealand. New Zealand Journal of Geology and Geophysics 23: 395-405.

Evison, F.F. 1971: Seismicity of the Alpine Fault, New Zealand. In: Collins, B.W. & Fraser, R. ed. Recent Crustal Movements. Royal Society of New Zealand Bulletin 9: 161-165.

Farmer, R.T. 1967: Stratigrphy and structure of Paleozoic rocks near Springs Junction, Southwest Nelson. Unpublished M.Sc. thesis, lodged in the Library, University of Canterbury.

Fleitout, L.; Froidevaux, C. 1980: Thermal and mechanical evolution of shear zones. Journal of Structural Geology 2: 159-164.

Freund, R. 1971: The Hope Fault, a strike slip fault in New Zealand, New Zealand Geological Survey Bulletin 86: 49p.

Fyfe, H.E. 1929: Maruia Subdivision. Geological Survey, 23rd Annual Report (n.s.): 8-9.

Fyfe, H.E. 1930: Murchison and Maruia Subdivisions. Geological Survey, 24th Annual Report (n.s.):. 13-19.

Fyfe, H.E. 1968: Geology of the Murchison Subdivision. Suggate, R.P. ed.: New Zealand Geological Survey Bulletin n.s. 36.

Ghosh, S.K. 1966: Experimental tests of buckling folds in relation to strain ellipsoid in simple shear deformations. Tectonophysics 3: 169-185.

Ghosh, S.K. 1982: The problem of shearing along axial plane foliations. Journal of Structural Geology 4: 63-67.

Grindley, G.W. 1963: Structure of the Alpine Schists of South Westland, Southern Alps, New Zealand. New Zealand Journal of Geology and Geophysics 6: 872-930.

Haast, J. von 1861: Report of the Topographical and Geological Exploration of the Western District of the Nelson Province. Printed C. and J. Elliot, 1861.
Hafner, W. 1951: Stress distributions and faulting. Geological Society of America Bulletin 62: 373-399.

Haines, A.J.; Calhaem, I.M.; Ware, D.E. 1979: Crustal seismicity near Lake Pukaki South Island, New Zealand, between June 1975 and October 1978. In: Walcott, R.I.; Cresswell, M.M. ed.: The origin of the Southern Alps. Royal Society of New Zealand Bulletin 18: 87-94.

Harper, C.T. and Landis, C.A. 1967: K-Ar ages from regionally metamorphosed rocks, South Island, New Zealand and some tectonic implications. Earthand Planetary Science Letters 2: 419-429.

Harris, L.B.; Cobbold, P.R. 1984: Development of conjugate shear bands during bulk simple shearing. Journal of Structural Geology 7: 37-44.

Hatherton, T. 1980: Crustal seismicity in New Zealand, 1956-75. Journal of the Royal Society of New Zealand 10: 19-25.

Hatherton, T.; Hunt, T.M. 1968: Gravity profiles across the Alpine Fault, New Zealand. Journal of Geophysical Research 73: 5343-5351.

Hawkes, M.R. 1981: The effect of bedrock geology on sediment yield in an alpine area of extreme rainfall. Unpublished M.Sc. thesis, lodged in the Library, University of Canterbury, Christchurch, New Zealand.

Henderson, J. 1937: The West Nelson earthquakes of 1929. New Zealand Journal of Science and Technology 19(2): 65-144.

Hicks, D.M. 1981: Deep-sea fan sediments in the Torlesse zone, Lake Ohau, South Canterbury, New Zealand. New Zealand Journal of Geology and Geophysics 24: 209-230.

Hobbs, B.E.; Means, W.D.; Williams, P.F. 1976: An Outline of Structural Geology. John Wiley and Sons, New York. 571pp.

Howell, D.J. 1981: Submarine fan facies in the Torlesse terrane, New Zealand. Journal of the Royal Society of New Zealand 11: 113-122.

Hutton, C.O.; Turner, F.J. 1936: Metamorphic zones in Northwest Otago. Transactions of the Royal Society of New Zealand 65: 405-406.

Hurley, P.M.; Hughes, H.; Pinson, W.H. Jr.; Fairbairn, H.W. 1962: Radiogenic argon and strontium diffusion parameters in biotite at low temperature obtained from Alpine Fault uplift in New Zealand. Geochemica Cosmochemica Acta: 67-80.

Johnston, D.C.; White, S.H. 1983: Shear heating associated with movement along the Alpine Fault, New Zealand. Tectonophysics 92: 241-252.

Kingma, J.T. 1959: The tectonic history of New Zealand. New Zealand Journal of Geology and Geophysics 2: 1-55.

Kingma, J.T. 1974: The Geological Structure of New Zealand. John Wiley and Sons. Koons, P.O. 1978: The Pounamu Ultramafics: a study of metasomatism. Unpublished M.Sc. thesis, lodged inthe Library, University of Otago, Dunedin, New Zealand.

Kupfer, D. 1964: Width of the Alpine Fault Zone, New Zealand. New Zealand Journal of Geology and Geophysics 7: 685-701.

Lensen, G.J. 1958: Rationalized fault interpretation. Zealand Journal of Geology and Geophysics 1: 307-317.

Lensen, G.J. 1960: A 12 mile long drag along the Awatere Fault. 9th Royal Society of New Zealand Congress 1960 Report (Abstracts): 47.

Lensen, G.J. 1977: Late Quaternary tectonic map of New Zealand 1:2 000 000 (1st edition). New Zealand Geological Survey Miscellaneous Series Map 12. Department of Scientific and Industrdial Research.

Le Pichon, X.J. 1968: Seafloor spreading and continental drift. Journal of Geophysical Research 73: 3661-97.

Lister, G.S.; Hobbs, B.E. 1980: The simulation of fabric development during plastic deformation and its application to quartzite: the influence of deformation history. Journal of Structural Geology 2: 355-370.

Lister, G.S.; Patterson, M.S.; Hobbs, B.E. 1978: The simulation of fabric development in plastic deformation and its application to quartzite: the model. Tectonophysics 45: 107-158.

Lister, G.S.; Snoke, A.W. 1984: S-C mylonites. Journal of Structural Geology 6: 167-638.

Lister, G.S.; Williams, P.F. 1979: Fabric development in shear zones: theoretical controls and observed phenomena. Journal of Structural Geology 1: 283-297.

McKay, A. 1985: Report on the geology the the southwest part of Nelson and the northern part ofthe Westland District. Appendix to the Journal of the House of Representatives. New Zealand Government - B.

Mackie, J.B. 1969: The New Zealand Alpine Fault (Letter to the Editor). New Zealand Journal of Geology and Geophysics 12: 578-579.

Mackinnon, T.C. 1980: Geology of Monotis-bearing Torlesse rocks in Temple Basin near Arthurs Pass, South Island, New Zealand. New Zealand Journal of Geology and Geophysics 23: 63-81.

Mackinnon, T.C. 1983: Origin of the Torlesse terrane and coeval rocks, South Island, New Zealand. Geological Society of America Bulletin 94: 967-985.

McLean, G. 1986: Structure and metamorphism near the Alpine and Awatere Faults, Lewis Pass. Unpublished M.Sc. thesis, lodged in the Library, University of Canterbury, Christchurch, New Zealand.

Malahoff, A. 1965: Gravity and geological studies of an ultramafic mass in New Zealand. Hawaii Institute of Geophysics, Report HIG-65-2.

Manz, R.; Wickham, J. 1978: Development of internal structures in deformed anisotropic rocks. Tectonophysics 12: 23-53.

Mason, B.H. 1961: Potassium-argon ages of metamorphic rocks and granites from Westland, New Zealand. New Zealand Journal of Geology and Geophysics 4: 352-356.

Means, W.D. 1963: Comments on dynamic interpretation of faulting. New Zealand Journal of Geology and Geophysics 6: 757-768.

Molnar, P.; Atwater, T.; Mammerickx, J.; Smith, S.M. 1975: Magnetic anomalies, bathymetry and tectonic evolution of the South Pacific since the Late Cretaceous. Geophysical Journal of the Royal Astronomical Society 40: 383-420.

Moody, J.D.; Hill, M.J. 1956: Wrench fault tectonics. Geological Society of America Bulletin 67: 1207-1246.

Morgan, P.G. 1908: The Geology of the Mikonui Subdivision. New Zealand Geological Survey Bulletin n.s. 6.

Murata, H.; Weber, K. 1983: Experimental study of subfluence tectonics in the Rheinische Schiefergebirge. In: Martin, H.; Eder, F.W. ed.: Intracontinental Fold Belts. Springer-Verlag, Berlin.

Norris, R.J.; Bishop, D.G. 1985: Deformed conglomerates, textural, and deformation mechanisms in the Haast Schists. Programme and Abstracts Christchurch Conference, Geological Society of New Zealand Miscellaneous Publications 32A: 67.

Paterson, M.S. & Weiss, L.E. 1966: Experimental deformation and folding in phyllite. Geological Society of America Bulletin 77: 343-374.

Platt, J.P. 1984: Secondary cleavages in ductile shear zones. Journal of Structural Geology 6: 439-442.

Platt, J.P.; Vissers, R.L.M. 1980: Extensional structures in anisotropic rocks. Journal of Structural Geology 2: 397-410.

Ramsay, J.G. 1980: Shear zone geometry. Journal of Structural Geology 2: 83-99.

Rattenbury, M.S. 1985: Timing of mylonitisation west of the Alpine Fault central Westland, New Zealand. Programme and Abstracts Christchurch Conference, Geological Society of New Zealand Miscellaneous Publications 32A: 71.

Reed, J.J. 1958: Regional metamorphism in Southeast Nelson. New Zealand Geological Survey Bulletin n.s. 60.

Reed, J.J. 1964: Mylonites, cataclasites and associated rocks along the Alpine Fault, South Island, New Zealand. New Zealand Journal of Geology and Geophysics 7: 645-684.

Rogers, D.A.; Rizer, W.D. 1981: Deformation and secondary faulting near the leading edge of a thrust sheet. In: McClay, K.R.; Price, N.J. ed.: Thrust and Nappe Tectonics. Geological Society of London.: 65-77.

Rynn, J.M.W.; Scholz, C.H. 1978: Seismotectonics of the Arthurs Pass region, South Island, New Zealand. Geological Society of America Bulletin 84: 1373-1388.

Sanderson, D.J.; Andrews, J.R.; Phillips, W.E.A.; Hutton, D.H.W. 1980: Deformation studies in the Irish Caledonoides. Journal of the Geological Society of London 137: 289-302.

Scholz, C.H.; Beavan, J.; Hanks, T.C. 1979: Frictional metamorphism, argon depletion, and tectonic stress on the Alpine Fault, New Zealand. Journal of Geophysical Research 84: 6770-6782.

Scholz, C.H.; Rynn, J.M.W.; Weed, R.W.; Frohlich C. 1973: Detailed seismicity of the Alpine Fault Zone Fiordland region, New Zealand. Geological Society of America Bulletin 84: 3297-3316.

Shelley, D. 1968: Ptygma-like veins in greywacke, mudstone, and low grade schist from New Zealand. Journal of Geology 76: 692-701.

Shelley, D. 1975: Manual of Optical Mineralogy. John Wiley and Sons, New York.

Sheppard, D.S.; Adams, C.J.; Bird, G.W. 1975: Age of metamorphism and uplift in the Alpine Schist belt of New Zealand. Geological Society of America Bulletin 86: 1147-1153.

Sibson, R.H.; White, S.H.; Atkinson, B.K. 1979: Fault rock distribution in the Alpine Fault Zone: a preliminary account. In: Walcott, R.I.; Cresswell, M.M. ed.: The Origin of the Southern Alps. Royal Society of New Zealand Bulletin 18: 55-65.

Sibson, R.H.; White, S.H.; Atkinson, B.K. 1981: Structure and Distrbution of fault rocks in the Alpine Fault Zone, New Zealand. In: McClay, K.R. & Price, N.J. eds: Thrust and Nappe Tectonics: 97-210.

Simpson, C.; Schmid, S.M. 1983: An evaluation of criteria to deduce the sense of movement in sheared rocks. Geological Society of America Bulletin 94: 1281-1288.

Skjernaa, L. 1980: Rotation and deformation of randomly oriented planar and linear structures in progressive simple shear. Journal of Structural Geology 2: 101-109.

Smith, W.D. 1971: Earthquakes at shallow and intermediate depth in Fiordland, New Zealand. Journal of Geophysical Research 76: 4901-4907.

Suggate, R.P. 1961: Rock-stratigraphic names and undifferentiated sediments of the New Zealand Geosyncline. New Zealand Journal of Geology and Geophysics 4: 392-399.

Suggate, R.P. 1963: The Alpine Fault. Transactions of the Royal Society of New Zealand 2: 105-129.

Suggate,R.P. 1979: The Alpine Fault bends and the Marlborough Faults. In: Walcott, R.I.; Cresswell, M.M. ed.: The Origin of the Southern Alps. Royal Society of New Zealand Bulletin 18: 67-72.

Tchalenko, J.S. 1970: Similarities between shear zones of different magnitude. Geological Society of America Bulletin 81: 1625-1639.

Turnbull, I.M.; Forsyth, P.J. (in press): Schist structure east of the Alpine Fault bend, southeast Nelson, New Zealand. New Zealand Journal of Geology and Geophysics.

Walcott, R.I. 1978: Present tectonics and Late Cenozoic evolution of New Zealand. Geophysical Journal of the Royal Astronomical Society 52: 137-164.

Walcott, R.I. 1979: Plate motion and shear strain rates in the vicinity of the Southern Alps. In: Walcott, R.I.; Cresswell, M.M. ed.: The Origin of the Southern Alps. Royal Society of New Zealand Bulletin 18: 5-12.

Walker, R.G. 1979: Turbidites and associated coarse clastic deposits. In: Walker, R.G. ed: Facies Models. Geoscience Canada, Reprint Series 1.

Webby,B.D. 1959: Sedimentation of the alternating greywacke and argillite strata in the Porirua District. New Zealand Journal of Geology and Geophysics 2: 461-478.

Wellman, H.W. 1949: Address to the Pacific Science Conference.

Wellman, H.W. 1955: The Geology between Bruce Bay and Haast River, South Westland. New Zealand Geological Survey Bulletin n.s. 48 (2nd ed.).

Wellman, H.W. 1979: An uplift map for the South Island of New Zealand, and a model for uplift of the Southern Alps. in: Walcott, R.I.; Cresswell, M.M. ed.: The origin of the Southern Alps. Royal Society of New Zealand Bulletin 18: 5-12.

Wellman, H.W.; Willet, R.W. 1942: The geology of the West Coast from Abut Head to Milford Sound. Part 1. Transactions of the Royal Society of New Zealand 71: 282-306.

Wellman, P.; Cooper, A. 1971: K-Ar age of some New Zealand lamprophyre dikes near the Alpine Fault. New Zealand Journal of Geology and Geophysics 14: 341-350.

White, J.C.; White, S.H. 1983: Semi-brittle deformation within the Alpine Fault Zone, New Zealand. Journal of Structural Geology 5: 579-589.

Wilcox, R.E.; Harding, T.P.; Seely, D.R. 1973: Basic wrench tectonics. American Association of Petroluem Geologists Bulletin 57: 74-96.

Wilson, J.T. 1963: Hypothesis of the earths behaviour. Nature 198: 925-929.

Woodland, B.G. 1982: Gradational development of domainal slaty cleavage, its origin and relation to chlorite porphyroblasts in the Martinsburg Formation, Eastern Pennsylvania. Tectonophysics 83: 89-124.

Woodward, D.J. 1972: Gravity anomalies in Fiordland, southwest New Zealand. New Zealand Journal of Geology and Geophysics 15: 22-32.

Woodward, D.J. 1979: The crustal structure in the Southern Alps, New Zealand, as determined by gravity. in: Walcott, R.I.; Cresswelol, M.M. eds.; The origin of the Southern Alps. Royal Society of New Zealand Bulletin 18: 95-99.

Young, D.J. 1968: The Fraser Fault in central Westland, New Zealand and its associated rocks. New Zealand Journal of Geology and Geophysics 11: 291-311.